

Current noise and Keldysh vertex function of an Anderson impurity in the Fermi liquid regime

Akira Oguri and Yoshimichi Teratani

*Department of Physics, Osaka City University, Sumiyoshi-ku, Osaka 558-8585, Japan and
Nambu Yoichiro Institute of Theoretical and Experimental Physics, Osaka City University, Osaka 558-8585, Japan*

Kazuhiko Tsutsumi

Department of Physics, Osaka City University, Sumiyoshi-ku, Osaka 558-8585, Japan

Rui Sakano

The Institute for Solid State Physics, the University of Tokyo, Kashiwa, Chiba 277-8581, Japan

(Dated: May 26, 2022)

We present a complete microscopic Fermi-liquid description for next-to-leading order transport through an Anderson impurity under a finite bias voltage V . It is applicable to multilevel quantum dots without particle-hole nor time-reversal symmetry, and is constructed based on the nonequilibrium Keldysh formalism, taking into account the current conservation between electrons in the impurity levels and the conduction bands. Specifically, we derive the formula for the current noise generated in the steady flow up to terms of order $(eV)^3$ at zero temperature $T = 0$. To this end, we calculate the Keldysh vertex functions $\Gamma_{\sigma\sigma';\sigma'\sigma}^{\nu_1\nu_2;\nu_3\nu_4}(\omega, \omega'; \omega', \omega)$, which depend on branches ν_1, ν_2, ν_3 and ν_4 of the time-loop contour and on spin degrees of freedom σ and σ' , up to linear-order terms with respect to eV , T , and frequencies ω and ω' . The coefficients of these linear-order terms are determined by a set of the parameters, defined with respect to the equilibrium ground state: the phase shift, static susceptibilities, and nonlinear three-body susceptibilities of the impurity electrons. The low-energy expressions of the vertex components are shown to satisfy the Ward identities with the Keldysh Green's functions expanded up to terms of order ω^2 , $(eV)^2$, and T^2 . We also find that the imaginary part of the Ward identities can be described in terms of the eV -dependent collision integrals for a single-quasiparticle excitation and that for a single quasiparticle-quasihole pair excitation. These collision integrals ensure the current conservation of the next-to-leading order Fermi-liquid transport due to the quasiparticles with a finite damping rate.

PACS numbers: 71.10.Ay, 71.27.+a, 72.15.Qm

I. INTRODUCTION

Highly correlated low-energy quantum states of the Kondo systems show universal behaviors which can be described by the Fermi liquid theory.¹ It was originally developed for dilute magnetic alloys, and has been applied later to quantum dots, for which the universal Fermi-liquid behaviors have been observed in nonlinear current-voltage characteristics^{2,3} and also in the nonequilibrium current noise.⁴⁻⁷ Furthermore, novel quantum systems having various kinds of internal degrees of freedom, such as orbitals, nuclear spins and flavors, bring an interesting variety to the Kondo effects, and have been being studied for carbon nanotubes,^{7,8} ultracold atomic gases,⁹ quark matters,¹⁰ etc.

The Fermi liquid (FL) theory for quantum impurity systems has been constructed based on the Kondo model¹¹ or Anderson model.¹²⁻¹⁶ The ground state properties such as the residual resistivity of magnetic alloys and the zero-bias conductance of quantum dots can be described by the scattering phase shift δ_σ . The Friedel sum rule states that at zero temperature $T = 0$ it also corresponds to a one-point correlation function $\delta_\sigma/\pi = \langle n_{d\sigma} \rangle$: the occupation number of an impurity level with σ the index for spin or the other internal degrees of free-

dom. The phase shift also determines the spectral weight of the impurity state at the Fermi level and the energy shift of the impurity level due to the Clo

Leading order behavior of the Fermi liquid approaching the limit $T \rightarrow 0$ occurs, for instance, as a T -linear specific heat of impurity electrons $\mathcal{C}_{\text{imp}} \propto T/T^*$. The Kondo energy scale T^* and the Wilson ratio R together with the phase shift δ_σ completely describe the leading-order behaviors. These additional parameters, T^* and R , can be expressed in terms of two-point correlation functions: the static susceptibilities of impurity electrons $\chi_{\sigma\sigma'}$, which can also be related to the derivative of the self-energy with respect to the frequency ω and the value of the vertex corrections at zero frequencies.¹²⁻¹⁴

Next leading-order behavior occurs especially in transport phenomena, such as the T^2 resistivity of magnetic alloys¹²⁻¹⁴ and the nonlinear $(eV)^2$ conductance through quantum dots under a finite bias voltage V .¹⁷⁻²⁰ In an ideal situation where quantum impurity systems have the particle-hole (PH) and time-reversal (TR) symmetries, these next leading-order terms can be described in terms of the two-point correlation functions, mentioned above. This is because in this highly symmetric case the quadratic ω^2 , T^2 , and $(eV)^2$ dependences occur only through the damping rate of quasiparticles. However,

these symmetries are easily broken by external fields, such as a gate voltage and a magnetic field. When the PH or TR symmetry is broken, the energy of a quasiparticle also shows the quadratic ω^2 , T^2 , and $(eV)^2$ dependences which enter through the real part of the self-energy.^{16,21}

It has recently been clarified that the energy shift of the quadratic order can be described in terms of three-point correlation functions. Extending Nozières' phenomenological Fermi-liquid theory,¹¹ the next-to-leading order terms for some transport coefficients have been derived for the $SU(N)$ Kondo model by Mora, Vitushinsky *et al*^{22–25}, and also for the Anderson model with²⁶ and without²⁷ a magnetic field by Filippone *et al* and Mora *et al*, respectively. Correspondingly, we have presented a fully microscopic description^{28–30} based on the standard many-body Green's-function approach of Yamada-Yosida, Shiba, and Yshimori,^{12–16} and have shown without assuming the PH nor TR symmetry that the order ω^2 , T^2 , and $(eV)^2$ real parts of the self-energy for the Anderson impurity are determined completely by the static three-body susceptibilities $\chi_{\sigma\sigma'\sigma''}^{[3]}$, defined in Eq. (3.7). We have also examined behaviors of the three-body susceptibilities of multilevel Anderson models in a wide range of impurity-electron fillings,^{31–33} using the numerical renormalization group (NRG) approach.^{34,35} Moreover, three-body correlations between electrons in quantum dots have recently been deduced successfully from nonlinear magnetoconductance measurements.³⁶

The current noise becomes one of the most important probes in recent years for exploring quantum fluctuations. The nonlinear current noise in the low-energy Fermi-liquid regime was studied, in early days, mainly in the situation where both the PH and TR symmetries are present.^{22,37–41} A major milestone has been achieved by Mora *et al*, without assuming the PH symmetry: formula for the next-leading order terms of the current noise has been derived for the $SU(N)$ Kondo model,²² and for the single-orbital Anderson model at zero magnetic field.²⁷ However, more general current-noise formulas applicable to the cases without the PH nor TR symmetry are necessary for studying nonequilibrium quantum fluctuations in a wide class of Kondo systems with various kinds of internal degrees of freedom.

The purpose of this paper is to present a complete microscopic description applicable to next-to-leading order Fermi-liquid behaviors of the current noise in a wide class of quantum impurity models. To this end, we investigate the low-energy asymptotic form of the Keldysh vertex function $\Gamma_{\sigma\sigma';\sigma'\sigma}^{\nu_1\nu_2;\nu_3\nu_4}(\omega,\omega';\omega'\omega)$ up to linear-order terms with respect to ω , ω' , T , and (eV) , for all branch-components $\nu_1, \nu_2, \nu_3, \nu_4$ of the Keldysh time-loop contour. The low-energy results of the vertex function satisfy the Ward identities with the Keldysh self-energy $\Sigma_{U,\sigma}^{\nu_4\nu_1}(\omega)$ which has been obtained up to terms of order ω^2 , $(eV)^2$ and T^2 . It ensures the current conservation is full filled for the next-to-leading order transport of the quasiparticles with a finite damping rate, and verifies the consistency in the Fermi-liquid description for nonlinear quan-

tum fluctuations.^{17,42}

In this paper, we also provide two alternative derivations for the Ward identities for the nonequilibrium Keldysh correlation functions at finite bias voltage and temperature. The first one is based on perturbation expansion in U , and the second one is deduced from a more general Ward-Takahashi identity for the Anderson impurity. We find that in the low-energy Fermi-liquid regime the imaginary parts of the Ward identities can be described in terms of the collision integrals,^{43,44} listed in TABLES V and VI: the fermionic collision integral $\mathcal{I}_K(\omega)$ describes the damping of a single quasiparticle, and the bosonic collision integrals $\mathcal{W}_K^{\text{ph}}(\omega)$ and $\mathcal{W}_K^{\text{pp}}(\omega)$ represent the damping of a single particle-hole pair and a single particle-particle pair, respectively. Furthermore, using the Ward identities, we find that the causal component of the vertex function $\Gamma_{\sigma\sigma';\sigma'\sigma}^{\bar{-};\bar{-}}(0,0;0,0)$ for $\sigma \neq \sigma'$ has an eV -linear real part, as shown in TABLE VIII.

The paper is organized as follows. In Sec. II, we describe the definition of the steady-state averages for the current and current fluctuations through the Anderson impurity at finite bias voltage. In Sec. III, we introduce the Fermi-liquid parameters necessary for describing low-energy properties up to the next-leading order, and demonstrated how the asymptotic form of the retarded Green's function can be expressed in terms of these parameters. In Sec. IV, we discuss some properties of the nonlinear current noise in the Fermi-liquid regime, leaving the derivation of the formula to the last part of this paper. In Sec. V, we provide a perturbative derivation of the Ward identities for the Keldysh Green's functions at finite eV and T . In Sec. VI and Appendix B, the nonequilibrium Ward-Takahashi identity is derived from the equation of continuity, and the three-point vertex functions are introduced in order to extract systematically the symmetrized vertex components with respect to the Keldysh time-loop branches. In Sec. VII, we show that the imaginary part of the Keldysh self-energies can be described by the fermionic collision integral in the Fermi-liquid regime, and introduce the bosonic collision integrals for the particle-hole pair and particle-particle pair excitations. In Sec. VIII and Appendix C, we calculate the low-energy asymptotic form of the Keldysh vertex functions, and show that the imaginary parts of the Ward identities are full filled through the relations between the fermionic and bosonic collision integrals. In Sec. IX, using the low-energy asymptotic form of the Keldysh vertex functions and self-energies, the nonlinear current-noise formula is derived up to terms order $|eV|^3$ at $T = 0$. Summary is given in Sec. X.

II. FORMULATION

A. Anderson impurity model

We study low-energy transport of quantum impurities in the Fermi-liquid regime over a wide range of electron

fillings, using a multilevel Anderson model coupled to two different reservoirs on the left (L) and right (R): $\mathcal{H} = \mathcal{H}_d + \mathcal{H}_c + \mathcal{H}_T$,

$$\mathcal{H}_d = \sum_{\sigma=1}^N \epsilon_{d\sigma} n_{d\sigma} + \frac{1}{2} \sum_{\sigma \neq \sigma'} U n_{d\sigma} n_{d\sigma'}, \quad (2.1a)$$

$$\mathcal{H}_c = \sum_{j=L,R} \sum_{\sigma=1}^N \int_{-D}^D d\xi \xi c_{\xi j \sigma}^\dagger c_{\xi j \sigma}, \quad (2.1b)$$

$$\mathcal{H}_T = - \sum_{j=L,R} \sum_{\sigma=1}^N v_j \left(\psi_{j\sigma}^\dagger d_\sigma + d_\sigma^\dagger \psi_{j\sigma} \right). \quad (2.1c)$$

Here, d_σ^\dagger for $\sigma = 1, 2, \dots, N$ creates an impurity electron with energy $\epsilon_{d\sigma}$. The operator $n_{d\sigma} = d_\sigma^\dagger d_\sigma$ represents the occupation number, and U is the Coulomb interaction between electrons in the different levels. For $N = 2$, this Hamiltonian corresponds to the usual spin-1/2 Anderson model. In this paper, we will hereafter cite the internal σ degrees of freedom as ‘*spin*’ also for $N > 2$, for simplicity. Conduction electrons with energy ξ in each of the two bands on the left and right are normalized such that $\{c_{\xi j \sigma}, c_{\xi' j' \sigma'}^\dagger\} = \delta_{jj'} \delta_{\sigma\sigma'} \delta(\xi - \xi')$ for $j = L, R$. The linear combination of these continuous states, $\psi_{j\sigma} \equiv \int_{-D}^D d\xi \sqrt{\rho_c} c_{\xi j \sigma}$ with $\rho_c = 1/(2D)$, couples to the discrete impurity level with the same σ via a tunnel matrix element v_j . It determines the width of the resonance as $\Delta \equiv \Gamma_L + \Gamma_R$ with $\Gamma_j = \pi \rho_c v_j^2$. Specifically, we consider the parameter region, where the relevant energy scales are much smaller than the half band width D , i.e. $\max(U, \Delta, |\epsilon_{d\sigma}|, |\omega|, T, |eV|) \ll D$.

In this paper, we study nonlinear fluctuations of the current $\hat{J}_{j,\sigma}$ through a quantum dot in the low-energy Fermi-liquid regime:

$$\hat{J}_{L,\sigma} = -i v_L \left(\psi_{L\sigma}^\dagger d_\sigma - d_\sigma^\dagger \psi_{L\sigma} \right), \quad (2.2a)$$

$$\hat{J}_{R,\sigma} = +i v_R \left(\psi_{R\sigma}^\dagger d_\sigma - d_\sigma^\dagger \psi_{R\sigma} \right). \quad (2.2b)$$

Here, $\hat{J}_{L,\sigma}$ represents the current following from the left lead to the dot, and $\hat{J}_{R,\sigma}$ represents the current from the dot to the right lead. These currents satisfy the conservation law which follows from the Heisenberg equation

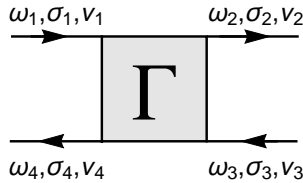


FIG. 1. Vertex correction $\Gamma_{\sigma_1 \sigma_2; \sigma_3 \sigma_4}^{\nu_1 \nu_2; \nu_3 \nu_4}(\omega_1, \omega_2; \omega_3, \omega_4)$ between the electron in the levels σ_i ($i = 1, 2, 3, 4$). The superscript ν_i specifies the branches of Keldysh time-loop contour, for which $\nu = -$ and $+$ represent the forward and return paths, respectively. The frequencies are conserved such that $\omega_1 + \omega_3 = \omega_2 + \omega_4$.

motion, $\partial n_{d\sigma} / \partial t = -i [n_{d\sigma}, \mathcal{H}]$, and preserves the spin σ ,

$$\frac{\partial n_{d\sigma}}{\partial t} + \hat{J}_{R,\sigma} - \hat{J}_{L,\sigma} = 0. \quad (2.3)$$

These two current operators can also be classified in to the symmetrized part

$$\hat{J}_\sigma \equiv \frac{\Gamma_L \hat{J}_{R,\sigma} + \Gamma_R \hat{J}_{L,\sigma}}{\Gamma_L + \Gamma_R}, \quad (2.4)$$

and the difference $\hat{J}_{R,\sigma} - \hat{J}_{L,\sigma}$.

B. Average current and current fluctuations

We consider a nonequilibrium steady state under a finite bias voltage $eV \equiv \mu_L - \mu_R$, applied between the two leads by setting the chemical potentials of the left and right leads to be μ_L and μ_R , respectively. The statistical density operator which describes the steady state in this situation can be described, using the time evolution along the Keldysh time-loop contour.⁴⁵

Specifically, the steady-state average of the electric current $J \equiv e \sum_\sigma \langle \hat{J}_\sigma \rangle$ can be expressed in the following form,^{17,46}

$$J = \frac{e}{h} \sum_\sigma \int_{-\infty}^{\infty} d\omega [f_L(\omega) - f_R(\omega)] \mathcal{T}_\sigma(\omega). \quad (2.5)$$

Here, $\mathcal{T}_\sigma(\omega)$ is the transmission probability that is deter-

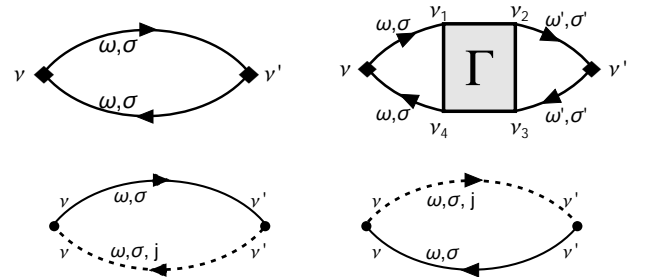


FIG. 2. Feynman diagrams for the current-current correlation function $\int_{-\infty}^{\infty} dt \mathcal{K}_{\sigma'\sigma}^{\nu'\nu}(t, 0)$ of symmetrized current fluctuations \hat{J}_σ defined in Eq. (2.4) with $\mathcal{K}_{\sigma'\sigma}^{+-}(t, 0) \equiv -i \langle \delta \hat{J}_{\sigma'}(t) \delta \hat{J}_\sigma(0) \rangle$ and $\mathcal{K}_{\sigma'\sigma}^{-+}(t, 0) \equiv -i \langle \delta \hat{J}_\sigma(0) \delta \hat{J}_{\sigma'}(t) \rangle$. The solid line represents the Keldysh Green's function $G_{\sigma'}^{\nu'\nu}(\omega)$ of the quantum dot. The black diamond (\blacklozenge) in the two diagrams on the top represents a matrix the bare current vertex $\lambda_{\text{sym}}^\alpha(\epsilon, \epsilon)$ for $\alpha = \nu, \nu'$ defined in Eq. (6.12). The dashed line in the last two diagrams at the bottom denotes the Green's function $g_{j\sigma}^{\nu'\nu}(\omega)$ of the isolated lead on $j = L$ and R .

TABLE I. Low-energy expansion of dJ/dV up to terms of order T^2 and $(eV)^2$ for $\Gamma_L = \Gamma_R = \Delta/2$ and $\mu_L = -\mu_R = eV/2$.

$$\begin{aligned}
\frac{dJ}{dV} &= \frac{e^2}{h} \sum_{\sigma} \left[\sin^2 \delta_{\sigma} - c_{T,\sigma} (\pi T)^2 - c_{V,\sigma} (eV)^2 + \dots \right], \\
c_{T,\sigma} &\equiv \frac{\pi^2}{3} \left[- \left(\chi_{\sigma\sigma}^2 + 2 \sum_{\sigma'(\neq\sigma)} \chi_{\sigma\sigma'}^2 \right) \cos 2\delta_{\sigma} + \frac{1}{2\pi} \left(\chi_{\sigma\sigma\sigma}^{[3]} + \sum_{\sigma'(\neq\sigma)} \chi_{\sigma\sigma'\sigma'}^{[3]} \right) \sin 2\delta_{\sigma} \right], \\
c_{V,\sigma} &\equiv \frac{\pi^2}{4} \left[- \left(\chi_{\sigma\sigma}^2 + 5 \sum_{\sigma'(\neq\sigma)} \chi_{\sigma\sigma'}^2 \right) \cos 2\delta_{\sigma} + \frac{1}{2\pi} \left(\chi_{\sigma\sigma\sigma}^{[3]} + 3 \sum_{\sigma'(\neq\sigma)} \chi_{\sigma\sigma'\sigma'}^{[3]} \right) \sin 2\delta_{\sigma} \right].
\end{aligned}$$

TABLE II. Low-bias expansion of the noise $S_{\text{noise}}^{\text{QD}}$, obtained at $T = 0$ up to terms of order $|eV|^3$ for $\Gamma_L = \Gamma_R = \Delta/2$ and $\mu_L = -\mu_R = eV/2$.

$$\begin{aligned}
S_{\text{noise}}^{\text{QD}} &= \frac{2e^2}{h} |eV| \sum_{\sigma} \left[\frac{1}{4} \sin^2 2\delta_{\sigma} + c_{S,\sigma} (eV)^2 + \dots \right], \\
c_{S,\sigma} &\equiv \frac{\pi^2}{12} \left[\cos 4\delta_{\sigma} \chi_{\sigma\sigma}^2 + (2 + 3 \cos 4\delta_{\sigma}) \sum_{\sigma'(\neq\sigma)} \chi_{\sigma\sigma'}^2 + 4 \sum_{\sigma'(\neq\sigma)} \cos 2\delta_{\sigma} \cos 2\delta_{\sigma'} \chi_{\sigma\sigma'}^2 \right. \\
&\quad \left. + 3 \sum_{\sigma'(\neq\sigma)} \sum_{\sigma''(\neq\sigma,\sigma')} \sin 2\delta_{\sigma} \sin 2\delta_{\sigma'} \chi_{\sigma\sigma''} \chi_{\sigma'\sigma''} - \frac{1}{4\pi} \left(\chi_{\sigma\sigma\sigma}^{[3]} + 3 \sum_{\sigma'(\neq\sigma)} \chi_{\sigma\sigma'\sigma'}^{[3]} \right) \sin 4\delta_{\sigma} \right]
\end{aligned}$$

mined by the retarded Green's function $G_{\sigma}^r(\omega)$,

$$\mathcal{T}_{\sigma}(\omega) = - \frac{4\Gamma_L\Gamma_R}{\Gamma_L + \Gamma_R} \text{Im} G_{\sigma}^r(\omega), \quad (2.6)$$

$$\begin{aligned}
G_{\sigma}^r(\omega) &\equiv -i \int_0^{\infty} dt e^{i(\omega+i0^+)t} \langle \{d_{\sigma}(t), d_{\sigma}^{\dagger}(0)\} \rangle \\
&= \frac{1}{\omega - \epsilon_{d\sigma} + i\Delta - \Sigma_{U,\sigma}^r(\omega)}. \quad (2.7)
\end{aligned}$$

Effects of the Coulomb repulsion on the average current J enters through the retarded self-energy $\Sigma_{U,\sigma}^r(\omega)$ which also depends on eV and temperature T . In Eq. (2.5), $f_j(\omega) \equiv f(\omega - \mu_j)$ with $f(\omega) \equiv [e^{\omega/T} + 1]^{-1}$ the Fermi distribution function. We will choose the chemical potentials μ_L and μ_R in a way such that

$$\mu_L = \alpha_L eV, \quad \mu_R = -\alpha_R eV, \quad \alpha_L + \alpha_R = 1. \quad (2.8)$$

The parameters α_L and α_R specify how the bias is applied relative to the Fermi level at equilibrium which is chosen to be the origin of one-particle energies $E_F = 0$.

The main subject of this paper is low-energy behavior of current noise of a quantum dot,⁴²

$$S_{\text{noise}}^{\text{QD}} = e^2 \sum_{\sigma\sigma'} \int_{-\infty}^{\infty} dt \langle \delta \hat{J}_{\sigma}(t) \delta \hat{J}_{\sigma'}(0) + \delta \hat{J}_{\sigma'}(0) \delta \hat{J}_{\sigma}(t) \rangle. \quad (2.9)$$

Here, $\delta \hat{J}_{\sigma}(t) \equiv \hat{J}_{\sigma}(t) - \langle \hat{J}_{\sigma}(0) \rangle$ represents fluctuations of the symmetrized current. The current-current correlation function $S_{\text{noise}}^{\text{QD}}$ depends not only the single-quasiparticle properties that enter through $G_{\sigma}^r(\omega)$ but

also on the collision term of two quasiparticles. It is described microscopically by the Keldysh vertex corrections $\Gamma_{\sigma\sigma';\sigma'\sigma}^{\nu_1\nu_2;\nu_3\nu_4}(\omega, \omega'; \omega'\omega)$, illustrated in Fig. 1.

We calculate $S_{\text{noise}}^{\text{QD}}$ later in Sec. IX up to terms of order $(eV)^3$, taking into account all multiple collision processes described in Fig. 2. Before giving the proof, the results of the average current and the current noise are summarized in TABLES I and II, respectively. The expansion coefficients $c_{T,\sigma}$, $c_{V,\sigma}$, and $c_{S,\sigma}$ of the next-leading order terms of the low-energy expansion can be expressed in terms of the static correlation functions $\chi_{\sigma\sigma'}$ and $\chi_{\sigma\sigma'\sigma''}^{[3]}$, defined with respect to the equilibrium ground state. We describe the definition of these static correlation functions, which also determine the behavior of the self-energy and vertex corrections, in the next section. We also present, in Sec. IV, some application examples of the transport formulas listed in TABLES I and II.

III. MICROSCOPIC FERMI-LIQUID THEORY

The main subject of this paper, i.e. low-energy behavior of the current noise, is based on the microscopic Fermi-liquid theory for which the roles of the three-body correlations have been clarified recently. In this section, we describe the latest version of FL theory for the retarded Green's function and the causal vertex function $\Gamma_{\sigma\sigma';\sigma'\sigma}^{-;-}(\omega, \omega'; \omega', \omega)$.

A. Fermi-liquid parameters

Low-energy transport in the Fermi-liquid regime are mostly determined by a set of the parameters which can be derived from the retarded Green's function with respect to the equilibrium ground state $G_{\text{eq},\sigma}^r(\omega) \equiv G_{\sigma}^r(\omega)|_{T=\epsilon V=0}$. In particular, the behavior of the retarded self-energy $\Sigma_{\text{eq},\sigma}^r(\omega)$ at small frequencies ω plays a central role,

$$\Sigma_{\text{eq},\sigma}^r(\omega) \equiv \Sigma_{U,\sigma}^r(\omega)|_{T=\epsilon V=0}. \quad (3.1)$$

The density of states of the impurity electrons at equilibrium is given by

$$\rho_{d\sigma}(\omega) \equiv -\frac{1}{\pi} \text{Im} G_{\text{eq},\sigma}^r(\omega). \quad (3.2)$$

We will write the value at the Fermi energy $\omega = 0$ as $\rho_{d\sigma} \equiv \rho_{d\sigma}(0)$ hereafter, suppressing the frequency argument. It can also be expressed, as $\rho_{d\sigma} = \sin^2 \delta_{\sigma}/\pi\Delta$, in terms of the phase shift δ_{σ} , defined by

$$\delta_{\sigma} = \cot^{-1} \left[\frac{\epsilon_{d\sigma} + \Sigma_{\text{eq},\sigma}^r(0)}{\Delta} \right]. \quad (3.3)$$

At zero temperature $T = 0$, the Friedel sum rule relates the phase shift to the occupation number of the impurity level $\langle n_{d\sigma} \rangle_{\text{eq}} = \delta_{\sigma}/\pi$. It can also be calculated from the free energy $\Omega \equiv -T \log [\text{Tr} e^{-\mathcal{H}/T}]$,

$$\langle n_{d\sigma} \rangle_{\text{eq}} = \frac{\partial \Omega}{\partial \epsilon_{d\sigma}}. \quad (3.4)$$

Fermi-liquid corrections beyond the constant energy shift $\Sigma_{\text{eq},\sigma}^r(0)$ can be described in terms of the linear susceptibilities, as shown by Yamada-Yosida and Shiba:^{12,14,15}

$$\begin{aligned} \chi_{\sigma\sigma'} &\equiv \int_0^{1/T} d\tau \langle \delta n_{d\sigma}(\tau) \delta n_{d\sigma'} \rangle_{\text{eq}} \\ &= -\frac{\partial^2 \Omega}{\partial \epsilon_{d\sigma'} \partial \epsilon_{d\sigma}} = -\frac{\partial \langle n_{d\sigma} \rangle_{\text{eq}}}{\partial \epsilon_{d\sigma'}} \\ &\xrightarrow{T \rightarrow 0} -\frac{1}{\pi} \frac{\partial \delta_{\sigma}}{\partial \epsilon_{d\sigma'}} = \rho_{d\sigma} \tilde{\chi}_{\sigma\sigma'}. \end{aligned} \quad (3.5)$$

Here, $\delta n_{d\sigma} \equiv n_{d\sigma} - \langle n_{d\sigma} \rangle_{\text{eq}}$, and the reciprocal relations hold between the components: $\chi_{\sigma\sigma'} = \chi_{\sigma'\sigma}$. The last line of Eq. (3.5) follows from the Friedel sum rule with the renormalized parameters $\tilde{\chi}_{\sigma\sigma'}$, defined by

$$\tilde{\chi}_{\sigma\sigma'} \equiv \delta_{\sigma\sigma'} + \frac{\partial \Sigma_{\text{eq},\sigma}^r(0)}{\partial \epsilon_{d\sigma'}}. \quad (3.6)$$

Furthermore, the next-leading-order FL corrections have been shown recently to be described in terms of the static nonlinear susceptibilities,²⁶⁻³⁰

$$\begin{aligned} \chi_{\sigma_1\sigma_2\sigma_3}^{[3]} &\equiv -\int_0^{\frac{1}{T}} d\tau_3 \int_0^{\frac{1}{T}} d\tau_2 \langle T_{\tau} \delta n_{d\sigma_3}(\tau_3) \delta n_{d\sigma_2}(\tau_2) \delta n_{d\sigma_1} \rangle_{\text{eq}} \\ &= -\frac{\partial^3 \Omega}{\partial \epsilon_{d\sigma_1} \partial \epsilon_{d\sigma_2} \partial \epsilon_{d\sigma_3}} = \frac{\partial \chi_{\sigma_2\sigma_3}}{\partial \epsilon_{d\sigma_1}}, \end{aligned} \quad (3.7)$$

where T_{τ} is the imaginary-time ordering operator. These three-body correlation functions become finite when the PH or TR symmetry is broken. In such situations, $\chi_{\sigma_1\sigma_2\sigma_3}^{[3]}$ contribute to the next-leading-order terms of the transport coefficients, together with the derivative of the density of states $\rho'_{d\sigma}$:

$$\rho'_{d\sigma} \equiv \left. \frac{\partial \rho_{d\sigma}(\omega)}{\partial \omega} \right|_{\omega=0} = -\frac{\partial \rho_{d\sigma}}{\partial \epsilon_{d\sigma}} = \frac{\sin 2\delta_{\sigma}}{\Delta} \chi_{\sigma\sigma}. \quad (3.8)$$

The three-body correlations are also related to the second derivative of the real part of the retarded self-energy which determines the higher-order energy shift of quasiparticles, as shown later in Sec. III C.

B. Fermi-liquid relations

Why can the transport coefficients are determined by the static linear and nonlinear susceptibilities at low energies as listed in TABLES I and II while they are originally defined in terms of time-dependent correlation functions as Eqs. (2.5) and (2.9)? It is owing to the current conservation law described in Eq. (2.3), from which the Ward identity can be deduced for various kinds of the Green's functions. The Ward identities for the Matsubara Green's function have systematically been explored by Yoshimori¹⁶ in the limit of $T \rightarrow 0$, which can be rewritten into the following form as a relation between the causal self-energy $\Sigma_{\text{eq},\sigma}^{--}$ and vertex function $\Gamma_{\sigma\sigma';\sigma'\sigma}^{--;--}$ of the zero-temperature formalism,

$$\delta_{\sigma\sigma'} \frac{\partial \Sigma_{\text{eq},\sigma}^{--}(\omega)}{\partial \omega} + \frac{\partial \Sigma_{\text{eq},\sigma}^{--}(\omega)}{\partial \epsilon_{d\sigma'}} = -\Gamma_{\sigma\sigma';\sigma'\sigma}^{--;--}(\omega, 0; 0, \omega) \rho_{d\sigma'}. \quad (3.9)$$

At $T = 0$, the retarded self-energy is related to the causal one, as $\Sigma_{\text{eq},\sigma}^r(\omega) = \theta(\omega) \Sigma_{\text{eq},\sigma}^{--}(\omega) + \theta(-\omega) \{ \Sigma_{\text{eq},\sigma}^{--}(\omega) \}^*$ with $\theta(\omega)$ the Heaviside step function.

The diagonal $\sigma = \sigma'$ components of the identity Eq. (3.9) gives the Yamada-Yosida relation between the renormalization factor z_{σ} and the enhancement factor for the susceptibility $\tilde{\chi}_{\sigma\sigma}$ at $\omega = 0$,^{12,16}

$$\frac{1}{z_{\sigma}} \equiv 1 - \left. \frac{\partial \Sigma_{\text{eq},\sigma}^r(\omega)}{\partial \omega} \right|_{\omega=0} = \tilde{\chi}_{\sigma\sigma}, \quad (3.10)$$

which follows from the fact that $\Gamma_{\sigma\sigma';\sigma'\sigma}^{--;--}(0, 0; 0, 0) = 0$. Furthermore, it also follows from Eq. (3.10) that the renormalized density of states $\tilde{\rho}_{d\sigma}$ is identical to $\chi_{\sigma\sigma}$,

$$\tilde{\rho}_{d\sigma} \equiv \frac{\rho_{d\sigma}}{z_{\sigma}} = \chi_{\sigma\sigma}. \quad (3.11)$$

Therefore, the T -linear specific heat of the impurity electrons can also be written in terms of the diagonal susceptibility, as $\mathcal{C}_{\text{imp}} = \frac{\pi^2}{3} \sum_{\sigma} \chi_{\sigma\sigma} T$.

Similarly, at $\omega = 0$, the off-diagonal $\sigma \neq \sigma'$ components of Eq. (3.9) can be written, as

$$\tilde{\chi}_{\sigma\sigma'} = -\Gamma_{\sigma\sigma';\sigma'\sigma}^{--;--}(0, 0; 0, 0) \rho_{d\sigma'}. \quad (3.12)$$

It also corresponds to the residual interaction between quasiparticles $\tilde{U}_{\sigma\sigma'}$ which is proportional to the off-diagonal susceptibilities for $\sigma \neq \sigma'$,⁴⁷

$$\tilde{U}_{\sigma\sigma'} \equiv z_\sigma z_{\sigma'} \Gamma_{\sigma\sigma';\sigma'\sigma}^{--;--}(0,0;0,0) = \frac{-\chi_{\sigma\sigma'}}{\chi_{\sigma\sigma} \chi_{\sigma'\sigma'}}. \quad (3.13)$$

Furthermore, a generalized form of the Wilson ratio $R_{\sigma\sigma'}$, which is applicable to the systems without the PH or TR symmetry, is given by a dimensionless residual interaction,

$$R_{\sigma\sigma'} - 1 \equiv \sqrt{\tilde{\rho}_{d\sigma} \tilde{\rho}_{d\sigma'}} \tilde{U}_{\sigma\sigma'} = \frac{-\chi_{\sigma\sigma'}}{\sqrt{\chi_{\sigma\sigma} \chi_{\sigma'\sigma'}}}. \quad (3.14)$$

C. Higher-order Fermi-liquid corrections

The renormalized parameters described in the above are related to the first derivatives of the self-energy. In order to explore next-leading-order behaviors of the transport coefficients, information about order ω^2 , T^2 , and $(eV)^2$ terms of $\Sigma_{U,\sigma}^r(\omega)$ are also necessary.^{26,28,29} Similarly, the low-energy expansion of $\Gamma_{\sigma\sigma';\sigma'\sigma}^{--;--}(\omega, \omega'; \omega', \omega)$ up to linear-order terms with respect to frequencies, T , and eV also includes alternative information. Here we briefly summarize the recent FL description for these high-order corrections, including some extensions carried out in this work. These corrections are also essential for our purpose to explore the low-energy behavior of the current noise.

1. ω^2 dependence of $\Sigma_{U,\sigma}^{--}$

The antisymmetry property of the vertex function imposes a strong restriction on the two-quasiparticle collision processes,

$$\begin{aligned} \Gamma_{\sigma_1\sigma_2;\sigma_3\sigma_4}^{--;--}(\omega_1, \omega_2; \omega_3, \omega_4) &= -\Gamma_{\sigma_3\sigma_2;\sigma_1\sigma_4}^{--;--}(\omega_3, \omega_2; \omega_1, \omega_4) \\ &= \Gamma_{\sigma_3\sigma_4;\sigma_1\sigma_2}^{--;--}(\omega_3, \omega_4; \omega_1, \omega_2) = -\Gamma_{\sigma_1\sigma_4;\sigma_3\sigma_2}^{--;--}(\omega_1, \omega_4; \omega_3, \omega_2). \end{aligned} \quad (3.15)$$

The diagonal $\sigma_1 = \sigma_2 = \sigma_3 = \sigma_4$ components of the causal vertex vanish $\Gamma_{\sigma\sigma;\sigma\sigma}^{--;--}(0,0;0,0) = 0$ at zero frequencies, and it has been used for the proof of Eq. (3.10).¹⁶ We have shown in the previous paper that the ω -linear real part of the diagonal vertex components also vanish at zero frequencies at $T = eV = 0$,²⁹ as

$$\left. \frac{\partial}{\partial \omega} \text{Re} \Gamma_{\sigma\sigma;\sigma\sigma}^{--;--}(\omega, 0; 0, \omega) \right|_{\omega \rightarrow 0} = 0. \quad (3.16)$$

Order ω^2 real part of the self-energy can be deduced from this information, taking a derivative of the both sides of Eq. (3.9) with respect to ω ,

$$\left. \frac{\partial^2}{\partial \omega^2} \text{Re} \Sigma_{\text{eq},\sigma}^{--}(\omega) \right|_{\omega \rightarrow 0} = \frac{\partial^2 \Sigma_{\text{eq},\sigma}^r(0)}{\partial \epsilon_{d\sigma}^2} = \frac{\partial \tilde{\chi}_{\sigma\sigma}}{\partial \epsilon_{d\sigma}}. \quad (3.17)$$

It shows that the ω^2 real part is determined by the intra-level component of the three-body correlation function $\chi_{\sigma\sigma\sigma}^{[3]}$. Physically, this term of the self-energy induces higher-order energy shifts for single-quasiparticle excitations.

It can also be deduced from Eq. (3.17) that the diagonal $\sigma = \sigma'$ components of the vertex function is pure imaginary up to linear order with respect to ω and ω' , and takes the following form at $T = eV = 0$,²⁹

$$\Gamma_{\sigma\sigma';\sigma'\sigma}^{--;--}(\omega, \omega'; \omega', \omega) \rho_{d\sigma}^2 = i\pi \sum_{\sigma'(\neq\sigma)} \chi_{\sigma\sigma'}^2 |\omega - \omega'| + \dots. \quad (3.18)$$

Furthermore, using also the identity Eq. (3.9), the off-diagonal $\sigma \neq \sigma'$ component can be deduced at $T = eV = 0$, as

$$\begin{aligned} \Gamma_{\sigma\sigma';\sigma'\sigma}^{--;--}(\omega, \omega'; \omega', \omega) \rho_{d\sigma} \rho_{d\sigma'} \\ = -\chi_{\sigma\sigma'} + \rho_{d\sigma} \frac{\partial \tilde{\chi}_{\sigma\sigma'}}{\partial \epsilon_{d\sigma}} \omega + \rho_{d\sigma'} \frac{\partial \tilde{\chi}_{\sigma'\sigma}}{\partial \epsilon_{d\sigma'}} \omega' \\ + i\pi \chi_{\sigma\sigma'}^2 \left(|\omega - \omega'| - |\omega + \omega'| \right) + \dots. \end{aligned} \quad (3.19)$$

Note that the imaginary parts of the vertex functions, which show non-analytic $|\omega - \omega'|$ and $|\omega + \omega'|$ dependence, determine the damping of the two-quasiparticle collisions.^{16,18,48,49} In this paper, we also calculate all the Keldysh vertex components at finite temperature and bias voltage up to terms of order T and eV in Sec. VIII and Appendix C.

2. T^2 dependence of $\Sigma_{U,\sigma}^{--}$

We have described in the previous paper that order T^2 term of the retarded self-energy $\Sigma_{\text{eq},\sigma}^r$ can be expressed in terms of the derivative of the causal vertex at $T = 0$,²⁹ rewriting the proof of Yamada-Yosida¹⁴ in the following form,

$$\Sigma_{\text{eq},\sigma}^r(0) - \Sigma_{\text{eq},\sigma}^r(0)|_{T=0} = \frac{(\pi T)^2}{6} \lim_{\omega \rightarrow 0^+} \Psi_{\sigma}^{--}(\omega) + \dots, \quad (3.20)$$

$$\Psi_{\sigma}^{--}(\omega) \equiv \lim_{\omega' \rightarrow 0} \frac{\partial}{\partial \omega'} \sum_{\sigma'} \Gamma_{\sigma\sigma';\sigma'\sigma}^{--;--}(\omega, \omega'; \omega', \omega) \rho_{d\sigma'}(\omega'). \quad (3.21)$$

The derivative with respect to ω' in the right-hand side can explicitly be carried out, using the results of the low-energy asymptotic form Eqs. (3.18) and (3.19) at finite ω , and then the coefficient for order T^2 term follows by taking the limit $\omega \rightarrow 0$,

$$\lim_{\omega \rightarrow 0} \Psi_{\sigma}^{--}(\omega) = \frac{1}{\rho_{d\sigma}} \sum_{\sigma'(\neq\sigma)} \left[\frac{\partial \chi_{\sigma\sigma'}}{\partial \epsilon_{d\sigma'}} - i 3\pi \frac{1}{\rho_{d\sigma}} \chi_{\sigma\sigma'}^2 \text{sgn}(\omega) \right]. \quad (3.22)$$

The non-analytic $\text{sgn}(\omega)$ dependence, appearing in the right-hand side, reflects the branch cut of the vertex function $\Gamma_{\sigma\sigma';\sigma'\sigma}^-(\omega, \omega'; \omega', \omega)$ along the lines $|\omega - \omega'| = 0$ and $|\omega + \omega'| = 0$ in the ω - ω' plane.^{16,29,48,49}

3. Retarded self-energy up to order ω^2 , T^2 , and $(eV)^2$

Low-energy behavior of the retarded self-energy under a finite bias voltage has been determined previously

$$\begin{aligned} \text{Re } \Sigma_{U,\sigma}^r(\omega) = & \Sigma_{\text{eq},\sigma}^r(0) + (1 - \tilde{\chi}_{\sigma\sigma})\omega + \frac{1}{2} \frac{\partial \tilde{\chi}_{\sigma\sigma}}{\partial \epsilon_{d\sigma}} \omega^2 + \frac{1}{6} \frac{1}{\rho_{d\sigma}} \sum_{\sigma'(\neq\sigma)} \frac{\partial \chi_{\sigma\sigma'}}{\partial \epsilon_{d\sigma'}} \left[\frac{3\Gamma_L\Gamma_R}{(\Gamma_L + \Gamma_R)^2} (eV)^2 + (\pi T)^2 \right] \\ & - \sum_{\sigma'(\neq\sigma)} \tilde{\chi}_{\sigma\sigma'} \alpha_{\text{sh}} eV + \sum_{\sigma'(\neq\sigma)} \frac{\partial \tilde{\chi}_{\sigma\sigma'}}{\partial \epsilon_{d\sigma}} \alpha_{\text{sh}} eV \omega + \frac{1}{2} \sum_{\sigma'(\neq\sigma)} \sum_{\sigma''(\neq\sigma)} \frac{\partial \tilde{\chi}_{\sigma\sigma'}}{\partial \epsilon_{d\sigma''}} \alpha_{\text{sh}}^2 (eV)^2 + \dots, \end{aligned} \quad (3.23a)$$

$$\text{Im } \Sigma_{U,\sigma}^r(\omega) = -\frac{\pi}{2} \frac{1}{\rho_{d\sigma}} \sum_{\sigma'(\neq\sigma)} \chi_{\sigma\sigma'}^2 \left[(\omega - \alpha_{\text{sh}} eV)^2 + \frac{3\Gamma_L\Gamma_R}{(\Gamma_L + \Gamma_R)^2} (eV)^2 + (\pi T)^2 \right] + \dots, \quad (3.23b)$$

and $\alpha_{\text{sh}} \equiv (\alpha_L\Gamma_L - \alpha_R\Gamma_R)/(\Gamma_L + \Gamma_R)$. The parameters α_L and α_R are defined in Eq. (2.8), and specify the position of the chemical potentials of the left and right leads, respectively, with a constraint $\alpha_L + \alpha_R = 1$. For multilevel quantum dots $N > 2$, the nonlinear susceptibilities $\chi_{\sigma\sigma'\sigma''}^{[3]}$ between electrons occupying three different levels ($\sigma \neq \sigma' \neq \sigma'' \neq \sigma$) give finite contributions to order $(eV)^2$ part of $\text{Re } \Sigma_{U,\sigma}^r(\omega)$ in the case where $\alpha_{\text{sh}} \neq 0$. In contrast, for $\alpha_{\text{sh}} = 0$, the correlations $\chi_{\sigma\sigma'\sigma'}^{[3]}$ between three electrons in two different levels ($\sigma \neq \sigma'$) determine order $(eV)^2$ and T^2 terms of the real part. Contributions of these three-body correlation functions play an important role when the PH or TR symmetry is broken by external fields, such as gate voltages and magnetic fields.

IV. NONLINEAR CURRENT NOISE IN THE FERMI LIQUID REGIME

We describe here properties of the current noise in the Fermi-liquid regime, leaving the complete proof later in Sec. IX as the derivation needs precise information about the low-energy behavior of the Keldysh vertex corrections which we will show in Secs. V–VIII and Appendix C.

A. Conductance and thermal noise

We consider first the differential conductance dJ/dV that can be deduced up to terms of order T^2 and $(eV)^2$ from the Landauer-type formula Eq. (2.5), using the

up to terms of order $(eV)^2$ as well as order ω^2 and T^2 terms, mentioned above.^{30,32} We will describe alternative derivation later in Sec. V in an extended way, using the generalized Ward identity which we have obtained in the present work at finite eV and T . Here we present the low-energy asymptotic form of the retarded self-energy, which is extended to multilevel quantum dots with $N > 2$,

low-energy expansion of $\Sigma_{U,\sigma}^r(\omega)$ given in Eq. (3.23). Specifically, for symmetric junctions with $\Gamma_L = \Gamma_R$ and $\mu_L = -\mu_R = eV/2$, the asymptotic form spectral function is given by

$$\begin{aligned} -\Delta \text{Im } G_{\sigma}^r(\omega) = & \sin^2 \delta_{\sigma} + \pi \sin 2\delta_{\sigma} \chi_{\sigma\sigma} \omega \\ & + \pi^2 \left[\cos 2\delta_{\sigma} \left(\chi_{\sigma\sigma}^2 + \frac{1}{2} \sum_{\sigma'(\neq\sigma)} \chi_{\sigma\sigma'}^2 \right) - \frac{\sin 2\delta_{\sigma}}{2\pi} \chi_{\sigma\sigma\sigma}^{[3]} \right] \omega^2 \\ & + \frac{\pi^2}{3} \left[\frac{3}{2} \cos 2\delta_{\sigma} \sum_{\sigma'(\neq\sigma)} \chi_{\sigma\sigma'}^2 - \frac{\sin 2\delta_{\sigma}}{2\pi} \sum_{\sigma'(\neq\sigma)} \chi_{\sigma\sigma'\sigma'}^{[3]} \right] \\ & \times \left\{ \frac{3}{4} (eV)^2 + (\pi T)^2 \right\} + \dots. \end{aligned} \quad (4.1)$$

TABLE I shows the explicit expressions of the coefficients $c_{T,\sigma}$ and $c_{V,\sigma}$ for the next-leading order terms of dJ/eV , which are applicable to a wide class of quantum dots without the PH or TR symmetries:

$$\frac{dJ}{dV} = \frac{e^2}{h} \sum_{\sigma=1}^N \left[\sin^2 \delta_{\sigma} - c_{T,\sigma} (\pi T)^2 - c_{V,\sigma} (eV)^2 + \dots \right]. \quad (4.2)$$

The first two terms in the right-hand side of Eq. (4.2) correspond to the linear conductance. It also determines the thermal current noise at equilibrium, as it can be

deduced from the fluctuation-dissipation theorem,⁴²

$$S_{\text{noise}}^{\text{QD}} \Big|_{V=0} = 4T \frac{dJ}{dV} \Big|_{V=0} = \frac{4e^2}{h} T \sum_{\sigma} \left[\sin^2 \delta_{\sigma} - c_{T,\sigma} (\pi T)^2 + \dots \right]. \quad (4.3)$$

We will also describe a diagrammatic derivation of the equilibrium noise in the Fermi-liquid regime in Sec. IX A as a preparation for calculating nonlinear current noise at finite eV .

B. Nonlinear current noise

We will calculate $S_{\text{noise}}^{\text{QD}}$ up to terms of order $|eV|^3$ later in Sec. IX, using the diagrammatic representations shown in Fig. 2. In order to carry it out, the Keldysh Green's functions $G_{\sigma}^{\nu'\nu}(\omega)$ should also be expanded up to terms of order ω^2 and $(eV)^2$. Furthermore, all components of the Keldysh vertex function $\Gamma_{\sigma\sigma';\sigma'\sigma}^{\nu_1\nu_2;\nu_3\nu_4}(\omega, \omega'; \omega'\omega)$ are needed to be determined up to linear order terms with respect to ω , ω' and eV . Leaving all these details in Secs. V–VIII, we discuss here the result of the nonlinear current noise, is obtained for symmetric junctions with $\Gamma_L = \Gamma_R$ and $\mu_L = -\mu_R = eV/2$:

$$S_{\text{noise}}^{\text{QD}} \Big|_{T=0} = \frac{2e^2}{h} |eV| \sum_{\sigma} \left[\frac{\sin^2 2\delta_{\sigma}}{4} + c_{S,\sigma} (eV)^2 + \dots \right]. \quad (4.4)$$

As shown in TABLE II, the coefficient $c_{S,\sigma}$ can be expressed in terms of the linear and nonlinear susceptibilities similarly to the other coefficients $c_{T,\sigma}$ and $c_{V,\sigma}$. Therefore, the nonlinear Fano factor which is defined as the ratio of order $(eV)^3$ current noise to the nonlinear current of the same order^{22,27} can be expressed in the following form,

$$F_K \equiv \lim_{|eV| \rightarrow 0} \frac{S_{\text{noise}}^{\text{QD}} - \frac{2e^2|eV|}{h} \sum_{\sigma} \frac{\sin^2 2\delta_{\sigma}}{4}}{-2|e| \left(J - \frac{e^2V}{h} \sum_{\sigma} \sin^2 \delta_{\sigma} \right)} = \frac{\sum_{\sigma} c_{S,\sigma}}{\sum_{\sigma} c_{V,\sigma}/3}. \quad (4.5)$$

1. Current noise in $SU(N)$ symmetric case

In a special case where the impurity level becomes degenerate $\epsilon_{d\sigma} \equiv \epsilon_d$ for all components $\sigma = 1, 2, \dots, N$, the Hamiltonian \mathcal{H} given in Eq. (2.1) has the $SU(N)$ symmetry. In this case, each of the levels equally contributes to the transport, and thus the nonlinear Fano Factor takes the form $F_K = c_{S,\sigma}/(c_{V,\sigma}/3)$, with the coefficients that

become independent of σ ,

$$c_{S,\sigma} = \frac{\pi^2 \chi_{\sigma\sigma}^2}{12} \left[\cos 4\delta + \left\{ 4 + 5 \cos 4\delta + \frac{3}{2} (1 - \cos 4\delta)(N-2) \right\} \frac{\tilde{K}^2}{N-1} - \cos 2\delta \left\{ \Theta_{\text{I}} + 3(N-1)\Theta_{\text{II}} \right\} \right], \quad (4.6)$$

$$c_{V,\sigma} = \frac{\pi^2 \chi_{\sigma\sigma}^2}{4} \left[- \left(1 + \frac{5\tilde{K}^2}{N-1} \right) \cos 2\delta + \Theta_{\text{I}} + 3(N-1)\Theta_{\text{II}} \right]. \quad (4.7)$$

Here, $\tilde{K} \equiv (N-1)(R-1)$ is a rescaled Wilson ratio: $R = 1 - \chi_{\sigma\sigma'}/\chi_{\sigma\sigma}$ for $\sigma' \neq \sigma$. The diagonal susceptibility $\chi_{\sigma\sigma}$ in the right-hand side of these equations determines a characteristic energy scale $T^* \equiv 1/(4\chi_{\sigma\sigma})$. The dimensionless parameters Θ_{I} and Θ_{II} are introduced for the three-body correlation functions for the diagonal and off-diagonal components, respectively,

$$\Theta_{\text{I}} \equiv \frac{\sin 2\delta}{2\pi} \frac{\chi_{\sigma\sigma\sigma}^{[3]}}{\chi_{\sigma\sigma}^2}, \quad \Theta_{\text{II}} \equiv \frac{\sin 2\delta}{2\pi} \frac{\chi_{\sigma\sigma'\sigma'}^{[3]}}{\chi_{\sigma\sigma}^2}. \quad (4.8)$$

The formula for $c_{S,\sigma}$ given in Eq. (4.6) reproduces the previous result as a special case for $N = 2$, obtained by Mora, Moca, *et al* for the spin-1/2 Anderson model at zero magnetic field.⁵⁰

The nonlinear Fano factor for the $SU(N)$ symmetric case is given by Eqs. (4.5)–(4.7). It also reproduces the previous result,⁴⁰ obtained just for the particle-hole symmetric case at which $\delta = \pi/2$ and all the three-body correlation functions vanish $\chi_{\sigma\sigma'\sigma''}^{[3]} = 0$,

$$F_K \xrightarrow{\epsilon_d \rightarrow -\frac{(N-1)U}{2}} \frac{1 + \frac{9\tilde{K}^2}{N-1}}{1 + \frac{5\tilde{K}^2}{N-1}} \xrightarrow{U \rightarrow \infty} \frac{1 + \frac{9}{N-1}}{1 + \frac{5}{N-1}}. \quad (4.9)$$

In the strong coupling limit $U \rightarrow \infty$, the occupation number $N_d \equiv \sum_{\sigma} \langle n_{d\sigma} \rangle$ takes integer values $M = 1, 2, \dots, N-1$ at $\epsilon_d = -(M-1/2)U$ and the phase is also locked at $\delta = \pi M/N$. In this limit, the charge and spin susceptibilities satisfy the stationary conditions, especially the charge susceptibility is suppressed $\chi_{\sigma\sigma} + (N-1)\chi_{\sigma\sigma'} \rightarrow 0$, and thus the scaled Wilson ratio approaches $\tilde{K} \rightarrow 1$. The three body correlation functions show the property $\Theta_{\text{I}} + (N-1)\Theta_{\text{II}} \rightarrow 0$ in the strong-coupling limit,³³ and thus F_K takes the value,

$$F_K \rightarrow \frac{1 + \sin^2 2\delta + \frac{9-13\sin^2 2\delta}{N-1} + 2\Theta_{\text{I}} \cos 2\delta}{- \left[1 + \frac{5}{N-1} \right] \cos 2\delta - 2\Theta_{\text{I}}}. \quad (4.10)$$

This expression agrees with F_K for the $SU(N)$ Kondo model, obtained previously by Mora, Vitushinsky, *et*

TABLE III. The coefficients C 's for the transport coefficients given in Eq. (4.12) at finite magnetic fields b for $N = 2$ at half filling $\epsilon_d = -\frac{U}{2}$. Dimensionless three-body correlation functions are defined as $\Theta_I^b \equiv -\frac{\sin(\pi m_d)}{2\pi} \frac{\chi_{\uparrow\uparrow\uparrow}^{[3]}}{\chi_{\uparrow\uparrow}^2}$, and $\Theta_{II}^b \equiv -\frac{\sin(\pi m_d)}{2\pi} \frac{\chi_{\uparrow\downarrow\downarrow}^{[3]}}{\chi_{\uparrow\downarrow}^2}$.

$C_S^b = \frac{\pi^2}{192} [W_S^b + (\Theta_I^b + 3\Theta_{II}^b) \cos(\pi m_d)]$	$W_S^b \equiv \cos(2\pi m_d) + [4 + 5 \cos(2\pi m_d)](R - 1)^2$
$C_V^b = \frac{\pi^2}{64} [W_V^b + \Theta_I^b + 3\Theta_{II}^b]$	$W_V^b \equiv [1 + 5(R - 1)^2] \cos(\pi m_d)$
$C_T^b = \frac{\pi^2}{48} [W_T^b + \Theta_I^b + \Theta_{II}^b]$	$W_T^b \equiv [1 + 2(R - 1)^2] \cos(\pi m_d)$
$C_{\kappa,b}^{\text{QD}} = \frac{7\pi^2}{80} [W_{\kappa,b}^{\text{QD}} + \Theta_I^b + \frac{5}{21}\Theta_{II}^b]$	$W_{\kappa,b}^{\text{QD}} \equiv [1 + \frac{6}{7}(R - 1)^2] \cos(\pi m_d)$

*al.*⁵¹ We have calculated the three-body correlation functions of the $SU(N)$ Anderson model for $N = 4, 6$, using the NRG in the previous paper.^{32,33} The results show that, for strong interactions $U \gg \Delta$, the three-body correlations are characterized by a single parameter over a wide continuous filling-range $1 \lesssim N_d \lesssim N - 1$, including the intermediate valence regions in between two adjacent integer-filling points M and $M+1$ for $M = 1, 2, \dots, N-2$.

2. Current noise at finite magnetic fields

We next provide another application of the current-noise formula to the case where the time-reversal symmetry is broken by an external magnetic field b . Specifically, we consider the spin 1/2 Anderson model ($N = 2$) at half filling, taking the impurity level to be $\epsilon_{d\sigma} \equiv \epsilon_d - \text{sgn}(\sigma)b$ with $\epsilon_d = -U/2$, $\text{sgn}(\uparrow) = +1$ and $\text{sgn}(\downarrow) = -1$. In this case, the phase shift takes the form $\delta_\sigma = \pi[1 + \text{sgn}(\sigma)m_d]/2$ with $m_d \equiv \langle n_{d\uparrow} \rangle - \langle n_{d\downarrow} \rangle$, and the correlation functions have the following properties: $\chi_{\uparrow\uparrow} = \chi_{\downarrow\downarrow}$, $\chi_{\uparrow\downarrow} = \chi_{\downarrow\uparrow}$, $\chi_{\downarrow\downarrow\downarrow}^{[3]} = -\chi_{\uparrow\uparrow\uparrow}^{[3]}$, and $\chi_{\uparrow\uparrow\downarrow}^{[3]} = -\chi_{\uparrow\downarrow\downarrow}^{[3]}$. Therefore, there are two independent three-body correlation functions $\chi_{\uparrow\uparrow\uparrow}^{[3]}$ and $\chi_{\uparrow\uparrow\downarrow}^{[3]}$ in this case, which can be evaluated from the derivative of the linear susceptibilities with respect to b ,

$$\begin{aligned} \frac{\partial \chi_{\uparrow\uparrow}}{\partial b} &= -\chi_{\uparrow\uparrow\uparrow}^{[3]} + \chi_{\uparrow\uparrow\downarrow}^{[3]} \xrightarrow{\epsilon_d = -U/2} -\chi_{\uparrow\uparrow\uparrow}^{[3]} - \chi_{\uparrow\uparrow\downarrow}^{[3]}, \\ \frac{\partial \chi_{\uparrow\downarrow}}{\partial b} &= -\chi_{\uparrow\uparrow\downarrow}^{[3]} + \chi_{\uparrow\downarrow\downarrow}^{[3]} \xrightarrow{\epsilon_d = -U/2} 2\chi_{\uparrow\uparrow\downarrow}^{[3]}. \end{aligned} \quad (4.11)$$

The transport coefficients up to the next-leading order terms can be described in terms of the five FL parameters: m_d , $T^* = 1/(4\chi_{\uparrow\uparrow})$, $R = 1 - \chi_{\uparrow\downarrow}/\chi_{\uparrow\uparrow}$, and two different three-body correlation functions, $\Theta_I^b \equiv -\sin(\pi m_d)\chi_{\uparrow\uparrow\uparrow}^{[3]}/(2\pi\chi_{\uparrow\uparrow}^2)$, and $\Theta_{II}^b \equiv -\sin(\pi m_d)\chi_{\uparrow\uparrow\downarrow}^{[3]}/(2\pi\chi_{\uparrow\uparrow}^2)$.

TABLE III shows the formulas for the coefficients of the low-energy expansion of the differential conductance dJ/dV , current noise $S_{\text{noise}}^{\text{QD}}$, and thermal conductivity

κ_{QD} for this case:

$$\begin{aligned} S_{\text{noise}}^{\text{QD}} &= 2 \frac{2e^2}{h} |eV| \left[\frac{\sin^2(\pi m_d)}{4} + C_S^b \left(\frac{eV}{T^*} \right)^2 + \dots \right], \\ \frac{dJ}{dV} &= \frac{2e^2}{h} \left[\cos^2 \left(\frac{\pi m_d}{2} \right) - C_T^b \left(\frac{\pi T}{T^*} \right)^2 - C_V^b \left(\frac{eV}{T^*} \right)^2 + \dots \right], \\ \kappa_{\text{QD}} &= \frac{2\pi^2 T}{3h} \left[\cos^2 \left(\frac{\pi m_d}{2} \right) - C_{\kappa,b}^{\text{QD}} \left(\frac{\pi T}{T^*} \right)^2 + \dots \right]. \end{aligned} \quad (4.12)$$

Here, the thermal conductivity is defined with respect to the heat current $J_Q = \kappa_{\text{QD}} \delta T$, induced by the temperature difference δT between the two leads. It is also determined by the transmission probability $\mathcal{T}_\sigma(\omega)$ defined in Eq. (2.6),⁵² as

$$\begin{aligned} \kappa_{\text{QD}} &\equiv \frac{1}{hT} \left[\sum_\sigma \mathcal{L}_{2,\sigma}^{\text{QD}} - \frac{(\sum_\sigma \mathcal{L}_{1,\sigma}^{\text{QD}})^2}{\sum_\sigma \mathcal{L}_{0,\sigma}^{\text{QD}}} \right], \quad (4.13) \\ \mathcal{L}_{n,\sigma}^{\text{QD}} &\equiv \int_{-\infty}^{\infty} d\omega \omega^n \mathcal{T}_\sigma(\omega) \left(-\frac{\partial f(\omega)}{\partial \omega} \right). \quad (4.14) \end{aligned}$$

We consider here behaviors of these coefficients for strong interactions $U \gg \Delta$, where the system can be described by the Kondo model. Specifically, the behavior of dI/dV in this limit has already been examined by Filippone *et al.*, i.e. Eq. (17) of Ref. 26, using a different notation. Here we consider mainly the current $S_{\text{noise}}^{\text{QD}}$ and κ_{QD} . In the Kondo limit, the Wilson ratio approaches $R \rightarrow 2$ as the charge fluctuations are suppressed $\chi_{\uparrow\downarrow} + \chi_{\uparrow\uparrow} \rightarrow 0$. Correspondingly, two different components of the three-body correlation functions take an identical value $\chi_{\uparrow\downarrow\downarrow}^{[3]} \rightarrow \chi_{\uparrow\uparrow\uparrow}^{[3]}$, and thus $\Theta_{II}^b \rightarrow \Theta_I^b$. Therefore, in the strong-interaction limit, the transport coefficients defined in Eq. (4.12) and TABLE III are determined by the following three FL parameters: m_d , Θ_I^b , and T^* . These parameters can be calculated from the spin susceptibility χ_s of the Kondo model with the Zeeman coupling $\mathcal{H}_z = -2S_d^z b$ between the impurity spin

$S_d^z = (n_{d\uparrow} - n_{d\downarrow})/2$ and magnetic field b ,

$$\chi_{\uparrow\uparrow} \xrightarrow{U \gg \Delta} \frac{\chi_s}{4} \equiv \int_0^{1/T} d\tau \langle S_d^z(\tau) S_d^z \rangle, \quad (4.15)$$

$$\chi_{\uparrow\uparrow}^{[3]} \xrightarrow{U \gg \Delta} -\frac{1}{8} \frac{\partial \chi_s}{\partial b}. \quad (4.16)$$

The field-dependent energy scale can be defined by the inverse of the spin susceptibility $T^* \xrightarrow{U \gg \Delta} 1/\chi_s$.

In the Kondo limit, the nonlinear Fano factor takes the form³³

$$\frac{C_S^b}{C_V^b/3} \xrightarrow{U \gg \Delta} \frac{4 + 6 \cos(2\pi m_d) + 4 \Theta_1^b \cos(\pi m_d)}{6 \cos(\pi m_d) + 4 \Theta_1^b}. \quad (4.17)$$

We also find that the ratio of the T^3 thermal conductivity to the T^2 conductance takes a constant value which does not depend on magnetic field strength b or the Kondo coupling $J_K \propto \Delta/(\rho_c U)$,

$$\frac{C_{\kappa,b}^{\text{QD}}}{C_T^b} \xrightarrow{U \gg \Delta} \frac{13}{5}. \quad (4.18)$$

Figure 3 shows the NRG results of these coefficients for strong interactions $U/(\pi\Delta) \gtrsim 2.5$ plotted against b/T_K .⁵³ The coefficients are rescaled in a way such that $\bar{C}_{\kappa,b}^{\text{QD}} \equiv (T_K/T^*)^2 C_{\kappa,b}^{\text{QD}}$, $\bar{C}_T^b \equiv (T_K/T^*)^2 C_T^b$, $\bar{C}_S^b \equiv (T_K/T^*)^2 C_S^b$, and $F_K^b \equiv C_S^b/(C_V^b/3)$, with the Kondo temperature $T_K \equiv T^*|_{b=0}$ defined at zero field.³³ Each of these curves shows the Kondo scaling behavior. We can see that the universal curve for $\bar{C}_{\kappa,b}^{\text{QD}}$ and that for $(15/3)\bar{C}_T^b$ are almost identical and overlap each other showing a good agreement with Eq. (4.18). Note that similar relation does not hold for magnetic alloys for the T^3 thermal conductivity and the T^2 electrical resistivity.^{30,54} Equation (4.18) clarifies one of the FL properties appearing in the temperature dependence. The nonlinear Fano factor $F_K^b \equiv \bar{C}_S^b/(\bar{C}_V^b/3)$ can be regarded as a nonequilibrium analogue. As the zero-points of \bar{C}_S^b and that of \bar{C}_V^b appear at different magnetic fields, F_K^b diverges at the zero-point of \bar{C}_V^b .

V. KELDYSH GREEN'S FUNCTION FOR ANDERSON IMPURITY

The current conservation is an essential requirement that transport theories must satisfy, and it is particularly important for strongly correlated electron systems. In this and next sections, we extend the Ward identities for the Keldysh Green's function which were previously obtained for nonequilibrium steady states but only for the zero-bias limit $eV \rightarrow 0$.¹⁸ Specifically, in this section, we perturbatively derive the Ward identities which hold for finite eV and can be expressed in terms of the

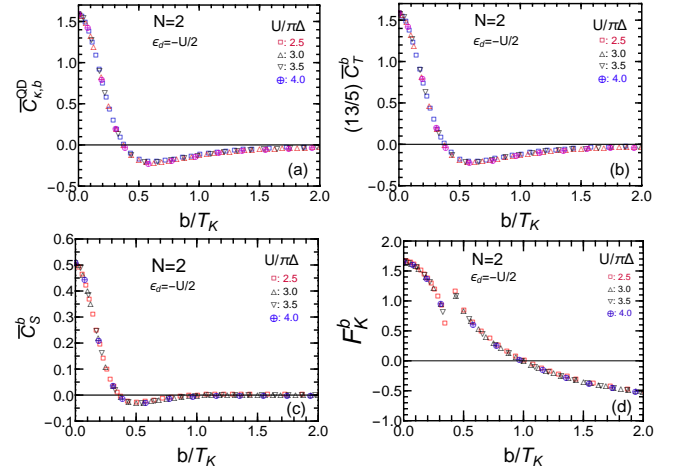


FIG. 3. Magnetic-field scaling of the coefficients that determine the next-leading-order transport of the $N = 2$ Anderson impurity model. These results are obtained at half-filling $\epsilon_d = -U/2$ for strong interactions $U/(\pi\Delta) = 2.5, 3.0, 3.5, 4.0$, using the NRG approach. Figures (a)–(d) show that (a): $\bar{C}_{\kappa,b}^{\text{QD}} \equiv (T_K/T^*)^2 C_{\kappa,b}^{\text{QD}}$, (b): $\bar{C}_T^b \equiv (T_K/T^*)^2 C_T^b$ multiplied by a factor of $13/5$, (c): $\bar{C}_S^b \equiv (T_K/T^*)^2 C_S^b$, and (d): $F_K^b \equiv \bar{C}_S^b/(\bar{C}_V^b/3)$. The Kondo temperature is defined as $T_K \equiv T^*|_{b=0}$, at zero field with $T^* = 1/(4\chi_{\uparrow\uparrow})$.

Keldysh self-energy and vertex functions. We will also present more general Ward-Takahashi identity for the three-point current vertex which reflects directly the current conservation between the quantum dot and leads in Sec. VI.

A. General properties

We summarize in this subsection the general properties of the Keldysh Green's function of the Anderson impurity, defined by⁵⁵

$$G_{\sigma}^{--}(t_1, t_2) \equiv -i \langle T d_{\sigma}(t_1) d_{\sigma}^{\dagger}(t_2) \rangle, \quad (5.1a)$$

$$G_{\sigma}^{++}(t_1, t_2) \equiv -i \langle \tilde{T} d_{\sigma}(t_1) d_{\sigma}^{\dagger}(t_2) \rangle, \quad (5.1b)$$

$$G_{\sigma}^{+-}(t_1, t_2) \equiv -i \langle d_{\sigma}(t_1) d_{\sigma}^{\dagger}(t_2) \rangle, \quad (5.1c)$$

$$G_{\sigma}^{-+}(t_1, t_2) \equiv i \langle d_{\sigma}^{\dagger}(t_2) d_{\sigma}(t_1) \rangle, \quad (5.1d)$$

where T and \tilde{T} are the time-ordering and anti-time-ordering operators, respectively. These correlation functions are defined along the Keldysh time-loop contour and are linearly dependent on each other, as summarized in TABLE IV. Thus the above four Green's functions can be written in terms of three components: the retarded G_{σ}^r , the advanced G_{σ}^a , and the symmetrized G_{σ}^K functions,

$$G_{\sigma}^r = G_{\sigma}^{--} - G_{\sigma}^{-+}, \quad G_{\sigma}^a = G_{\sigma}^{--} - G_{\sigma}^{++}, \quad (5.2a)$$

$$G_{\sigma}^K \equiv G_{\sigma}^{+-} + G_{\sigma}^{-+} = G_{\sigma}^{--} + G_{\sigma}^{++}. \quad (5.2b)$$

TABLE IV. Linear dependency of the Keldysh correlation functions. The three-point functions $\Phi_{\gamma,\sigma\sigma'}^{\alpha;\mu\nu}$ and $\Lambda_{\gamma,\sigma\sigma'}^{\alpha;\mu\nu}$ for $\gamma = L, R, d$ are defined in Eqs. (6.1) and (6.3). Outline of the derivation is given in Appendix A.

$$\begin{aligned}
& \overline{G_{\sigma}^{-} + G_{\sigma}^{+} = G_{\sigma}^{-+} + G_{\sigma}^{+-}, \quad \Sigma_{\sigma}^{-} + \Sigma_{\sigma}^{+} = -\Sigma_{\sigma}^{-+} - \Sigma_{\sigma}^{+-},} \\
& \overline{\Phi_{\gamma,\sigma\sigma'}^{-;-} + \Phi_{\gamma,\sigma\sigma'}^{-;+-} - \Phi_{\gamma,\sigma\sigma'}^{-;-+} - \Phi_{\gamma,\sigma\sigma'}^{-;-+} = \Phi_{\gamma,\sigma\sigma'}^{+;++} + \Phi_{\gamma,\sigma\sigma'}^{+;--} - \Phi_{\gamma,\sigma\sigma'}^{+;-+} - \Phi_{\gamma,\sigma\sigma'}^{+;-+},} \\
& \overline{\Lambda_{\gamma,\sigma\sigma'}^{-;-} + \Lambda_{\gamma,\sigma\sigma'}^{-;+-} + \Lambda_{\gamma,\sigma\sigma'}^{-;-+} + \Lambda_{\gamma,\sigma\sigma'}^{-;-+} = \Lambda_{\gamma,\sigma\sigma'}^{+;--} + \Lambda_{\gamma,\sigma\sigma'}^{+;++} + \Lambda_{\gamma,\sigma\sigma'}^{+;-+} + \Lambda_{\gamma,\sigma\sigma'}^{+;-+},} \\
& \overline{\Gamma_{\sigma\sigma';\sigma'\sigma}^{-;-} + \Gamma_{\sigma\sigma';\sigma'\sigma}^{+;++} + \Gamma_{\sigma\sigma';\sigma'\sigma}^{-;-+} + \Gamma_{\sigma\sigma';\sigma'\sigma}^{-;-+} + \Gamma_{\sigma\sigma';\sigma'\sigma}^{+;--} + \Gamma_{\sigma\sigma';\sigma'\sigma}^{+;--} + \Gamma_{\sigma\sigma';\sigma'\sigma}^{-;-+} + \Gamma_{\sigma\sigma';\sigma'\sigma}^{-;-+}} \\
& \quad = -\Gamma_{\sigma\sigma';\sigma'\sigma}^{-;-+} - \Gamma_{\sigma\sigma';\sigma'\sigma}^{-;-+} - \Gamma_{\sigma\sigma';\sigma'\sigma}^{-;-+} - \Gamma_{\sigma\sigma';\sigma'\sigma}^{-;-+} - \Gamma_{\sigma\sigma';\sigma'\sigma}^{-;-+} - \Gamma_{\sigma\sigma';\sigma'\sigma}^{-;-+} - \Gamma_{\sigma\sigma';\sigma'\sigma}^{-;-+} - \Gamma_{\sigma\sigma';\sigma'\sigma}^{-;-+}.
\end{aligned}$$

These Green's functions can also be written in a matrix form,

$$\begin{aligned}
\mathbf{G}_{\sigma} &\equiv \begin{bmatrix} G_{\sigma}^{-} & G_{\sigma}^{-+} \\ G_{\sigma}^{+-} & G_{\sigma}^{+} \end{bmatrix} \quad (5.3) \\
&= \frac{G_{\sigma}^{\text{K}}}{2} (\mathbf{1} + \boldsymbol{\tau}_1) + \frac{G_{\sigma}^r + G_{\sigma}^a}{2} \boldsymbol{\tau}_3 - \frac{G_{\sigma}^r - G_{\sigma}^a}{2} i\boldsymbol{\tau}_2.
\end{aligned}$$

Here, $\mathbf{1}$ is the 2×2 unit matrix and $\boldsymbol{\tau}_j$ for $j = 1, 2, 3$ are the Pauli matrices, defined by

$$\boldsymbol{\tau}_1 = \begin{bmatrix} 0 & 1 \\ 1 & 0 \end{bmatrix}, \quad \boldsymbol{\tau}_2 = \begin{bmatrix} 0 & -i \\ i & 0 \end{bmatrix}, \quad \boldsymbol{\tau}_3 = \begin{bmatrix} 1 & 0 \\ 0 & -1 \end{bmatrix}. \quad (5.4)$$

Therefore, the determinant of \mathbf{G}_{σ} can be expressed, as

$$\det \{\mathbf{G}_{\sigma}\} \equiv G_{\sigma}^{-} G_{\sigma}^{+} - G_{\sigma}^{-+} G_{\sigma}^{+-} = -G_{\sigma}^r G_{\sigma}^a, \quad (5.5)$$

and this product $G_{\sigma}^r G_{\sigma}^a$ of the retarded and advanced Green's functions plays an important role in the transport theory. We will also use later the following matrix identity which appears when we take the derivative of \mathbf{G}_{σ} ,

$$\mathbf{G}_{\sigma} (\mathbf{1} - \boldsymbol{\tau}_1) \mathbf{G}_{\sigma} = (\mathbf{1} + \boldsymbol{\tau}_1) G_{\sigma}^r G_{\sigma}^a. \quad (5.6)$$

The Fourier transform of the Green's function defined with respect to the steady state at eV becomes a function of a single frequency ω ,

$$G_{\sigma}^{\nu_1\nu_2}(\omega) = \int_{-\infty}^{\infty} dt e^{i\omega t} G_{\sigma}^{\nu_1\nu_2}(t, 0). \quad (5.7)$$

For $U = 0$, it can be expressed in the following form,

$$G_{0\sigma}^{-+}(\omega) = i 2 f_{\text{eff}}(\omega) \Delta G_{0\sigma}^r(\omega) G_{0\sigma}^a(\omega), \quad (5.8a)$$

$$G_{0\sigma}^{+-}(\omega) = -i 2 [1 - f_{\text{eff}}(\omega)] \Delta G_{0\sigma}^r(\omega) G_{0\sigma}^a(\omega), \quad (5.8b)$$

$$G_{0\sigma}^{-}(\omega) = G_{0\sigma}^r(\omega) + G_{0\sigma}^{-+}(\omega), \quad (5.8c)$$

$$G_{0\sigma}^{+}(\omega) = -G_{0\sigma}^a(\omega) + G_{0\sigma}^{+-}(\omega). \quad (5.8d)$$

Here, $\Delta = \Gamma_L + \Gamma_R$, and the retarded function is given by

$$G_{0\sigma}^r(\omega) = \frac{1}{\omega - \epsilon_{d\sigma} + i(\Gamma_L + \Gamma_R)}. \quad (5.9)$$

The Fourier transformed Green's functions have additional relations, $G_{\sigma}^a(\omega) = \{G_{\sigma}^r(\omega)\}^*$, and $G_{\sigma}^{+-}(\omega) = -\{G_{\sigma}^{-+}(\omega)\}^*$. Furthermore, the greater $G_{\sigma}^{-+}(\omega)$ and lesser $G_{\sigma}^{+-}(\omega)$ functions become pure imaginary.

The bias voltage eV and temperature T enter the Green functions through the distribution function

$$f_{\text{eff}}(\omega) \equiv \frac{f_L(\omega) \Gamma_L + f_R(\omega) \Gamma_R}{\Gamma_L + \Gamma_R} = \sum_{j=L,R} \frac{\Gamma_j}{\Delta} f(\omega - \mu_j). \quad (5.10)$$

It shows jump discontinuities at $\omega = \mu_L$ and μ_R at $T = 0$, as depicted in Fig. 4. The noninteracting Green's function can also be written in the following form,

$$\{\mathbf{G}_{0\sigma}(\omega)\}^{-1} = (\omega - \epsilon_{d\sigma}) \boldsymbol{\tau}_3 - \boldsymbol{\Sigma}_0(\omega). \quad (5.11)$$

It is this noninteracting self-energy $\boldsymbol{\Sigma}_0(\omega)$ that brings $f_{\text{eff}}(\omega)$ into $\mathbf{G}_{0\sigma}(\omega)$ through the tunneling processes,

$$\begin{aligned}
\boldsymbol{\Sigma}_0(\omega) &\equiv \boldsymbol{\tau}_3 v_L^2 \mathbf{g}_L(\omega) \boldsymbol{\tau}_3 + \boldsymbol{\tau}_3 v_R^2 \mathbf{g}_R(\omega) \boldsymbol{\tau}_3 \\
&= -i\Delta [1 - 2f_{\text{eff}}(\omega)] (\mathbf{1} - \boldsymbol{\tau}_1) + \Delta \boldsymbol{\tau}_2. \quad (5.12)
\end{aligned}$$

Here, $\mathbf{g}_j(\omega)$ is the Keldysh Green's function for the isolated lead on $j = L$ and R ,

$$v_j^2 \mathbf{g}_j(\omega) = -i\Gamma_j [1 - 2f_j(\omega)] (\mathbf{1} + \boldsymbol{\tau}_1) - \Gamma_j \boldsymbol{\tau}_2. \quad (5.13)$$

Note that $\boldsymbol{\Sigma}_0(\omega)$ does not depend on $\epsilon_{d\sigma}$, and the derivative with respect to ω takes the following form,

$$\frac{\partial \boldsymbol{\Sigma}_0(\omega)}{\partial \omega} = 2i\Delta \frac{\partial f_{\text{eff}}(\omega)}{\partial \omega} (\mathbf{1} - \boldsymbol{\tau}_1). \quad (5.14)$$

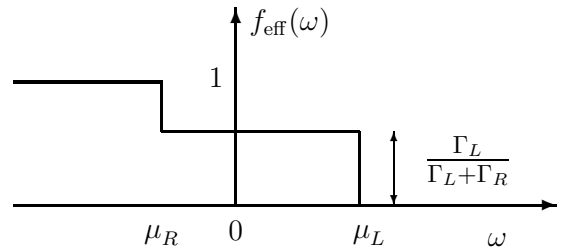


FIG. 4. The nonequilibrium distribution function $f_{\text{eff}}(\omega)$ for $\mu_L - \mu_R = eV$ and $T = 0$. The Fermi level at equilibrium is chosen to be the origin of single-particle energy $\omega = 0$.

Effects of the Coulomb repulsion U enter through the interacting self-energy,

$$\Sigma_{U,\sigma} = \begin{bmatrix} \Sigma_{U,\sigma}^{--} & \Sigma_{U,\sigma}^{+-} \\ \Sigma_{U,\sigma}^{+-} & \Sigma_{U,\sigma}^{++} \end{bmatrix}, \quad (5.15)$$

with $\{\mathbf{G}_\sigma(\omega)\}^{-1} = \{\mathbf{G}_{0\sigma}(\omega)\}^{-1} - \Sigma_{U,\sigma}(\omega)$. The Dyson equation can also be rewritten into the following form, using Eq. (5.11),

$$\{\mathbf{G}_\sigma(\omega)\}^{-1} = (\omega - \epsilon_{d\sigma})\boldsymbol{\tau}_3 - \Sigma_{\text{tot},\sigma}(\omega), \quad (5.16a)$$

$$\Sigma_{\text{tot},\sigma}(\omega) \equiv \Sigma_0(\omega) + \Sigma_{U,\sigma}(\omega). \quad (5.16b)$$

The retarded, advanced, and symmetrized self-energies are given by linear combinations of the four elements of $\Sigma_{U,\sigma}$:

$$\Sigma_{U,\sigma}^r = \Sigma_{U,\sigma}^{--} + \Sigma_{U,\sigma}^{+-}, \quad \Sigma_{U,\sigma}^a = \Sigma_{U,\sigma}^{--} + \Sigma_{U,\sigma}^{+-}, \quad (5.17a)$$

$$\Sigma_{U,\sigma}^K \equiv -\Sigma_{U,\sigma}^{+-} - \Sigma_{U,\sigma}^{+-} = \Sigma_{U,\sigma}^{--} + \Sigma_{U,\sigma}^{++}. \quad (5.17b)$$

Note that $\Sigma_{U,\sigma}^a(\omega) = \{\Sigma_{U,\sigma}^r(\omega)\}^*$. The lesser and greater self-energies, namely $\Sigma_{U,\sigma}^{+-}(\omega)$ and $\Sigma_{U,\sigma}^{+-}(\omega)$, are pure imaginary. Similarly, $\Sigma_{U,\sigma}^{++}(\omega) = -\{\Sigma_{U,\sigma}^{--}(\omega)\}^*$, and the imaginary part of the causal self-energy corresponds to $\Sigma_{U,\sigma}^K(\omega)/2$,

$$\Sigma_{U,\sigma}^{--}(\omega) = \frac{\Sigma_{U,\sigma}^r(\omega) + \Sigma_{U,\sigma}^a(\omega)}{2} + \frac{\Sigma_{U,\sigma}^K(\omega)}{2}. \quad (5.18)$$

Furthermore, using Eq. (5.5), the Green's function for the impurity electrons can also be expressed in the form,

$$\mathbf{G}_\sigma(\omega) = G_\sigma^r(\omega) G_\sigma^a(\omega) \times \begin{bmatrix} \omega - \epsilon_{d\sigma} + \Sigma_{\text{tot},\sigma}^{++}(\omega) & -\Sigma_{\text{tot},\sigma}^{+-}(\omega) \\ -\Sigma_{\text{tot},\sigma}^{+-}(\omega) & -(\omega - \epsilon_{d\sigma}) + \Sigma_{\text{tot},\sigma}^{--}(\omega) \end{bmatrix}. \quad (5.19)$$

Note that the off-diagonal Green's functions are proportional to the lesser or the greater self-energies. From this property, it can be deduced that the lesser and greater self-energies takes the following form in the limit of $eV \rightarrow 0$,

$$\Sigma_{\text{eq},\sigma}^{+-}(\omega) = f(\omega) [\Sigma_{\text{eq},\sigma}^r(\omega) - \Sigma_{\text{eq},\sigma}^a(\omega)], \quad (5.20a)$$

$$\Sigma_{\text{eq},\sigma}^{+-}(\omega) = -[1 - f(\omega)] [\Sigma_{\text{eq},\sigma}^r(\omega) - \Sigma_{\text{eq},\sigma}^a(\omega)]. \quad (5.20b)$$

This is because at equilibrium $eV = 0$ the lesser and greater Green's functions can be expressed in the following form, using the Lehmann representation,⁵⁶ as

$$G_{\text{eq},\sigma}^{+-}(\epsilon) = i2\pi f(\omega) \rho_{d\sigma}(\omega), \quad (5.21a)$$

$$G_{\text{eq},\sigma}^{+-}(\omega) = -i2\pi [1 - f(\omega)] \rho_{d\sigma}(\omega). \quad (5.21b)$$

Here, $\rho_{d\sigma}(\omega)$ is the density of states of impurity electrons, defined in Eq. (3.2).



FIG. 5. Feynman diagrams for the derivatives $\frac{\partial}{\partial \epsilon_{d\sigma'}} \mathbf{G}_{0\sigma}(\omega)$ and $\left(\frac{\partial}{\partial \omega} + \frac{\partial}{\partial \epsilon_{d\sigma}}\right) \mathbf{G}_{0\sigma}(\omega)$, given in Eqs. (5.22a) and (5.22b). Here, \times and \otimes placed in between two propagators denote the matrices $\boldsymbol{\tau}_3 \delta_{\sigma\sigma'}$ and $-\frac{\partial f_{\text{eff}}(\omega)}{\partial \omega} (-2i\Delta) (\mathbf{1} - \boldsymbol{\tau}_1)$, respectively.

B. Nonequilibrium Ward identities

We describe here a perturbative derivation of the Ward identity for the Anderson impurity at finite bias voltages. To this end, we start with the derivatives of the noninteracting Green's function $\mathbf{G}_{0\sigma}$ with respect to external fields and a frequency. First of all, the derivative with respect to $\epsilon_{d\sigma'}$ is given by

$$\frac{\partial \mathbf{G}_{0\sigma}(\omega)}{\partial \epsilon_{d\sigma'}} = \delta_{\sigma\sigma'} \mathbf{G}_{0\sigma}(\omega) \boldsymbol{\tau}_3 \mathbf{G}_{0\sigma}(\omega). \quad (5.22a)$$

This can be verified using Eq. (5.11), using a matrix identity $\delta \mathbf{G} = -\mathbf{G} \{\delta \mathbf{G}^{-1}\} \mathbf{G}$ for a small variation of the Green's function $\delta \mathbf{G}$. Next one is the the frequency derivative, which can be calculated from Eq. (5.8), using the property that $G_{0\sigma}^r(\omega)$ and $G_{0\sigma}^a(\omega)$ are functions of the difference $\omega - \epsilon_{d\sigma}$,

$$\begin{aligned} & \left(\frac{\partial}{\partial \omega} + \frac{\partial}{\partial \epsilon_{d\sigma}}\right)^n \mathbf{G}_{0\sigma}(\omega) \\ &= -\frac{\partial^n f_{\text{eff}}(\omega)}{\partial \omega^n} (-2i\Delta) G_{0\sigma}^r(\omega) G_{0\sigma}^a(\omega) \begin{bmatrix} 1 & 1 \\ 1 & 1 \end{bmatrix} \\ &= -\frac{\partial^n f_{\text{eff}}(\omega)}{\partial \omega^n} (-2i\Delta) \mathbf{G}_{0\sigma}(\omega) (\mathbf{1} - \boldsymbol{\tau}_1) \mathbf{G}_{0\sigma}(\omega). \end{aligned} \quad (5.22b)$$

Here, we have used Eq. (5.6) to obtain the last line. Similarly, as the bias voltage enters $\mathbf{G}_{0\sigma}(\omega)$ only through $f_{\text{eff}}(\omega)$, the eV derivative can be expressed in the form,

$$\begin{aligned} & \frac{\partial^n \mathbf{G}_{0\sigma}(\omega)}{\partial (eV)^n} \\ &= -\frac{\partial^n f_{\text{eff}}(\omega)}{\partial (eV)^n} (-2i\Delta) \mathbf{G}_{0\sigma}(\omega) (\mathbf{1} - \boldsymbol{\tau}_1) \mathbf{G}_{0\sigma}(\omega). \end{aligned} \quad (5.22c)$$

These derivatives for $\mathbf{G}_{0\sigma}(\omega)$ can diagrammatically be represented as shown in Fig. 5. The Ward identities for the interacting self-energy $\Sigma_{U,\sigma}^{\nu\mu}(\epsilon)$ can be derived using the Feynman diagrammatic approach.¹⁶

1. Ward identities for the ω and $\epsilon_{d\sigma'}$ derivatives

We consider the derivative of $\Sigma_{U,\sigma}^{\nu\mu}(\epsilon)$ with respect to $\epsilon_{d\sigma'}$. It can be carried out by using the chain rule with Eq. (5.22a), taking the $\epsilon_{d\sigma'}$ derivative for the internal

$\mathbf{G}_{0\sigma}$'s which constitute the diagrams for the self-energy,

$$\begin{aligned} & \frac{\partial \Sigma_{U,\sigma}^{\nu_4\nu_1}(\epsilon)}{\partial \epsilon_{d\sigma'}} \\ &= \int_{-\infty}^{\infty} \frac{d\epsilon'}{2\pi i} \sum_{\nu_2\nu_3} \Gamma_{\sigma\sigma';\sigma'\sigma}^{\nu_1\nu_2;\nu_3\nu_4}(\epsilon, \epsilon'; \epsilon', \epsilon) \{ \mathbf{G}_{\sigma'}(\epsilon') \boldsymbol{\tau}_3 \mathbf{G}_{\sigma'}(\epsilon') \}^{\nu_3\nu_2}. \end{aligned} \quad (5.23)$$

Here, all contributions of the perturbation series in U are included in the Keldysh vertex functions and the full Green's functions that appeared as a matrix product of the form $\mathbf{G}_{\sigma'} \boldsymbol{\tau}_3 \mathbf{G}_{\sigma'}$. Note that this identity Eq. (5.23) holds for arbitrary eV and T .

In a similar way, the Ward identity for the ω can also be derived, using Eq. (5.22b),

$$\left(\delta_{\sigma\sigma'} \frac{\partial}{\partial \omega} + \frac{\partial}{\partial \epsilon_{d\sigma'}} \right) \Sigma_{U,\sigma}^{\nu_4\nu_1}(\omega) = - \int_{-\infty}^{\infty} \frac{d\omega'}{2\pi} \sum_{\nu_2\nu_3} \Gamma_{\sigma\sigma';\sigma'\sigma}^{\nu_1\nu_2;\nu_3\nu_4}(\omega, \omega'; \omega', \omega) 2\Delta G_{\sigma'}^r(\omega') G_{\sigma'}^a(\omega') \left(-\frac{\partial f_{\text{eff}}(\omega')}{\partial \omega'} \right) \quad (5.24a)$$

$$\xrightarrow{T \rightarrow 0} - \sum_{\nu_2\nu_3} \sum_{j=L,R} \Gamma_{\sigma\sigma';\sigma'\sigma}^{\nu_1\nu_2;\nu_3\nu_4}(\omega, \mu_j; \mu_j, \omega) \frac{\Delta}{\pi} G_{\sigma'}^r(\mu_j) G_{\sigma'}^a(\mu_j) \frac{\Gamma_j}{\Gamma_L + \Gamma_R} \quad (5.24b)$$

$$\xrightarrow{T \rightarrow 0, eV \rightarrow 0} - \sum_{\nu_2\nu_3} \Gamma_{\sigma\sigma';\sigma'\sigma}^{\nu_1\nu_2;\nu_3\nu_4}(\omega, 0; 0, \omega) \rho_{d\sigma'}. \quad (5.24c)$$

In order to obtain the Ward identities of this form, we have also used the property that the value of $\Sigma_{U,\sigma}(\omega)$ remains unchanged when the frequencies ω_{in} 's for all the internal Green's functions along each closed loop that carries level index σ' are uniformly sifted by an arbitrary amount of ω_0 in a way such that $\omega_{\text{in}} \rightarrow \omega_{\text{in}} + \omega_0$.¹⁶ Specifically, for the diagonal $\sigma = \sigma'$ components of Eq. (5.24a), the internal frequencies for the closed loops that carry the same level index σ as that of the external one is shifted, choosing ω_0 to be equal to the external frequency ω , and then the derivative $(\partial/\partial\omega + \partial/\partial\epsilon_{d\sigma})$ is carried out.

The off-diagonal $\sigma \neq \sigma'$ components of Eq. (5.24a) are obtained in a similar way: shifting the frequencies of the closed loops carrying level index σ' by an arbitrary amount ω_0 independent of the external frequency ω , and then taking the following derivative

$$\left(\frac{\partial}{\partial \omega_0} + \frac{\partial}{\partial \epsilon_{d\sigma'}} \right) \Sigma_{U,\sigma}(\omega) = \frac{\partial \Sigma_{U,\sigma}(\omega)}{\partial \epsilon_{d\sigma'}}. \quad (5.25)$$

Here, the ω_0 -derivative vanishes $\partial \Sigma_{U,\sigma}(\omega)/\partial \omega_0 = 0$, and thus only $\partial \Sigma_{U,\sigma}(\omega)/\partial \epsilon_{d\sigma'}$ remains in the left-hand of Eq. (5.24a). For obtaining the right-hand side of Eq. (5.24a) for $\sigma \neq \sigma'$, the operator $(\partial/\partial\omega_0 + \partial/\partial\epsilon_{d\sigma'})$ is applied to the internal Green's functions along the closed loops carrying the index σ' . We have also used Eq. (5.6) with Eq. (5.22b) in order to rewrite the matrix product of the full Green's function $\mathbf{G}_{\sigma'}(\mathbf{1} - \boldsymbol{\tau}_1)\mathbf{G}_{\sigma'}$ in terms of the

retarded and advanced Green's functions. The diagonal and off-diagonal components of Eq. (5.24a) are also derived from more general Ward-Takahashi identity that reflects the current conservation at the junctions between the dot and leads in Sec. VI.

We next describe some properties of the Keldysh vertex function that can be deduced from the Ward identity Eq. (5.24). In the second line that describes the $T \rightarrow 0$ limit, Eq. (5.24b), the derivative of $f_{\text{eff}}(\omega')$ in the integrand has been replaced by a sum of the two Dirac delta functions,

$$-\frac{\partial f_{\text{eff}}(\omega)}{\partial \omega} \xrightarrow{T \rightarrow 0} \sum_{j=L,R} \frac{\Gamma_j}{\Delta} \delta(\omega - \mu_j). \quad (5.26)$$

In particular, at $T = eV = 0$, the causal component ($\nu_4 = \nu_1 = -$) of Eq. (5.24c) can be compared to the identity Eq. (3.9) which has been obtained by using the zero-temperature formalism.¹⁶ Comparing these two results, we find that

$$\sum_{\nu_2\nu_3} \Gamma_{\sigma\sigma';\sigma'\sigma}^{-\nu_2;\nu_3-}(\omega, 0; 0, \omega) = \Gamma_{\sigma\sigma';\sigma'\sigma}^{--;--}(\omega, 0; 0, \omega), \quad (5.27a)$$

$$\sum_{\nu_2\nu_3} \Gamma_{\sigma\sigma';\sigma'\sigma}^{+\nu_2;\nu_3+}(\omega, 0; 0, \omega) = \Gamma_{\sigma\sigma';\sigma'\sigma}^{++;++}(\omega, 0; 0, \omega). \quad (5.27b)$$

Furthermore, at $T = eV = 0$, the left-hand side of Eq. (5.24c) can be rewritten into the following form, specifically for the lesser component ($\nu_4 = -, \nu_1 = +$) by

using the property $\Sigma_{\text{eq},\sigma}^{-+}(\omega) = -2if(\omega) \text{Im} \Sigma_{\text{eq},\sigma}^{--}(\omega)$ and $\text{Im} \Sigma_{\text{eq},\sigma}^{--}(0) = 0$ mentioned above, as

$$\begin{aligned} & \left(\delta_{\sigma\sigma'} \frac{\partial}{\partial\omega} + \frac{\partial}{\partial\epsilon_{d\sigma'}} \right) \Sigma_{\text{eq},\sigma}^{-+}(\omega) \\ &= -2if(\omega) \text{Im} \left(\delta_{\sigma\sigma'} \frac{\partial}{\partial\omega} + \frac{\partial}{\partial\epsilon_{d\sigma'}} \right) \Sigma_{\text{eq},\sigma}^{--}(\omega) \\ &= 2if(\omega) \text{Im} \Gamma_{\sigma\sigma';\sigma'\sigma}^{--;--}(\omega, 0; 0, \omega) \rho_{d\sigma'}. \end{aligned} \quad (5.28)$$

Here, $\Sigma_{\text{eq},\sigma}^{\mu\nu}(\omega) \equiv \Sigma_{U,\sigma}^{\mu\nu}(\omega) \Big|_{T=eV=0}$ and we have used Eq. (3.9) to obtain the last line. Comparing the last line of Eq. (5.28) to the right-hand side of Eq. (5.24c) for $\nu_1 = +$ and $\nu_4 = -$, we find

$$\sum_{\nu_2\nu_3} \Gamma_{\sigma\sigma';\sigma'\sigma}^{+\nu_2;\nu_3-}(\omega, 0; 0, \omega) = -2if(\omega) \text{Im} \Gamma_{\sigma\sigma';\sigma'\sigma}^{--;--}(\omega, 0; 0, \omega). \quad (5.29a)$$

Similarly, the greater self-energy has the property $\Sigma_{\text{eq},\sigma}^{+-}(\omega) = -2i[1-f(\omega)] \text{Im} \Sigma_{\text{eq},\sigma}^{--}(\omega)$ at $T = eV = 0$. From this and the ($\nu_4 = +$, $\nu_1 = -$) component of Eq. (5.24c), it follows that

$$\begin{aligned} & \sum_{\nu_2\nu_3} \Gamma_{\sigma\sigma';\sigma'\sigma}^{-\nu_2;\nu_3+}(\omega, 0; 0, \omega) \\ &= -2i[1-f(\omega)] \text{Im} \Gamma_{\sigma\sigma';\sigma'\sigma}^{--;--}(\omega, 0; 0, \omega). \end{aligned} \quad (5.29b)$$

The vertex function also has another general property: sixteen different components defined with respect to the Keldysh time-loop contour are linearly dependent,

$$\sum_{\nu_1\nu_2\nu_3\nu_4} \Gamma_{\sigma\sigma';\sigma'\sigma}^{\nu_1\nu_2;\nu_3\nu_4}(\omega, \omega'; \omega', \omega) = 0, \quad (5.30)$$

for which a brief explanation is provided in Appendix A. We can verify that both sides of Eq. (5.24a) will vanish if summations over ν_1 and ν_4 are carried out, as a result of the linear dependence of the Keldysh self-energy and vertex function, listed in TABLE IV. Furthermore, at $T = eV = 0$, it can also be deduced from Eqs. (5.27) (5.29), and (5.30) that

$$\begin{aligned} & \Gamma_{\sigma\sigma';\sigma'\sigma}^{--;--}(\omega, 0; 0, \omega) + \Gamma_{\sigma\sigma';\sigma'\sigma}^{++;++}(\omega, 0; 0, \omega) \\ &= 2i \text{Im} \Gamma_{\sigma\sigma';\sigma'\sigma}^{--;--}(\omega, 0; 0, \omega), \end{aligned} \quad (5.31)$$

$$\text{and } \Gamma_{\sigma\sigma';\sigma'\sigma}^{++;++}(\omega, 0; 0, \omega) = - \left\{ \Gamma_{\sigma\sigma';\sigma'\sigma}^{--;--}(\omega, 0; 0, \omega) \right\}^*.$$

2. Ward identities for the eV derivatives

We have described in the above the Ward identities for the ω and $\epsilon_{d\sigma'}$ derivatives, i.e. Eqs. (5.23) and (5.24a), respectively. Here we present some related Ward identities for the derivative of $\Sigma_{U,\sigma}^{\nu_4\nu_1}(\omega)$ with respect to eV which also hold at finite bias voltages.

The bias derivative can be carried out by applying the differential operator $\partial/\partial(eV)$ to the internal Green's functions in the self-energy diagrams of all order in U . Using also the chain rule with Eq. (5.22c) and the properties of the Green's-function products shown in Eq. (5.6), we obtain

$$\frac{\partial \Sigma_{U,\sigma}^{\nu_4\nu_1}(\omega)}{\partial eV} = - \int_{-\infty}^{\infty} \frac{d\omega'}{2\pi} \sum_{\sigma'} \sum_{\nu_2\nu_3} \Gamma_{\sigma\sigma';\sigma'\sigma}^{\nu_1\nu_2;\nu_3\nu_4}(\omega, \omega'; \omega', \omega) 2\Delta G_{\sigma'}^r(\omega') G_{\sigma'}^a(\omega') \left(-\frac{\partial f_{\text{eff}}(\omega')}{\partial eV} \right) \quad (5.32a)$$

$$\xrightarrow{T \rightarrow 0} - \sum_{\sigma'} \sum_{\nu_2\nu_3} \sum_{j=L,R} \Gamma_{\sigma\sigma';\sigma'\sigma}^{\nu_1\nu_2;\nu_3\nu_4}(\omega, \mu_j; \mu_j, \omega) \frac{\Delta}{\pi} G_{\sigma'}^r(\mu_j) G_{\sigma'}^a(\mu_j) \left(\frac{-\Gamma_j \mu_j}{\Delta eV} \right). \quad (5.32b)$$

At $T = 0$, the derivative $\partial f_{\text{eff}}(\omega')/\partial(eV)$ is replaced by the two Dirac delta functions at $\omega' = \mu_L, \mu_R$, similarly to that for the ω' derivative, mentioned above for Eq. (5.26). It also takes the following form in the zero-bias limit $eV \rightarrow 0$,

$$\left. \frac{\partial f_{\text{eff}}(\omega)}{\partial eV} \right|_{eV \rightarrow 0} = -\alpha_{\text{sh}} \frac{\partial f(\omega)}{\partial \omega}, \quad \alpha_{\text{sh}} \equiv \frac{\alpha_L \Gamma_L - \alpha_R \Gamma_R}{\Gamma_L + \Gamma_R}. \quad (5.33)$$

This relation holds at finite temperatures $T \neq 0$. There-

fore, the extended Ward identities given in Eqs. (5.24a) and (5.32a), reproduce the previous result in the zero-bias limit:¹⁸

$$\left. \frac{\partial \Sigma_{U,\sigma}(\omega)}{\partial eV} \right|_{eV \rightarrow 0} = \alpha_{\text{sh}} \sum_{\sigma'} \left(\delta_{\sigma\sigma'} \frac{\partial}{\partial\omega} + \frac{\partial}{\partial\epsilon_{d\sigma'}} \right) \Sigma_{\text{eq},\sigma}(\omega). \quad (5.34)$$

Note that, at $T = 0$, the causal component ($\nu_4 = \nu_1 = -$) can be calculated directly from Eq. (5.32b), using Eq.

(5.27a), as

$$\left. \frac{\partial \Sigma_{U,\sigma}^{\bar{-}}(\omega)}{\partial eV} \right|_{\substack{T \rightarrow 0 \\ eV \rightarrow 0}} = \alpha_{\text{sh}} \sum_{\sigma'} \Gamma_{\sigma\sigma';\sigma'\sigma}^{\bar{-};\bar{-}}(\omega, 0; 0, \omega) \rho_{d\sigma'}. \quad (5.35)$$

We next consider the second derivative of $\Sigma_{\sigma}(\omega)$ with respect to eV , extending the derivation given in Ref. 18. The double derivative can be carried out, applying the formula Eq. (5.22c) for $n = 1$ and 2 to the internal

$$\begin{aligned} \left. \frac{\partial^2 \Sigma_{U,\sigma}^{\nu_4\nu_1}(\omega)}{\partial (eV)^2} \right|_{eV \rightarrow 0} &= \alpha_{\text{sh}}^2 \left(\frac{\partial}{\partial \omega} + \frac{\partial}{\partial \epsilon_d} \right)^2 \Sigma_{\text{eq},\sigma}^{\nu_4\nu_1}(\omega) \\ &\quad - \frac{\Gamma_L \Gamma_R}{(\Gamma_L + \Gamma_R)^2} \int_{-\infty}^{\infty} \frac{d\omega'}{2\pi} \sum_{\sigma'} \sum_{\nu_2\nu_3} \Gamma_{\sigma\sigma';\sigma'\sigma}^{\nu_1\nu_2;\nu_3\nu_4}(\omega, \omega'; \omega', \omega) 2\Delta G_{\sigma'}^r(\omega') G_{\sigma'}^a(\omega') \left(-\frac{\partial^2 f(\omega')}{\partial \omega'^2} \right). \end{aligned} \quad (5.36)$$

Here, we have used the property $\partial/\partial\epsilon_d = \sum_{\sigma''} \partial/\partial\epsilon_{d\sigma''}$ in the first term in the right-hand side. This identity for the double derivative holds at any finite temperature, and reproduces the previous result given for the causal component at $T = 0$,²⁹

$$\begin{aligned} \left. \frac{\partial^2 \Sigma_{U,\sigma}^{\bar{-}}(\omega)}{\partial (eV)^2} \right|_{eV \rightarrow 0} &\xrightarrow{T \rightarrow 0} \alpha_{\text{sh}}^2 \left(\frac{\partial}{\partial \omega} + \frac{\partial}{\partial \epsilon_d} \right)^2 \Sigma_{U,\sigma}^{\bar{-}}(\omega) \\ &\quad + \frac{\Gamma_L \Gamma_R}{(\Gamma_L + \Gamma_R)^2} \Psi_{\sigma}^{\bar{-}}(\omega). \end{aligned} \quad (5.37)$$

Here, $\Psi_{\sigma}^{\bar{-}}(\omega)$ in the right-hand side is the function which is defined in Eq. (3.21), and it also determines the T^2 dependence of the self-energy. The bias dependence of the retarded self-energy shown in Eq. (3.23) can be deduced from these results, i.e. Eqs. (5.35) and (5.37).

VI. WARD-TAKAHASHI IDENTITY AT FINITE BIAS VOLTAGES

A. Three-point current vertex

In this section, we describe more general Ward-Takahashi identity, from which the Ward identities discussed in the above can naturally be deduced. It reflects current conservation around the quantum dot, and is derived nonperturbatively from the equation of motion of the Keldysh three-point functions of the charge and current through the Anderson impurity. We also discuss some important properties of the three-point functions as a preparation for diagrammatic calculations of the current noise $S_{\text{noise}}^{\text{QD}}$. In order to carry these things out, we extend the approach that has been used previously for the three-point functions in the Matsubara formalism to the nonequilibrium Keldysh correlation functions.^{57,58}

Green's functions for the self-energy diagrams with two different first-differentiated propagators and one second-differentiated propagator, respectively. All contributions of the perturbation series in U can be taken into account, using the Keldysh vertex connected to the matrix product of the interacting propagators $\mathbf{G}_{\sigma'}(\mathbf{1} - \boldsymbol{\tau}_1)\mathbf{G}_{\sigma'}$ that can be simplified further using Eq. (5.6), and it yields the following result,

We consider the three-point correlation function of the charge fluctuation $\delta n_{d\sigma} \equiv n_{d\sigma} - \langle n_{d\sigma} \rangle$ and that of the current fluctuations $\delta \hat{J}_{j\sigma} \equiv \hat{J}_{j\sigma} - \langle \hat{J}_{j\sigma} \rangle$ for $j = L, R$, defined with respect to the nonequilibrium steady state,

$$\begin{aligned} \Phi_{d,\sigma\sigma'}^{\alpha;\mu\nu}(t; t_1, t_2) &= -\langle T_C \delta n_{d\sigma'}(t^\alpha) d_\sigma(t_1^\mu) d_\sigma^\dagger(t_2^\nu) \rangle, \\ \Phi_{L,\sigma\sigma'}^{\alpha;\mu\nu}(t; t_1, t_2) &= -\langle T_C \delta \hat{J}_{L,\sigma'}(t^\alpha) d_\sigma(t_1^\mu) d_\sigma^\dagger(t_2^\nu) \rangle, \\ \Phi_{R,\sigma\sigma'}^{\alpha;\mu\nu}(t; t_1, t_2) &= -\langle T_C \delta \hat{J}_{R,\sigma'}(t^\alpha) d_\sigma(t_1^\mu) d_\sigma^\dagger(t_2^\nu) \rangle. \end{aligned} \quad (6.1)$$

Here, T_C is the time-ordering operator along the Keldysh time-loop contour. The indexes α, μ , and ν specify at which branches of the contour, forward – or backward +, the three time variables t, t_1 , and t_2 belong, respectively. Therefore, each of these three-point functions has 2³ Keldysh components which are linearly dependent, as shown in TABLE IV and Appendix A.

In the steady state that we are considering, the system has the time translation symmetry. Therefore, these three-point functions depend only on two frequency variables ϵ and ω , and the Fourier transform can be written in the following form,

$$\begin{aligned} \Phi_{\gamma,\sigma\sigma'}^{\alpha;\mu\nu}(t; t_1, t_2) &= \int \frac{d\epsilon d\omega}{(2\pi)^2} \Phi_{\gamma,\sigma\sigma'}^{\alpha;\mu\nu}(\epsilon, \epsilon + \omega) e^{-i\epsilon(t_1-t)} e^{-i(\epsilon+\omega)(t-t_2)}, \end{aligned} \quad (6.2)$$

where $\gamma = L, R, d$. We will use the matrix notation to express the Keldysh components, as $\{\Phi_{\gamma,\sigma\sigma'}^\alpha\}^{\mu\nu} = \Phi_{\gamma,\sigma\sigma'}^{\alpha;\mu\nu}$. Similarly, we also introduce the 2×2 matrix for the current vertex $\mathbf{\Lambda}_{\gamma,\sigma\sigma'}^\alpha$ which includes all vertex corrections due to the Coulomb interaction, as

$$\mathbf{\Phi}_{\gamma,\sigma\sigma'}^\alpha(\epsilon, \epsilon + \omega) = \mathbf{G}_\sigma(\epsilon) \mathbf{\Lambda}_{\gamma,\sigma\sigma'}^\alpha(\epsilon, \epsilon + \omega) \mathbf{G}_\sigma(\epsilon + \omega). \quad (6.3)$$

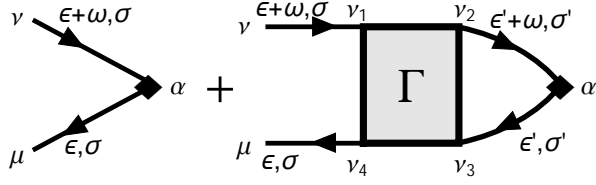


FIG. 6. Feynman diagrams for the three-point function $\Phi_{\gamma, \sigma \sigma'}^{\alpha; \mu \nu}(\epsilon, \epsilon + \omega)$ defined in Eq. (6.2) for $\gamma = L, R, d$. The black diamond (\blacklozenge) represents the bare current vertex $\lambda_{\gamma}^{\alpha}(\epsilon, \epsilon + \omega)$ defined in Eq. (6.9).

Figure 6 shows the Feynman diagrams for $\Phi_{\gamma, \sigma \sigma'}^{\alpha; \mu \nu}$. The current vertex $\Lambda_{\gamma, \sigma \sigma'}^{\alpha}$, corresponds to the remainder parts which are left over when the pair of the Green's functions with the frequency arguments $\epsilon + \omega$ and ϵ placed on the left side of each Feynman diagram are removed. We will discuss later that it can be expressed in terms of the four-point vertex functions, as Eq. (6.23).

1. Relation between current noise and $\Phi_{R/L, \sigma \sigma'}^{\alpha}$

It is essential for calculating the nonlinear current noise $S_{\text{noise}}^{\text{QD}}$ in the Fermi-liquid regime to know the low-energy behavior of these three-point correlations. For instance, the current-current correlations between $\hat{J}_{R, \sigma'}$ and $\hat{J}_{L, \sigma}$ can be expressed in terms of $\Phi_{R, \sigma \sigma'}^{\alpha}$, as

$$\begin{aligned}
 S_{RL} &\equiv e^2 \sum_{\sigma \sigma'} \int_{-\infty}^{\infty} dt \\
 &\quad \times \left[\langle \delta \hat{J}_{R, \sigma'}(t) \delta \hat{J}_{L, \sigma}(0) \rangle + \langle \delta \hat{J}_{L, \sigma}(0) \delta \hat{J}_{R, \sigma'}(t) \rangle \right] \\
 &= \frac{e^2}{\hbar} \sum_{\sigma \sigma'} \sum_{\alpha = +, -} \int_{-\infty}^{\infty} \frac{d\epsilon}{2\pi} \text{Tr} \left[\lambda_L^{-\alpha}(\epsilon, \epsilon) \Phi_{R, \sigma \sigma'}^{\alpha}(\epsilon, \epsilon) \right].
 \end{aligned} \tag{6.4}$$

Here, Tr denotes the trace that is taken over diagonal elements of the 2×2 Keldysh matrices. λ_L^{α} is the bare current vertex accompanied by the operator $\hat{J}_{L, \sigma}$. It is illustrated in Fig. 6 and its explicit form is given below in Eq. (6.9).

2. Current vertexes for $U = 0$: λ_L^{α} and λ_R^{α}

In the noninteracting case $U = 0$, the three-point correlation functions for the charge fluctuation $\delta n_{d\sigma}$ is given by,

$$\Phi_{d, \sigma \sigma'}^{(0)\alpha}(\epsilon, \epsilon + \omega) = \delta_{\sigma \sigma'} \mathbf{G}_{\sigma}^{(0)}(\epsilon) \boldsymbol{\rho}_3^{\alpha} \mathbf{G}_{\sigma}^{(0)}(\epsilon + \omega). \tag{6.5}$$

Here, the label (0) in superscript represents that the correlation function with this label is defined for noninteracting electrons $U = 0$, i.e. $\mathbf{G}_{\sigma}^{(0)} \equiv \mathbf{G}_{0\sigma}$. The matrix $\boldsymbol{\rho}_3^{\alpha}$ corresponds to the projection operator into the forward

(-) branch, or the backward (+) branch, of the Keldysh time-loop contour,

$$\boldsymbol{\rho}_3^{-} \equiv \frac{\mathbf{1} + \boldsymbol{\tau}_3}{2} = \begin{bmatrix} 1 & 0 \\ 0 & 0 \end{bmatrix}, \quad \boldsymbol{\rho}_3^{+} \equiv \frac{\mathbf{1} - \boldsymbol{\tau}_3}{2} = \begin{bmatrix} 0 & 0 \\ 0 & 1 \end{bmatrix}. \tag{6.6}$$

The corresponding three-point vertex $\Lambda_{d, \sigma \sigma'}^{(0)\alpha}$, can be derived from $\Phi_{d, \sigma \sigma'}^{(0)\alpha}$ using Eq. (6.5), as $\Lambda_{d, \sigma \sigma'}^{(0)\alpha} = \delta_{\sigma \sigma'} \lambda_d^{\alpha}$ with $\lambda_d^{\alpha} \equiv \boldsymbol{\rho}_3^{\alpha}$. This function $\Lambda_{d, \sigma \sigma'}^{(0)\alpha}$, becomes independent of the frequencies ϵ and ω for noninteracting electrons.

Similarly, for $U = 0$, the three-point correlation functions for current fluctuations take the following form, for $j = L, R$,

$$\begin{aligned}
 \Phi_{j, \sigma \sigma'}^{(0)\alpha}(\epsilon, \epsilon + \omega) &= i \eta_j v_j \delta_{\sigma \sigma'} \left[\mathbf{G}_{dj, \sigma}^{(0)}(\epsilon) \boldsymbol{\rho}_3^{\alpha} \mathbf{G}_{\sigma}^{(0)}(\epsilon + \omega) \right. \\
 &\quad \left. - \mathbf{G}_{\sigma}^{(0)}(\epsilon) \boldsymbol{\rho}_3^{\alpha} \mathbf{G}_{jd, \sigma}^{(0)}(\epsilon + \omega) \right] \\
 &= \delta_{\sigma \sigma'} \mathbf{G}_{\sigma}^{(0)}(\epsilon) \lambda_j^{\alpha}(\epsilon, \epsilon + \omega) \mathbf{G}_{\sigma}^{(0)}(\epsilon + \omega).
 \end{aligned} \tag{6.7}$$

Here, $\eta_L = -1$ and $\eta_R = +1$. The inter-site Green's functions between the dot and leads are written as $\mathbf{G}_{dj, \sigma}$ and $\mathbf{G}_{jd, \sigma}$. To obtain the last line of Eq. (6.7), we have used the recursive properties of these inter-site Green's functions which hold for both interacting and noninteracting electrons,

$$\begin{aligned}
 \mathbf{G}_{jd, \sigma}(\epsilon) &= -v_j \mathbf{g}_j(\epsilon) \boldsymbol{\tau}_3 \mathbf{G}_{\sigma}(\epsilon), \\
 \mathbf{G}_{dj, \sigma}(\epsilon) &= -v_j \mathbf{G}_{\sigma}(\epsilon) \boldsymbol{\tau}_3 \mathbf{g}_j(\epsilon).
 \end{aligned} \tag{6.8}$$

Here, \mathbf{g}_j is the Green's functions for the isolated lead on $j = L$ and R , defined in Eq. (5.13). Therefore, the bare current vertex can be written explicitly in the form,

$$\lambda_j^{\alpha}(\epsilon, \epsilon + \omega) \equiv i \eta_j v_j^2 \left[\boldsymbol{\rho}_3^{\alpha} \mathbf{g}_j(\epsilon + \omega) \boldsymbol{\tau}_3 - \boldsymbol{\tau}_3 \mathbf{g}_j(\epsilon) \boldsymbol{\rho}_3^{\alpha} \right]. \tag{6.9}$$

In particular, at $\omega = 0$, the bare current vertexes becomes independent of whether $\alpha = -$ or $+$, as

$$\begin{aligned}
 \lambda_R^{\alpha}(\epsilon, \epsilon) &= i \frac{v_R^2}{2} \left[\mathbf{g}_R(\epsilon) \boldsymbol{\tau}_3 - \boldsymbol{\tau}_3 \mathbf{g}_R(\epsilon) \right] \\
 &= 2\Gamma_R \begin{bmatrix} 0 & f_R \\ 1 - f_R & 0 \end{bmatrix},
 \end{aligned} \tag{6.10a}$$

$$\begin{aligned}
 \lambda_L^{\alpha}(\epsilon, \epsilon) &= -i \frac{v_L^2}{2} \left[\mathbf{g}_L(\epsilon) \boldsymbol{\tau}_3 - \boldsymbol{\tau}_3 \mathbf{g}_L(\epsilon) \right] \\
 &= -2\Gamma_L \begin{bmatrix} 0 & f_L \\ 1 - f_L & 0 \end{bmatrix}.
 \end{aligned} \tag{6.10b}$$

This can be verified, substituting the explicit form of the projection operator $\boldsymbol{\rho}_3^{\alpha}$ given in Eq. (6.6) into the right-hand side of Eq. (6.9).

For later convenience, we introduce the following two different linear combinations of λ_L^{α} and λ_R^{α} . One is for

the difference between incoming and outgoing currents through the dot $\hat{J}_{R,\sigma} - \hat{J}_{L,\sigma}$, and the other is for the symmetrized current $\hat{J}_\sigma \equiv (\Gamma_L \hat{J}_{R,\sigma} + \Gamma_R \hat{J}_{L,\sigma}) / (\Gamma_L + \Gamma_R)$ defined in Eq. (2.4),

$$\begin{aligned} \lambda_J^\alpha(\epsilon, \epsilon + \omega) &\equiv \lambda_R^\alpha(\epsilon, \epsilon + \omega) - \lambda_L^\alpha(\epsilon, \epsilon + \omega) \\ &\xrightarrow{\omega \rightarrow 0} 2(\Gamma_L + \Gamma_R) \begin{bmatrix} 0 & f_{\text{eff}}(\epsilon) \\ 1 - f_{\text{eff}}(\epsilon) & 0 \end{bmatrix}, \end{aligned} \quad (6.11)$$

$$\begin{aligned} \lambda_{\text{sym}}^\alpha(\epsilon, \epsilon + \omega) &\equiv \frac{\Gamma_L \lambda_R^\alpha(\epsilon, \epsilon + \omega) + \Gamma_R \lambda_L^\alpha(\epsilon, \epsilon + \omega)}{\Gamma_L + \Gamma_R} \\ &\xrightarrow{\omega \rightarrow 0} \frac{-2\Gamma_L \Gamma_R}{\Gamma_L + \Gamma_R} [f_L(\epsilon) - f_R(\epsilon)] \begin{bmatrix} 0 & 1 \\ -1 & 0 \end{bmatrix}. \end{aligned} \quad (6.12)$$

Each of these bare current vertexes shows a pronounced frequency dependence. While $\lambda_J^\alpha(\epsilon, \epsilon)$ represents the local nonequilibrium distribution $f_{\text{eff}}(\epsilon)$, the symmetrized part $\lambda_{\text{sym}}^\alpha(\epsilon, \epsilon)$ extracts the contributions of single-particle excitations inside the bias-window region through $f_L(\epsilon) - f_R(\epsilon)$.

B. Symmetrization of $\Lambda_{\gamma,\sigma\sigma'}^\alpha$ with respect to the forward and backward Keldysh contours

We also introduce another type symmetrization, defined with respect to the forward ($\alpha = -$) and the backward ($\alpha = +$) Keldysh branches: the symmetrized (S) part and anti-symmetrized (A) part of the three-point vertex functions are defined by

$$\Lambda_{p,\sigma\sigma'}^S(\epsilon, \epsilon + \omega) \equiv \Lambda_{p,\sigma\sigma'}^-(\epsilon, \epsilon + \omega) - \Lambda_{p,\sigma\sigma'}^+(\epsilon, \epsilon + \omega), \quad (6.13a)$$

$$\Lambda_{p,\sigma\sigma'}^A(\epsilon, \epsilon + \omega) \equiv \Lambda_{p,\sigma\sigma'}^-(\epsilon, \epsilon + \omega) + \Lambda_{p,\sigma\sigma'}^+(\epsilon, \epsilon + \omega). \quad (6.13b)$$

Here, the label p ($= L, R, d, J$, ‘‘sym’’) specifies the spatial components of the current and charge three-point vertex functions, including the difference $p = J$ and the average $p = \text{‘‘sym’’}$, the bare ones of which are defined in Eqs. (6.11) and (6.12), respectively.

For interacting electrons $U = 0$, the symmetrized and antisymmetrized three-point vertex functions for the impurity charge $\delta n_{d\sigma}$ are determined by Eqs. (6.5) and (6.6), as

$$\lambda_d^S \equiv \rho_3^- - \rho_3^+ = \tau_3, \quad \lambda_d^A \equiv \rho_3^- + \rho_3^+ = \mathbf{1}. \quad (6.14a)$$

Similarly, for the bare vertex functions for the current difference defined in Eq. (6.11), the symmetrized $\lambda_J^S \equiv \lambda_J^- - \lambda_J^+$ and anti-symmetrized $\lambda_J^A \equiv \lambda_J^- + \lambda_J^+$ vertexes

follow from Eq. (6.9), as

$$\lambda_J^S(\epsilon, \epsilon + \omega) = i \left[\Sigma_0(\epsilon + \omega) - \Sigma_0(\epsilon) \right] \quad (6.14b)$$

$$= -2(\Gamma_L + \Gamma_R) \left[f_{\text{eff}}(\epsilon + \omega) - f_{\text{eff}}(\epsilon) \right] \begin{bmatrix} 1 & -1 \\ -1 & 1 \end{bmatrix},$$

$$\lambda_J^A(\epsilon, \epsilon + \omega) = i \left[\tau_3 \Sigma_0(\epsilon + \omega) - \Sigma_0(\epsilon) \tau_3 \right] \quad (6.14c)$$

$$\xrightarrow{\omega \rightarrow 0} 4(\Gamma_L + \Gamma_R) \begin{bmatrix} 0 & f_{\text{eff}}(\epsilon) \\ 1 - f_{\text{eff}}(\epsilon) & 0 \end{bmatrix}.$$

While the symmetrized part $\lambda_J^S(\epsilon, \epsilon + \omega)$ is determined directly by the noninteracting self-energy Σ_0 given in Eq. (5.12), the antisymmetrized part λ_J^A is determined by the product of τ_3 and Σ_0 . Therefore, at $\omega = 0$, λ_J^A remains finite, whereas λ_J^S vanishes, but nevertheless its derivative has a pronounced property,

$$\begin{aligned} &\frac{\partial}{\partial \omega} \left[\mathbf{G}_\sigma(\epsilon) \lambda_J^S(\epsilon, \epsilon + \omega) \mathbf{G}_\sigma(\epsilon + \omega) \right]_{\omega \rightarrow 0} \\ &= \mathbf{G}_\sigma(\epsilon) i \frac{\partial \Sigma_0(\epsilon)}{\partial \epsilon} \mathbf{G}_\sigma(\epsilon) \\ &= -2\Delta G_\sigma^r(\epsilon) G_\sigma^a(\epsilon) \frac{\partial f_{\text{eff}}(\epsilon)}{\partial \epsilon} \begin{bmatrix} 1 & 1 \\ 1 & 1 \end{bmatrix}. \end{aligned} \quad (6.15)$$

For obtaining the last line, we have used Eqs. (5.6) and (5.14).

C. Ward-Takahashi identities for $\Phi_{\gamma,\sigma\sigma'}^\alpha$ and $\Lambda_{\gamma,\sigma\sigma'}^\alpha$

We now come to the point for discussing the Ward-Takahashi identity between the Keldysh three-point functions $\Phi_{d,\sigma\sigma'}^\alpha$, $\Phi_{R,\sigma\sigma'}^\alpha$, and $\Phi_{L,\sigma\sigma'}^\alpha$:

$$\begin{aligned} &i \frac{\partial}{\partial t} \Phi_{d,\sigma\sigma'}^\alpha(t; t_1, t_2) + i \Phi_{R,\sigma\sigma'}^\alpha(t; t_1, t_2) - i \Phi_{L,\sigma\sigma'}^\alpha(t; t_1, t_2) \\ &= -\delta_{\sigma\sigma'} \delta(t - t_1) \rho_3^\alpha \tau_3 \mathbf{G}_\sigma(t, t_2) \\ &\quad + \delta_{\sigma\sigma'} \delta(t_2 - t) \mathbf{G}_\sigma(t_1, t) \tau_3 \rho_3^\alpha. \end{aligned} \quad (6.16)$$

As shown in the proof given in Appendix B, this identity corresponds to the equation of motion of the charge component $\Phi_{d,\sigma\sigma'}^\alpha(t; t_1, t_2)$, and it reflects the current conservation between the dot and leads, described in Eq. (2.3). In the frequency domain, the Ward-Takahashi identity can be expressed in the following form, carrying out the Fourier transform as Eq. (6.2),

$$\begin{aligned} &\omega \Phi_{d,\sigma\sigma'}^\alpha(\epsilon, \epsilon + \omega) + i \Phi_{R,\sigma\sigma'}^\alpha(\epsilon, \epsilon + \omega) - i \Phi_{L,\sigma\sigma'}^\alpha(\epsilon, \epsilon + \omega) \\ &= -\delta_{\sigma\sigma'} \rho_3^\alpha \tau_3 \mathbf{G}_\sigma(\epsilon + \omega) + \delta_{\sigma\sigma'} \mathbf{G}_\sigma(\epsilon) \tau_3 \rho_3^\alpha. \end{aligned} \quad (6.17)$$

Furthermore, it can also be rewritten into the relation between the three-point vertex functions $\Lambda_{\gamma,\sigma\sigma'}^\alpha$ and the self-energy, using Eq. (6.3),

$$\begin{aligned} &\omega \Lambda_{d,\sigma\sigma'}^\alpha(\epsilon, \epsilon + \omega) + i \Lambda_{R,\sigma\sigma'}^\alpha(\epsilon, \epsilon + \omega) - i \Lambda_{L,\sigma\sigma'}^\alpha(\epsilon, \epsilon + \omega) \\ &= \delta_{\sigma\sigma'} \left[\omega \rho_3^\alpha - \rho_3^\alpha \tau_3 \Sigma_{\text{tot},\sigma}(\epsilon + \omega) + \Sigma_{\text{tot},\sigma}(\epsilon) \tau_3 \rho_3^\alpha \right]. \end{aligned} \quad (6.18)$$

Here, $\Sigma_{\text{tot},\sigma}(\epsilon) = \Sigma_0(\epsilon) + \Sigma_{U,\sigma}(\epsilon)$ is the total self-energy, and $\{\mathbf{G}_\sigma(\epsilon)\}^{-1} = (\epsilon - \epsilon_{d\sigma})\boldsymbol{\tau}_3 - \Sigma_{\text{tot},\sigma}(\epsilon)$, as shown in Eq. (5.16). We will show in the following that the Ward identity given in Eq. (5.24a) can be deduced non-perturbatively from the generalized one Eq. (6.18), in the limit where the external frequency to be $\omega \rightarrow 0$.

D. Symmetrized Ward-Takahashi identities

The Ward-Takahashi identity Eq. (6.18) can be rearranged into the symmetrized $\Lambda_{p,\sigma\sigma'}^S = \Lambda_{p,\sigma\sigma'}^- - \Lambda_{p,\sigma\sigma'}^+$ and the antisymmetrized $\Lambda_{p,\sigma\sigma'}^A = \Lambda_{p,\sigma\sigma'}^- + \Lambda_{p,\sigma\sigma'}^+$ parts, defined in Eq. (6.13), as

$$\omega \Lambda_{d,\sigma\sigma'}^S(\epsilon, \epsilon + \omega) + i \Lambda_{J,\sigma\sigma'}^S(\epsilon, \epsilon + \omega) = \delta_{\sigma\sigma'} \left[\omega \boldsymbol{\tau}_3 - \Sigma_{\text{tot},\sigma}(\epsilon + \omega) + \Sigma_{\text{tot},\sigma}(\epsilon) \right], \quad (6.19a)$$

$$\omega \Lambda_{d,\sigma\sigma'}^A(\epsilon, \epsilon + \omega) + i \Lambda_{J,\sigma\sigma'}^A(\epsilon, \epsilon + \omega) = \delta_{\sigma\sigma'} \left[\omega \mathbf{1} - \boldsymbol{\tau}_3 \Sigma_{\text{tot},\sigma}(\epsilon + \omega) + \Sigma_{\text{tot},\sigma}(\epsilon) \boldsymbol{\tau}_3 \right]. \quad (6.19b)$$

Here, $\Lambda_{J,\sigma\sigma'}^q \equiv \Lambda_{R,\sigma\sigma'}^q - \Lambda_{L,\sigma\sigma'}^q$ with the label q ($= -, +, S, A$) which specifies the time-loop components. Equation (6.19b) shows that the antisymmetrized current vertex $\Lambda_{J,\sigma\sigma'}^A$ remains finite for $\omega \rightarrow 0$, similarly to

the noninteracting one λ_J^A given in Eq. (6.14c),

$$i \Lambda_{J,\sigma\sigma'}^A(\epsilon, \epsilon) = \delta_{\sigma\sigma'} \left[\Sigma_{\text{tot},\sigma}(\epsilon) \boldsymbol{\tau}_3 - \boldsymbol{\tau}_3 \Sigma_{\text{tot},\sigma}(\epsilon) \right] = 2 \begin{bmatrix} 0 & -\Sigma_{\text{tot},\sigma}^+(\epsilon) \\ \Sigma_{\text{tot},\sigma}^+(\epsilon) & 0 \end{bmatrix} \delta_{\sigma\sigma'}. \quad (6.20)$$

In contrast, Eq. (6.19a) shows that the symmetrized component vanishes for $\omega \rightarrow 0$, i.e., $\Lambda_{J,\sigma\sigma'}^S(\epsilon, \epsilon) = 0$. Nevertheless, the ω derivative remains finite,

$$\Lambda_{d,\sigma\sigma'}^S(\epsilon, \epsilon) + i \left. \frac{\partial}{\partial \omega} \Lambda_{J,\sigma\sigma'}^S(\epsilon, \epsilon + \omega) \right|_{\omega \rightarrow 0} = \delta_{\sigma\sigma'} \left[\boldsymbol{\tau}_3 - \frac{\partial \Sigma_{\text{tot},\sigma}(\epsilon)}{\partial \epsilon} \right]. \quad (6.21)$$

This equation is identical to the Ward identity given in Eq. (5.24a). In order to see it more clearly, we rewrite the left-hand side of Eq. (6.21) further.

Contributions of the charge fluctuation term $\Lambda_{d,\sigma\sigma'}^S(\epsilon, \epsilon)$ in the left-hand side of Eq. (6.21) can be separated into two parts described diagrammatically shown in Fig. 6. The first diagram corresponds simply to the bare vertex $\boldsymbol{\tau}_3 \delta_{\sigma\sigma'}$, and the second diagram gives contributions which are exactly the same as the right-hand side of Eq. (5.23). Therefore, $\Lambda_{d,\sigma\sigma'}^S(\epsilon, \epsilon)$ can be expressed in terms of the self-energy, as

$$\Lambda_{d,\sigma\sigma'}^S(\epsilon, \epsilon) = \boldsymbol{\tau}_3 \delta_{\sigma\sigma'} + \frac{\partial \Sigma_{U,\sigma}(\epsilon)}{\partial \epsilon_{d\sigma'}}. \quad (6.22)$$

More generally, contributions of the two diagrams for $\Lambda_{p,\sigma\sigma'}^q(\epsilon, \epsilon + \omega)$ shown in Fig. 6 can be expressed in terms of the four-point Keldysh vertex functions,

$$\Lambda_{p,\sigma\sigma'}^{q:\nu\mu}(\epsilon, \epsilon + \omega) = \delta_{\sigma\sigma'} \lambda_p^{q:\nu\mu}(\epsilon, \epsilon + \omega) + \int_{-\infty}^{\infty} \frac{d\epsilon'}{2\pi i} \sum_{\mu'\nu'} \Gamma_{\sigma\sigma';\sigma'\sigma}^{\mu\mu';\nu'\nu}(\epsilon + \omega, \epsilon'; \epsilon', \epsilon) \{ \mathbf{G}_{\sigma'}(\epsilon') \boldsymbol{\lambda}_p^q(\epsilon', \epsilon' + \omega) \mathbf{G}_{\sigma'}(\epsilon' + \omega) \}^{\nu'\mu'}, \quad (6.23)$$

for any q ($= -, +, S, A$) and any p ($= d, L, R, J$, “sym”). Therefore, the second term $i \frac{\partial}{\partial \omega} \Lambda_{J,\sigma\sigma'}^S(\epsilon, \epsilon + \omega)$ in the left-hand side of Eq. (6.21) can be expressed in the following form, using Eq. (6.23) and the properties of the bare vertex $\lambda_J^S(\epsilon, \epsilon + \omega)$ shown in Eqs. (6.14b) and (6.15), as

$$i \left. \frac{\partial}{\partial \omega} \Lambda_{J,\sigma\sigma'}^{S:\nu\mu}(\epsilon, \epsilon + \omega) \right|_{\omega \rightarrow 0} = -\delta_{\sigma\sigma'} \left\{ \frac{\partial \Sigma_0(\epsilon)}{\partial \epsilon} \right\}^{\nu\mu} + \int_{-\infty}^{\infty} \frac{d\epsilon'}{2\pi} \sum_{\mu'\nu'} \Gamma_{\sigma\sigma';\sigma'\sigma}^{\mu\mu';\nu'\nu}(\epsilon, \epsilon'; \epsilon', \epsilon) 2\Delta G_{\sigma'}^r(\epsilon') G_{\sigma'}^a(\epsilon') \left(-\frac{\partial f_{\text{eff}}(\epsilon')}{\partial \epsilon'} \right). \quad (6.24)$$

Finally, substituting Eqs. (6.22) and (6.24) into Eq. (6.21), we obtain the same result as Eq. (5.24a) from the symmetrized part of the Ward-Takahashi identity,

$$\left(\delta_{\sigma\sigma'} \frac{\partial}{\partial \epsilon} + \frac{\partial}{\partial \epsilon_{d\sigma'}} \right) \Sigma_{U,\sigma}^{\nu\mu}(\epsilon) = - \int_{-\infty}^{\infty} \frac{d\epsilon'}{2\pi} \sum_{\mu'\nu'} \Gamma_{\sigma\sigma';\sigma'\sigma}^{\mu\mu';\nu'\nu}(\epsilon, \epsilon'; \epsilon', \epsilon) 2\Delta G_{\sigma'}^r(\epsilon') G_{\sigma'}^a(\epsilon') \left(-\frac{\partial f_{\text{eff}}(\epsilon')}{\partial \epsilon'} \right). \quad (6.25)$$

In addition, the antisymmetrized part of the Ward-Takahashi identity for $\Lambda_{J,\sigma\sigma'}^{A:\nu\mu}(\epsilon, \epsilon + \omega)$ also provides important information about the relation between the self-energy and the four-point vertex functions. For instance, at $\omega = 0$,

Eq. (6.20) can be rewritten as an integral-form relation, using Eq. (6.23) for $q = A$ and $p = J$ with the property of the bare vertex $\lambda_{J,\sigma\sigma'}^{A:\nu\mu}(\epsilon, \epsilon + \omega)$ shown in Eq. (6.14c):

$$\begin{bmatrix} 0 & -\Sigma_{U,\sigma}^{+-}(\epsilon) \\ \Sigma_{U,\sigma}^{+-}(\epsilon) & 0 \end{bmatrix}_{\nu\mu} \delta_{\sigma\sigma'} = \int_{-\infty}^{\infty} \frac{d\epsilon'}{2\pi} \sum_{\mu'\nu'} \Gamma_{\sigma\sigma';\sigma'\sigma}^{\mu\mu';\nu'\nu}(\epsilon, \epsilon'; \epsilon', \epsilon) 2\Delta \left\{ \mathbf{G}_{\sigma'}(\epsilon') \begin{bmatrix} 0 & f_{\text{eff}}(\epsilon') \\ 1 - f_{\text{eff}}(\epsilon') & 0 \end{bmatrix} \mathbf{G}_{\sigma'}(\epsilon') \right\}^{\nu'\mu'}. \quad (6.26)$$

Physically, it represents the relation between the damping of a single quasiparticle in the left-hand side and the effects of the multiple collisions of two quasiparticles in the right-hand side.

VII. COLLISION INTEGRALS FOR THE FERMI LIQUID AT FINITE BIAS VOLTAGES

In this section, we consider the low-energy behavior of the Keldysh self-energies other than the retarded $\Sigma_{U,\sigma}^r(\omega)$ or advanced $\Sigma_{U,\sigma}^a(\omega)$ one. We also describe the particle-hole and particle-particle excitations that determine the imaginary part of the Keldysh vertex functions in the Fermi-liquid regime.

A. Lesser and greater self-energies in the Fermi-liquid regime

The lesser and greater self-energies, $\Sigma_{U,\sigma}^{+-}(\omega)$ and $\Sigma_{U,\sigma}^{+}(\omega)$, are both pure imaginary in the frequency domain, and these two components determine the imaginary part of the other self-energy components, as it can be deduced from Eqs. (5.17) and (5.18). We have already discussed low-energy behavior of the retarded self-energy, the imaginary part of which is given by $2i \text{Im} \Sigma_{U,\sigma}^r(\omega) = \Sigma_{U,\sigma}^{+}(\omega) - \Sigma_{U,\sigma}^{+-}(\omega)$. However, for calculating the nonlinear current noise $S_{\text{noise}}^{\text{QD}}$ up to terms of order $(eV)^3$, the low-energy asymptotic of another independent component $\Sigma_{U,\sigma}^K(\omega) = \Sigma_{U,\sigma}^{+}(\omega) + \Sigma_{U,\sigma}^{+-}(\omega)$ is also necessary.

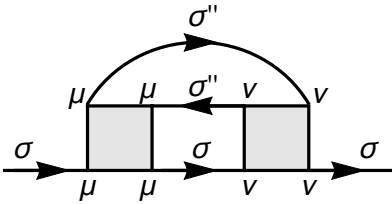


FIG. 7. Feynman diagram for $\Sigma_{\sigma}^{\nu\mu}(\omega)$ which yields order ω^2 , $(eV)^2$, T^2 imaginary part. The shaded square represents the scattering amplitude of quasiparticles that is given by the full vertex correction $\Gamma_{\sigma,\sigma'';\sigma''\sigma}^{\nu\nu;\nu\nu}(0,0;0,0)$ defined at $T = eV = 0$. The inter-level components $\sigma'' \neq \sigma$ of the scattering amplitude is real and finite, whereas the intra-level ones identically vanish since $\Gamma_{\sigma\sigma;\sigma\sigma}^{\nu\nu;\nu\nu}(0,0;0,0) = 0$ at zero frequencies as a result of the Pauli exclusion rule.^{14,56}

1. Fermionic collision integrals for quasiparticles

The imaginary part of the self-energy $\Sigma_{U,\sigma}^{\nu\mu}(\omega)$ can be deduced exactly from the scattering process shown in Fig. 7 up to terms of order ω^2 , T^2 , and $(eV)^2$.^{14,56} In particular, the low-energy asymptotic forms of the lesser and greater self-energies can be expressed in terms of the collision integrals of quasiparticles, which in the equilibrium limit $eV \rightarrow 0$ take the form,⁵⁹

$$\begin{aligned} \mathcal{I}_{\text{eq}}^{+-}(\omega) &\equiv \int d\varepsilon_1 \int d\varepsilon_2 [1 - f(\varepsilon_1)] [1 - f(\varepsilon_2)] f(\varepsilon_1 + \varepsilon_2 - \omega) \\ &= \frac{\omega^2 + (\pi T)^2}{2} [1 - f(\omega)], \end{aligned} \quad (7.1a)$$

$$\begin{aligned} \mathcal{I}_{\text{eq}}^{-+}(\omega) &\equiv \int d\varepsilon_1 \int d\varepsilon_2 f(\varepsilon_1) f(\varepsilon_2) [1 - f(\varepsilon_1 + \varepsilon_2 - \omega)] \\ &= \frac{\omega^2 + (\pi T)^2}{2} f(\omega). \end{aligned} \quad (7.1b)$$

Physically, $\mathcal{I}_{\text{eq}}^{+-}(\omega)$ and $\mathcal{I}_{\text{eq}}^{-+}(\omega)$ determine the damping rate of a single quasiparticle and a single quasihole, respectively. At finite eV , these collision integrals are extended to the following form, replacing the Fermi function in Eq. (7.1) by the nonequilibrium distribution function $f_{\text{eff}}(\omega)$, as

$$\begin{aligned} \mathcal{I}^{+-}(\omega) &\equiv \int_{-\infty}^{\infty} d\omega_1 \int_{-\infty}^{\infty} d\omega_2 \\ &\times [1 - f_{\text{eff}}(\omega_1)] [1 - f_{\text{eff}}(\omega_2)] f_{\text{eff}}(\omega_1 + \omega_2 - \omega) \\ &= \sum_{\substack{j,k,\ell \\ =L,R}} \frac{\Gamma_j \Gamma_k \Gamma_\ell}{\Delta^3} \mathcal{I}_{\text{eq}}^{+-}(\omega - \mu_j - \mu_k + \mu_\ell), \end{aligned} \quad (7.2a)$$

$$\begin{aligned} \mathcal{I}^{-+}(\omega) &\equiv \int_{-\infty}^{\infty} d\omega_1 \int_{-\infty}^{\infty} d\omega_2 \\ &\times f_{\text{eff}}(\omega_1) f_{\text{eff}}(\omega_2) [1 - f_{\text{eff}}(\omega_1 + \omega_2 - \omega)] \\ &= \sum_{\substack{j,k,\ell \\ =L,R}} \frac{\Gamma_j \Gamma_k \Gamma_\ell}{\Delta^3} \mathcal{I}_{\text{eq}}^{-+}(\omega - \mu_j - \mu_k + \mu_\ell). \end{aligned} \quad (7.2b)$$

In the Fermi-liquid regime, the damping rate of a quasiparticle is determined by the collision processes, illustrated in Fig. 7, in which a single particle-hole

pair with spin σ'' is virtually excited in the intermediate states by an incident quasiparticle with spin σ via the scattering amplitude, given by the vertex functions $\Gamma_{\sigma\sigma'';\sigma''\sigma}^{\nu\nu;\nu\nu}(0,0;0,0)$ at $\omega = eV = T = 0$ that include all effects of multiple scatterings. The lesser and greater self-energies caused by this processes can be expressed in terms of $\mathcal{I}^{-+}(\omega)$ and $\mathcal{I}^{+-}(\omega)$,

$$\begin{aligned}\Sigma_{U,\sigma}^{-+}(\omega) &= \sum_{\sigma''(\neq\sigma)} \int \frac{d\omega_1}{2\pi} \int \frac{d\omega_2}{2\pi} \\ &\quad \times \Gamma_{\sigma''\sigma;\sigma\sigma''}^{-;-;--}(0,0;0,0) \Gamma_{\sigma\sigma'';\sigma''\sigma}^{++;++;++}(0,0;0,0) \\ &\quad \times G_{\sigma}^{-+}(\omega_1) G_{\sigma''}^{-+}(\omega_2) G_{\sigma''}^{+-}(\omega_1 + \omega_2 - \omega) + \dots \\ &= -i2\pi \sum_{\sigma''(\neq\sigma)} \left| \Gamma_{\sigma\sigma'';\sigma''\sigma}^{-;-;--}(0,0;0,0) \right|^2 \rho_{d\sigma} \{ \rho_{d\sigma''} \}^2 \mathcal{I}^{-+}(\omega) \\ &\quad + \dots, \quad (7.3)\end{aligned}$$

$$\begin{aligned}\Sigma_{U,\sigma}^{+-}(\omega) &= \sum_{\sigma''(\neq\sigma)} \int \frac{d\omega_1}{2\pi} \int \frac{d\omega_2}{2\pi} \\ &\quad \times \Gamma_{\sigma\sigma'';\sigma''\sigma}^{++;++;++}(0,0;0,0) \Gamma_{\sigma''\sigma;\sigma\sigma''}^{-;-;--}(0,0;0,0) \\ &\quad \times G_{\sigma}^{+-}(\omega_1) G_{\sigma''}^{+-}(\omega_2) G_{\sigma''}^{-+}(\omega_1 + \omega_2 - \omega) + \dots \\ &= i2\pi \sum_{\sigma''(\neq\sigma)} \left| \Gamma_{\sigma\sigma'';\sigma''\sigma}^{-;-;--}(0,0;0,0) \right|^2 \rho_{d\sigma} \{ \rho_{d\sigma''} \}^2 \mathcal{I}^{+-}(\omega) \\ &\quad + \dots. \quad (7.4)\end{aligned}$$

These expressions are exact up to terms of order ω^2 , $(eV)^2$, and T^2 , and reproduce the previous results calculated specifically at $T = 0$ by Aligia,¹⁹ using the renormalized perturbation theory.⁴⁷ In order to obtain the last lines of Eq. (7.3) and Eq. (7.4), we have rewritten the lesser and greater Green's functions in the integrands in the following form, using Eq. (5.19),

$$\begin{aligned}G_{\sigma}^{-+}(\omega) &= - \left[\Sigma_0^{-+}(\omega) + \Sigma_{U,\sigma}^{-+}(\omega) \right] G_{\sigma}^r(\omega) G_{\sigma}^a(\omega) \\ &\simeq - \Sigma_0^{-+}(\omega) G_{\text{eq},\sigma}^r(0) G_{\text{eq},\sigma}^a(0), \quad (7.5a)\end{aligned}$$

$$\begin{aligned}G_{\sigma}^{+-}(\omega) &= - \left[\Sigma_0^{+-}(\omega) + \Sigma_{U,\sigma}^{+-}(\omega) \right] G_{\sigma}^r(\omega) G_{\sigma}^a(\omega) \\ &\simeq - \Sigma_0^{+-}(\omega) G_{\text{eq},\sigma}^r(0) G_{\text{eq},\sigma}^a(0). \quad (7.5b)\end{aligned}$$

In the second line of each equations the total self-energy in the first line has been replaced by the the noninteracting one: $\Sigma_0^{-+}(\omega) = -2i\Delta f_{\text{eff}}(\omega)$, or $\Sigma_0^{+-}(\omega) = 2i\Delta[1 - f_{\text{eff}}(\omega)]$, given in Eq. (5.12). This is because the interacting self-energies $\Sigma_{U,\sigma}^{-+}(\omega)$ and $\Sigma_{U,\sigma}^{+-}(\omega)$ themselves show ω^2 , $(eV)^2$, and T^2 dependences at low energies as it can be deduced from the perturbation theory in U , and they yield corrections that are higher than the leading-order ones for Eq. (7.3) and Eq. (7.4). Furthermore, in Eq. (7.5), the retarded and advanced Green's functions have been replaced by the value at $\omega = eV = T = 0$, i.e. $G_{\text{eq},\sigma}^r(0) G_{\text{eq},\sigma}^a(0) = \pi\rho_{d\sigma}/\Delta$ in the last line of each equation.

Note that the vertex correction that appeared in Eqs. (7.3) and (7.4) can be expressed in terms of the static susceptibility $\chi_{\sigma\sigma''}$ for different spin components $\sigma \neq \sigma''$, using the Fermi-liquid relations given in Eqs. (3.5) and (3.12), as

$$\chi_{\sigma\sigma''} = -\rho_{d\sigma}\rho_{d\sigma''}\Gamma_{\sigma\sigma'';\sigma''\sigma}^{-;-;--}(0,0;0,0). \quad (7.6)$$

2. Symmetrization of the fermionic collision integrals

One can also deduce the imaginary part of the retarded self-energy given in Eq. (3.23b) in another way, from the difference between the lesser and greater ones $2i \text{Im} \Sigma_{U,\sigma}^r(\omega) = \Sigma_{U,\sigma}^{-+}(\omega) - \Sigma_{U,\sigma}^{+-}(\omega)$, using Eqs. (7.1)–(7.4). The leading-order terms in the Fermi-liquid regime are determined by the sum of the single-quasiparticle collision integrals $\mathcal{I}^{+-}(\omega) + \mathcal{I}^{-+}(\omega)$,

$$\begin{aligned}\mathcal{I}_{\text{diff}}(\omega) &\equiv 2 \left[\mathcal{I}^{+-}(\omega) + \mathcal{I}^{-+}(\omega) \right] \\ &= \left(\omega - \alpha_{eV} eV \right)^2 + \frac{3\Gamma_L \Gamma_R}{(\Gamma_L + \Gamma_R)^2} (eV)^2 + (\pi T)^2. \quad (7.7)\end{aligned}$$

Note that $\mathcal{I}_{\text{eq}}^{+-}(\omega) + \mathcal{I}_{\text{eq}}^{-+}(\omega) = \omega^2 + (\pi T)^2$ and the Fermi distribution disappears from this sum Eq. (7.1).

In contrast, $\Sigma_{U,\sigma}^K(\omega)$ component is determined by the difference $\mathcal{I}^{+-}(\omega) - \mathcal{I}^{-+}(\omega)$ between the two collision terms, up to terms of order ω^2 , T^2 , and $(eV)^2$, as

$$\frac{\Sigma_{U,\sigma}^{-+}(\omega) + \Sigma_{U,\sigma}^{+-}(\omega)}{2i} = \frac{\pi}{2\rho_{d\sigma}} \sum_{\sigma''(\neq\sigma)} \chi_{\sigma\sigma''}^2 \mathcal{I}_K(\omega) + \dots. \quad (7.8)$$

$$\begin{aligned}\mathcal{I}_K(\omega) &\equiv 2 \left[\mathcal{I}^{+-}(\omega) - \mathcal{I}^{-+}(\omega) \right] \\ &= \sum_{j,k,\ell=L,R} \frac{\Gamma_j \Gamma_k \Gamma_\ell}{\Delta^3} \left[(\pi T)^2 + (\omega - \mu_j - \mu_k + \mu_\ell)^2 \right] \\ &\quad \times \tanh \left(\frac{\omega - \mu_j - \mu_k + \mu_\ell}{2T} \right). \quad (7.9)\end{aligned}$$

We have also shown in TABLE V an alternative expression, carrying out the summation over j, k, ℓ explicitly. In some special cases, it takes a simplified form. For example, at equilibrium $eV \rightarrow 0$, it is given by $\mathcal{I}_K(\omega) \xrightarrow{eV \rightarrow 0} [\omega^2 + (\pi T)^2] \tanh(\frac{\omega}{2T})$. At zero temperature, the hyperbolic function that comes from the Fermi function is replaced by the sign function, as $1 - 2f(\omega) = \tanh \frac{\omega}{2T} \xrightarrow{T \rightarrow 0} \text{sgn} \omega$. Furthermore, for symmetric junctions $\Gamma_L = \Gamma_R = \Delta/2$ and symmetric bias voltages

$\mu_L = -\mu_R = eV/2$, it takes the following form at $T = 0$,

$$\begin{aligned} \mathcal{I}_K(\omega) \rightarrow \frac{1}{8} & \left[\left(\omega - \frac{3eV}{2} \right)^2 \operatorname{sgn} \left(\omega - \frac{3eV}{2} \right) \right. \\ & + 3 \left(\omega - \frac{eV}{2} \right)^2 \operatorname{sgn} \left(\omega - \frac{eV}{2} \right) \\ & + 3 \left(\omega + \frac{eV}{2} \right)^2 \operatorname{sgn} \left(\omega + \frac{eV}{2} \right) \\ & \left. + \left(\omega + \frac{3eV}{2} \right)^2 \operatorname{sgn} \left(\omega + \frac{3eV}{2} \right) \right]. \quad (7.10) \end{aligned}$$

We will show later in Sec. VIII that these results of the self-energies satisfy the Ward identities with the low-energy results of the vertex corrections listed in TABLES VII and VIII.

B. Particle-hole pair and particle-particle pair excitations in the Fermi-liquid regime

We have reexamined in the above that the leading-order terms of the imaginary part of the self-energies are determined by the three internal propagators which represent virtually excited quasiparticles and holes. Correspondingly, the leading-order terms of the imaginary part of the vertex functions $\Gamma_{\sigma\sigma';\sigma''\sigma}^{\nu\nu';\nu\nu''}(\omega, \omega'; \omega', \omega)$ are determined by four types of collision processes, illustrated in

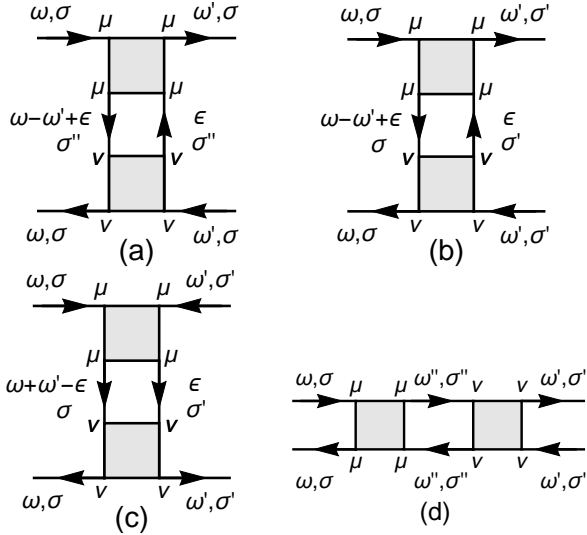


FIG. 8. Feynman diagrams for the Keldysh vertex functions $\Gamma_{\sigma\sigma';\sigma''\sigma}^{\nu\nu';\nu\nu''}(\omega, \omega'; \omega', \omega)$ which yield the imaginary part up to linear-order terms with respect to ω , ω' , eV , and T . The shaded square represents the scattering amplitude of quasiparticles that is given by the full vertex correction $\Gamma_{\sigma\sigma';\sigma''\sigma}^{\nu\nu';\nu\nu''}(0, 0; 0, 0)$ defined at $T = eV = 0$. The inter-level components $\sigma'' \neq \sigma$ of the scattering amplitude is real and finite, whereas the intra-level ones identically vanish since $\Gamma_{\sigma\sigma';\sigma\sigma}^{\nu\nu';\nu\nu''}(0, 0; 0, 0) = 0$ at zero frequencies as a result of the Pauli exclusion rule.

Fig. 8. The particle-hole (PH) and particle-particle (PP) pairs which propagate in between the shaded squares (vertex functions) determine the damping rate up to terms of order ω , ω' , eV , and T .

1. Bosonic collision integrals for PH and PP excitations

Leaving precise calculations of the Keldysh vertex functions to Appendix C, here we consider the low-energy behavior of the PH and PP propagators, $X_{\sigma\sigma'}^{\mu\nu}(\omega)$ and $Y_{\sigma\sigma'}^{\mu\nu}(\omega)$, defined later in Eq. (7.16). The low-energy behaviors of the imaginary parts of the PH and PP propagators up to the linear-order terms with respect to ω , eV , and T can be described in terms of the collision integrals $\mathcal{W}^{\text{ph}}(\omega)$, $\mathcal{W}^{\text{pp}}(\omega)$, and $\mathcal{W}^{\text{hh}}(\omega)$, defined below in Eq. (7.12)–(7.14). In this and the next section, we provide a nonequilibrium Fermi-liquid description, using these bosonic collision integrals.

To this end, we start with the equilibrium case $eV = 0$, at which the damping of the PH and PP excitations are determined by a single bosonic collision integral,

$$\begin{aligned} \mathcal{W}_{\text{eq}}(\omega) & \equiv \int_{-\infty}^{\infty} d\varepsilon f(\varepsilon) \left[1 - f(\varepsilon + \omega) \right] \\ & = \left[1 + b(\omega) \right] \lim_{D \rightarrow \infty} \int_{-D}^{\infty} d\varepsilon \left[f(\varepsilon) - f(\varepsilon + \omega) \right] \\ & = \frac{\omega}{2} \left[\coth \frac{\omega}{2T} + 1 \right]. \quad (7.11) \end{aligned}$$

Here, $b(\omega) = [e^{\omega/T} - 1]^{-1}$ is the Bose function. Note that $\omega \coth(\frac{\omega}{2T}) \simeq 2T$ for $|\omega| \ll T$, and $\omega \coth(\frac{\omega}{2T}) \simeq |\omega|$ for $|\omega| \gg T$. Thus, $\mathcal{W}_{\text{eq}}(\omega) \xrightarrow{T \rightarrow 0} |\omega| \theta(\omega)$ at $T \rightarrow 0$.

We now introduce the nonequilibrium bosonic collision integral $\mathcal{W}^{\text{ph}}(\omega)$ which determines the imaginary part of the PH propagator at finite eV , replacing the Fermi function $f(\varepsilon)$ in Eq. (7.11) by $f_{\text{eff}}(\varepsilon)$,

$$\begin{aligned} \mathcal{W}^{\text{ph}}(\omega) & \equiv \int_{-\infty}^{\infty} d\varepsilon f_{\text{eff}}(\varepsilon) \left[1 - f_{\text{eff}}(\varepsilon + \omega) \right] \\ & = \sum_{j,k=L,R} \frac{\Gamma_j \Gamma_k}{\Delta^2} \mathcal{W}_{\text{eq}}(\omega + \mu_j - \mu_k). \quad (7.12) \end{aligned}$$

Furthermore, the time-reversal processes describes the propagation of a single pair which consists of a quasiparticle with frequency ε' and a quasihole with $\varepsilon' + \omega$, as

$$\mathcal{W}^{\text{ph}}(-\omega) = \int_{-\infty}^{\infty} d\varepsilon' f_{\text{eff}}(\varepsilon' + \omega) \left[1 - f_{\text{eff}}(\varepsilon') \right]. \quad (7.13)$$

Similarly, the collision integrals for the single particle-particle pair and hole-hole pair are also given, respec-

TABLE V. Fermionic collision integral $\mathcal{I}_K(\omega)$, and low-energy asymptotic form of the self-energy at finite bias $eV = \mu_L - \mu_R$. The parameter α_{sh} is defined such that $\alpha_{\text{sh}} eV = (\Gamma_L \mu_L + \Gamma_R \mu_R)/(\Gamma_L + \Gamma_R)$.

$$\begin{aligned}
\mathcal{I}_K(\omega) &\equiv 2 \int d\varepsilon_1 \int d\varepsilon_2 \left\{ \left[1 - f_{\text{eff}}(\varepsilon_1) \right] \left[1 - f_{\text{eff}}(\varepsilon_2) \right] f_{\text{eff}}(\varepsilon_1 + \varepsilon_2 - \omega) - f_{\text{eff}}(\varepsilon_1) f_{\text{eff}}(\varepsilon_2) \left[1 - f_{\text{eff}}(\varepsilon_1 + \varepsilon_2 - \omega) \right] \right\}, \\
&= \frac{\Gamma_L^2 \Gamma_R}{(\Gamma_L + \Gamma_R)^3} \left[(\pi T)^2 + (\omega - \mu_L - eV)^2 \right] \tanh \frac{\omega - \mu_L - eV}{2T} + \frac{\Gamma_L^3 + 2\Gamma_L \Gamma_R^2}{(\Gamma_L + \Gamma_R)^3} \left[(\pi T)^2 + (\omega - \mu_L)^2 \right] \tanh \frac{\omega - \mu_L}{2T} \\
&\quad + \frac{\Gamma_R^3 + 2\Gamma_L^2 \Gamma_R}{(\Gamma_L + \Gamma_R)^3} \left[(\pi T)^2 + (\omega - \mu_R)^2 \right] \tanh \frac{\omega - \mu_R}{2T} + \frac{\Gamma_L \Gamma_R^2}{(\Gamma_L + \Gamma_R)^3} \left[(\pi T)^2 + (\omega - \mu_R + eV)^2 \right] \tanh \frac{\omega - \mu_R + eV}{2T}.
\end{aligned}$$

$$\begin{aligned}
\Sigma_{U,\sigma}^{+}(\omega) + \Sigma_{U,\sigma}^{+-}(\omega) &= i \frac{\pi}{\rho_{d\sigma}} \sum_{\sigma'(\neq\sigma)} \chi_{\sigma\sigma'}^2 \mathcal{I}_K(\omega) + \dots, \\
\Sigma_{U,\sigma}^{+}(\omega) - \Sigma_{U,\sigma}^{+-}(\omega) &= -i \frac{\pi}{\rho_{d\sigma}} \sum_{\sigma'(\neq\sigma)} \chi_{\sigma\sigma'}^2 \left[(\omega - \alpha_{\text{sh}} eV)^2 + \frac{3\Gamma_L \Gamma_R}{(\Gamma_L + \Gamma_R)^2} (eV)^2 + (\pi T)^2 \right] + \dots, \\
\text{Re } \Sigma_{U,\sigma}^r(\omega) &= \Sigma_{\text{eq},\sigma}^r(0) + (1 - \tilde{\chi}_{\sigma\sigma}) \omega + \frac{1}{2} \frac{\partial \tilde{\chi}_{\sigma\sigma}}{\partial \varepsilon_{d\sigma}} \omega^2 + \frac{1}{6} \frac{1}{\rho_{d\sigma}} \sum_{\sigma'(\neq\sigma)} \frac{\partial \chi_{\sigma\sigma'}}{\partial \varepsilon_{d\sigma'}} \left[(\pi T)^2 + \frac{3\Gamma_L \Gamma_R}{(\Gamma_L + \Gamma_R)^2} (eV)^2 \right] \\
&\quad - \sum_{\sigma'(\neq\sigma)} \tilde{\chi}_{\sigma\sigma'} \alpha_{\text{sh}} eV + \sum_{\sigma'(\neq\sigma)} \frac{\partial \tilde{\chi}_{\sigma\sigma'}}{\partial \varepsilon_{d\sigma}} \alpha_{\text{sh}} eV \omega + \frac{1}{2} \sum_{\sigma'(\neq\sigma)} \sum_{\sigma''(\neq\sigma)} \frac{\partial \tilde{\chi}_{\sigma\sigma'}}{\partial \varepsilon_{d\sigma''}} \alpha_{\text{sh}}^2 (eV)^2 + \dots.
\end{aligned}$$

TABLE VI. Bosonic collision integrals $\mathcal{W}_K^{\text{ph}}(\omega)$ and $\mathcal{W}_K^{\text{pp}}(\omega)$ that determine low-energy behavior of the PH propagator $X_{\sigma\sigma'}^{\mu\nu}$, and PP propagator $Y_{\sigma\sigma'}^{\mu\nu}$.

$$\begin{aligned}
\mathcal{W}_K^{\text{ph}}(\omega) &\equiv \int_{-\infty}^{\infty} d\varepsilon \left\{ f_{\text{eff}}(\varepsilon) \left[1 - f_{\text{eff}}(\varepsilon + \omega) \right] + f_{\text{eff}}(\varepsilon + \omega) \left[1 - f_{\text{eff}}(\varepsilon) \right] \right\} \\
&= \frac{\Gamma_L^2 + \Gamma_R^2}{(\Gamma_L + \Gamma_R)^2} \omega \coth \frac{\omega}{2T} + \frac{\Gamma_L \Gamma_R}{(\Gamma_L + \Gamma_R)^2} \left[(\omega + eV) \coth \frac{\omega + eV}{2T} + (\omega - eV) \coth \frac{\omega - eV}{2T} \right]. \\
\mathcal{W}_K^{\text{pp}}(\omega) &\equiv \int_{-\infty}^{\infty} d\varepsilon \left\{ \left[1 - f_{\text{eff}}(\varepsilon) \right] \left[1 - f_{\text{eff}}(\omega - \varepsilon) \right] + f_{\text{eff}}(\varepsilon) f_{\text{eff}}(\omega - \varepsilon) \right\} \\
&= \frac{\Gamma_L^2}{(\Gamma_L + \Gamma_R)^2} (\omega - 2\mu_L) \coth \frac{\omega - 2\mu_L}{2T} + \frac{\Gamma_R^2}{(\Gamma_L + \Gamma_R)^2} (\omega - 2\mu_R) \coth \frac{\omega - 2\mu_R}{2T} + \frac{2\Gamma_L \Gamma_R}{(\Gamma_L + \Gamma_R)^2} (\omega - \mu_L - \mu_R) \coth \frac{\omega - \mu_L - \mu_R}{2T}.
\end{aligned}$$

$$\begin{aligned}
X_{\sigma\sigma'}^{\mu\nu}(\omega) &\equiv - \int_{-\infty}^{\infty} \frac{d\varepsilon}{2\pi i} G_{\sigma\sigma'}^{\mu\nu}(\varepsilon + \omega) G_{\sigma'\sigma}^{\nu\mu}(\varepsilon), & Y_{\sigma\sigma'}^{\mu\nu}(\omega) &\equiv - \int_{-\infty}^{\infty} \frac{d\varepsilon}{2\pi i} G_{\sigma\sigma'}^{\mu\nu}(\omega - \varepsilon) G_{\sigma'\sigma}^{\nu\mu}(\varepsilon), \\
\text{Im } X_{\sigma\sigma'}^{--}(\omega) &= \frac{1}{2i} \left[X_{\sigma\sigma'}^{+-}(\omega) + X_{\sigma\sigma'}^{-+}(\omega) \right] = \pi \rho_{d\sigma} \rho_{d\sigma'} \mathcal{W}_K^{\text{ph}}(\omega) + O(\omega^2, (eV)^2, T^2), \\
\text{Im } Y_{\sigma\sigma'}^{--}(\omega) &= \frac{1}{2i} \left[Y_{\sigma\sigma'}^{+-}(\omega) + Y_{\sigma\sigma'}^{-+}(\omega) \right] = -\pi \rho_{d\sigma} \rho_{d\sigma'} \mathcal{W}_K^{\text{pp}}(\omega) + O(\omega^2, (eV)^2, T^2),
\end{aligned}$$

tively, by

$$\begin{aligned}
\mathcal{W}^{\text{pp}}(\omega) &\equiv \int d\varepsilon \left[1 - f_{\text{eff}}(\varepsilon) \right] \left[1 - f_{\text{eff}}(\omega - \varepsilon) \right], \\
&= \sum_{j,k=L,R} \frac{\Gamma_j \Gamma_k}{\Delta^2} \mathcal{W}_{\text{eq}}(\omega - \mu_j - \mu_k), \quad (7.14)
\end{aligned}$$

$$\begin{aligned}
\mathcal{W}^{\text{hh}}(\omega) &\equiv \int d\varepsilon f_{\text{eff}}(\varepsilon) f_{\text{eff}}(\omega - \varepsilon) \\
&= \sum_{j,k=L,R} \frac{\Gamma_j \Gamma_k}{\Delta^2} \mathcal{W}_{\text{eq}}(-\omega + \mu_j + \mu_k). \quad (7.15)
\end{aligned}$$

We have also presented in TABLE VI more explicit forms

of these bosonic collision integrals, carrying out the summations over j and k .

2. Imaginary part of the PH and PP propagators

We next consider the properties of the particle-hole and particle-particle propagators $X_{\sigma\sigma'}^{\mu\nu}(\omega)$ and $Y_{\sigma\sigma'}^{\mu\nu}(\omega)$,

defined by

$$X_{\sigma\sigma'}^{\mu\nu}(\omega) \equiv - \int \frac{d\varepsilon}{2\pi i} G_{\sigma}^{\mu\nu}(\varepsilon + \omega) G_{\sigma'}^{\nu\mu}(\varepsilon), \quad (7.16a)$$

$$Y_{\sigma\sigma'}^{\mu\nu}(\omega) \equiv - \int \frac{d\varepsilon}{2\pi i} G_{\sigma}^{\mu\nu}(\omega - \varepsilon) G_{\sigma'}^{\nu\mu}(\varepsilon). \quad (7.16b)$$

Note that the lesser and greater components of these propagators, i.e., $X_{\sigma\sigma'}^{+-}$, $X_{\sigma\sigma'}^{-+}$, $Y_{\sigma\sigma'}^{+-}$, and $Y_{\sigma\sigma'}^{-+}$, are pure imaginary. Furthermore, the diagonal components are related to each other, as $X_{\sigma\sigma'}^{++}(\omega) = -\{X_{\sigma\sigma'}^{--}(\omega)\}^*$ and $Y_{\sigma\sigma'}^{++}(\omega) = -\{Y_{\sigma\sigma'}^{--}(\omega)\}^*$ since the Green's function has the property $G_{\sigma}^{++}(\varepsilon) = -\{G_{\sigma}^{--}(\varepsilon)\}^*$. The components of the PH propagator and PP propagators are also linearly dependent, respectively, as $X_{\sigma\sigma'}^{--} + X_{\sigma\sigma'}^{++} - X_{\sigma\sigma'}^{-+} - X_{\sigma\sigma'}^{+-} = 0$, and $Y_{\sigma\sigma'}^{--} + Y_{\sigma\sigma'}^{++} - Y_{\sigma\sigma'}^{-+} - Y_{\sigma\sigma'}^{+-} = 0$. Thus, in the frequency domain, the imaginary part of the causal propagator can be described in terms of the lesser and greater components, as

$$\text{Im } X_{\sigma\sigma'}^{--}(\omega) = \frac{X_{\sigma\sigma'}^{\text{K}}(\omega)}{2i}, \quad \text{Im } Y_{\sigma\sigma'}^{--}(\omega) = \frac{Y_{\sigma\sigma'}^{\text{K}}(\omega)}{2i}. \quad (7.17)$$

Here, $X_{\sigma\sigma'}^{\text{K}} \equiv X_{\sigma\sigma'}^{+-} + X_{\sigma\sigma'}^{-+}$ and $Y_{\sigma\sigma'}^{\text{K}} \equiv Y_{\sigma\sigma'}^{+-} + Y_{\sigma\sigma'}^{-+}$. Note that the retarded and advanced PH propagators are given by $X_{\sigma\sigma'}^r = X_{\sigma\sigma'}^{--} - X_{\sigma\sigma'}^{-+}$ and $X_{\sigma\sigma'}^a = X_{\sigma\sigma'}^{--} - X_{\sigma\sigma'}^{+-}$, respectively. The retarded and advanced propagators for the PP excitations are also given by the same linear-combination forms.

This PH collision integral $\mathcal{W}^{\text{ph}}(\omega)$, defined in Eq. (7.12), determines the low-energy behavior of the greater component of the PH propagator $X_{\sigma\sigma'}^{+-}(\omega)$ exactly up to linear-order terms with respect to ω , T , and eV ,

$$\begin{aligned} X_{\sigma\sigma'}^{+-}(\omega) &\equiv - \int \frac{d\varepsilon}{2\pi i} G_{\sigma}^{+-}(\varepsilon + \omega) G_{\sigma'}^{-+}(\varepsilon) \\ &\simeq - \int \frac{d\varepsilon}{2\pi i} (2\pi)^2 \rho_{d\sigma'}(\varepsilon) \rho_{d\sigma}(\varepsilon + \omega) f_{\text{eff}}(\varepsilon) [1 - f_{\text{eff}}(\varepsilon + \omega)] \\ &= i 2\pi \rho_{d\sigma'} \rho_{d\sigma} \mathcal{W}^{\text{ph}}(\omega) + \dots \end{aligned} \quad (7.18)$$

To obtain the second line, the lesser and greater Green's functions in the integrand has been replaced by the lowest-order ones, i.e., $G_{\sigma}^{-+}(\omega) \simeq -i 2\pi \rho_{d\sigma} f_{\text{eff}}(\omega)$, and $G_{\sigma}^{+-}(\omega) \simeq i 2\pi \rho_{d\sigma} [1 - f_{\text{eff}}(\omega)]$ in the same way as that used for Eq. (7.5). Correspondingly, the low-energy asymptotic form of the lesser PH propagator $X_{\sigma\sigma'}^{-+}(\omega)$ can be expressed in terms of $\mathcal{W}^{\text{ph}}(-\omega)$, as

$$\begin{aligned} X_{\sigma\sigma'}^{-+}(\omega) &\equiv - \int \frac{d\varepsilon}{2\pi i} G_{\sigma}^{-+}(\varepsilon + \omega) G_{\sigma'}^{+-}(\varepsilon) \\ &= - \int \frac{d\varepsilon'}{2\pi i} G_{\sigma}^{-+}(\varepsilon' - \omega) G_{\sigma'}^{-+}(\varepsilon') = X_{\sigma\sigma'}^{+-}(-\omega) \\ &= i 2\pi \rho_{d\sigma'} \rho_{d\sigma} \mathcal{W}^{\text{ph}}(-\omega) + \dots \end{aligned} \quad (7.19)$$

Similarly, the low-energy behaviors of the PP propagators can be described in terms of the collision integrals $\mathcal{W}^{\text{pp}}(\omega)$ and $\mathcal{W}^{\text{hh}}(\omega)$. The greater $Y_{\sigma\sigma'}^{+-}(\omega)$ component

can be calculated up to linear-order terms in ω , eV and T , as

$$\begin{aligned} Y_{\sigma\sigma'}^{+-}(\omega) &\equiv - \int \frac{d\varepsilon}{2\pi i} G_{\sigma}^{+-}(\omega - \varepsilon) G_{\sigma'}^{-+}(\varepsilon) \\ &= \int \frac{d\varepsilon}{2\pi i} (2\pi)^2 \rho_{d\sigma} \rho_{d\sigma'} [1 - f_{\text{eff}}(\varepsilon)] [1 - f_{\text{eff}}(\omega - \varepsilon)] + \dots \\ &= -i 2\pi \rho_{d\sigma} \rho_{d\sigma'} \mathcal{W}^{\text{pp}}(\omega) + \dots \end{aligned} \quad (7.20)$$

The lesser component $Y_{\sigma\sigma'}^{-+}(\omega)$ is determined by the HH collision integral $\mathcal{W}^{\text{hh}}(\omega)$,

$$\begin{aligned} Y_{\sigma\sigma'}^{-+}(\omega) &\equiv - \int \frac{d\varepsilon}{2\pi i} G_{\sigma}^{-+}(\omega - \varepsilon) G_{\sigma'}^{-+}(\varepsilon) \\ &= \int \frac{d\varepsilon}{2\pi i} (2\pi)^2 \rho_{d\sigma} \rho_{d\sigma'} f_{\text{eff}}(\varepsilon) f_{\text{eff}}(\omega - \varepsilon) + \dots \\ &= -i 2\pi \rho_{d\sigma} \rho_{d\sigma'} \mathcal{W}^{\text{hh}}(\omega) + \dots \end{aligned} \quad (7.21)$$

3. Symmetrization of the bosonic collision integrals

These lesser and greater bosonic propagators can be simplified further, carrying out some symmetrizations. For the PH pair excitations, the difference between the two $X_{\sigma\sigma'}^{+-} - X_{\sigma\sigma'}^{-+} = X_{\sigma\sigma'}^r - X_{\sigma\sigma'}^a$, gives the imaginary part of the retarded propagator in the frequency domain. It shows the ω -linear dependence which is determined by the collision integrals in Eqs. (7.18) and (7.19) at low energies,

$$\mathcal{W}_{\text{dif}}^{\text{ph}}(\omega) \equiv \mathcal{W}^{\text{ph}}(\omega) - \mathcal{W}^{\text{ph}}(-\omega) = \omega. \quad (7.22)$$

In the zero-bias limit $eV \rightarrow 0$, the ω -linear imaginary part of the retarded function is closely related to the Korrington-Shiba relation of the impurity susceptibilities,¹⁵ and also to the fluctuation-dissipation theorem for the current noise.⁴²

In contrast, the symmetrized PH propagator $X_{\sigma\sigma'}^{\text{K}}(\omega)$, described in Eq. (7.17), is determined by the sum of the collision integrals $\mathcal{W}^{\text{ph}}(\omega)$ and $\mathcal{W}^{\text{ph}}(-\omega)$, as

$$\begin{aligned} \mathcal{W}_{\text{K}}^{\text{ph}}(\omega) &\equiv \mathcal{W}^{\text{ph}}(\omega) + \mathcal{W}^{\text{ph}}(-\omega) \\ &= \sum_{j,k=L,R} \frac{\Gamma_j \Gamma_k}{\Delta^2} (\omega + \mu_j - \mu_k) \coth \frac{\omega + \mu_j - \mu_k}{2T}. \end{aligned} \quad (7.23)$$

This symmetrized part $\mathcal{W}_{\text{K}}^{\text{ph}}(\omega)$ depends also on eV and T . The hyperbolic function represents the nonequilibrium distribution, and it interpolates the three different regions $(\omega, 0, 0)$, $(0, T, 0)$, and $(0, 0, eV)$ of the parameter space, consisting of (ω, T, eV) .

Similarly, the difference between the particle-particle and hole-hole (HH) collision integrals is given by

$$\begin{aligned} \mathcal{W}_{\text{dif}}^{\text{pp}}(\omega) &\equiv \mathcal{W}^{\text{pp}}(\omega) - \mathcal{W}^{\text{hh}}(\omega) \\ &= \omega - 2 \frac{\Gamma_L^2 \mu_L + \Gamma_R^2 \mu_R + \Gamma_L \Gamma_R (\mu_L + \mu_R)}{\Delta^2}, \end{aligned} \quad (7.24)$$

and the sum of the PP and HH collision integrals takes the form,

$$\begin{aligned} \mathcal{W}_K^{\text{PP}}(\omega) &\equiv \mathcal{W}^{\text{PP}}(\omega) + \mathcal{W}^{\text{hh}}(\omega) \\ &= \sum_{j,k=L,R} \frac{\Gamma_j \Gamma_k}{\Delta^2} (\omega - \mu_j - \mu_k) \coth \frac{\omega - \mu_j - \mu_k}{2T}. \end{aligned} \quad (7.25)$$

In particular, for symmetric junctions $\Gamma_L = \Gamma_R$ and $\mu_L = -\mu_R = eV/2$, the PP and HH collision integrals coincide with the PH ones, as

$$\mathcal{W}^{\text{PP}}(\omega) \rightarrow \mathcal{W}^{\text{ph}}(\omega), \quad \mathcal{W}^{\text{hh}}(\omega) \rightarrow \mathcal{W}^{\text{ph}}(-\omega) \quad (7.26)$$

In this case, the difference of these two takes the form $\mathcal{W}_{\text{diff}}^{\text{PP}}(\omega) \rightarrow \omega$ which does not depend on eV and T . The symmetrized part $\mathcal{W}_K^{\text{PP}}(\omega)$ also coincides with $\mathcal{W}_K^{\text{ph}}(\omega)$, and takes the following form at $T = 0$,

$$\begin{aligned} \mathcal{W}_K^{\text{ph}}(\omega) &\rightarrow \frac{1}{4} \left[|\omega + eV| + 2|\omega| + |\omega - eV| \right] \\ &= \begin{cases} |\omega|, & |\omega| > |eV| \\ \frac{1}{2}|\omega| + \frac{1}{2}|eV|, & |\omega| < |eV| \end{cases}. \end{aligned} \quad (7.27)$$

For symmetric junctions, the PP and PH propagators also become identical at low energies, $Y_{\sigma\sigma'}^{+-}(\omega) = -X_{\sigma\sigma'}^{+-}(\omega) + \dots$ and $Y_{\sigma\sigma'}^{-+}(\omega) = -X_{\sigma\sigma'}^{-+}(\omega) + \dots$, apart from the sign.

VIII. CURRENT CONSERVATION OF THE KELDYSH VERTEX FUNCTIONS IN THE FERMI-LIQUID REGIME

In order to calculate the nonlinear current noise $S_{\text{noise}}^{\text{QD}}$, up to terms of order $(eV)^3$, we also need information about low-energy behavior of the Keldysh vertex function in the Fermi-liquid regime $\Gamma_{\sigma\sigma';\sigma'\sigma}^{\mu\mu';\nu'\nu}(\omega, \omega'; \omega', \omega)$ up to terms of order ω, ω' , and eV . The collision processes which yield these linear-order terms in the imaginary part of the vertex functions are illustrated in Figs. 8 (a)–(d).

These diagrams can be calculated in such a way that is shown in Appendix C and we find that the low-energy behavior of the imaginary parts of the vertex functions can be described in terms of the collision integrals $\mathcal{W}_K^{\text{ph}}(\omega)$, and $\mathcal{W}_K^{\text{PP}}(\omega)$, as shown in TABLES VII and VIII for $\sigma = \sigma'$ and $\sigma \neq \sigma'$, respectively. These results explicitly show that all the Keldysh vertex components other than the causal one $\Gamma_{\sigma\sigma';\sigma'\sigma}^{-+;-+}(\omega, \omega'; \omega', \omega)$ and its counterpart $\Gamma_{\sigma\sigma';\sigma'\sigma}^{++;++}(\omega, \omega'; \omega', \omega)$ are pure imaginary in the frequency domain. Furthermore, the following sum over the time-loop indexes μ, μ', ν' , and ν vanishes,

$$\begin{aligned} &\Gamma_{\sigma\sigma';\sigma'\sigma}^{--;--} + \Gamma_{\sigma\sigma';\sigma'\sigma}^{++;++} + \Gamma_{\sigma\sigma';\sigma'\sigma}^{--;++} + \Gamma_{\sigma\sigma';\sigma'\sigma}^{++;--} + \Gamma_{\sigma\sigma';\sigma'\sigma}^{-+;-+} \\ &+ \Gamma_{\sigma\sigma';\sigma'\sigma}^{+-;-+} + \Gamma_{\sigma\sigma';\sigma'\sigma}^{-+;-+} + \Gamma_{\sigma\sigma';\sigma'\sigma}^{+-;-+} = 0 + O(\omega^2, |eV|^2, T^3), \end{aligned} \quad (8.1)$$

for both $\sigma = \sigma'$ and $\sigma \neq \sigma'$. Note that the vertex functions with three identical time-loop indexes, such as $\Gamma_{\sigma\sigma;\sigma\sigma}^{-+;-+}$ and $\Gamma_{\sigma\sigma;\sigma\sigma}^{+-;-+}$, do not yield linear-order terms with respect to ω, ω' , and eV . Therefore, Eq. (8.1) represents the linear dependency between the Keldysh vertex components at low energies (see also Appendix A),

$$\sum_{\mu\nu} \sum_{\mu'\nu'} \Gamma_{\sigma\sigma';\sigma'\sigma}^{\mu\mu';\nu'\nu}(\omega, \omega'; \omega', \omega) = 0. \quad (8.2)$$

In particular, in the frequency domain, it describes a relationship between the imaginary parts of the vertex components.

We show in this section that the Ward identities between the vertex corrections and self-energy, given in Eqs. (5.24) and (5.32), can be expressed in terms of the collision integrals $\mathcal{I}_K(\omega)$, $\mathcal{W}_K^{\text{ph}}(\omega)$, and $\mathcal{W}_K^{\text{PP}}(\omega)$, which is exact up to terms of order ω, ω', eV , and T . The Ward identities, which reflect the current conservation through quantum dots, also impose a strong requirement for the real part of causal vertex function $\Gamma_{\sigma\sigma';\sigma'\sigma}^{-+;-+}(\omega, \omega'; \omega', \omega)$. Specifically, it determines the expansion coefficient for the eV -linear real part, which contributes to the nonlinear current through tunnel junctions without the inversion symmetry, i.e. $\Gamma_L \neq \Gamma_R$ or $\mu_L \neq -\mu_R$.⁶⁰

A. Current conservation and imaginary part of the Keldysh self-energies

In order to clarify roles of the current conservation in the lesser and greater self-energies, the product of the retarded and advanced Green's functions in the right-hand side of Ward identities Eqs. (5.24a) and (5.32a) can be replaced by $\Delta G_{\sigma'}^r(\omega') G_{\sigma'}^a(\omega') = \pi \rho_{d\sigma'} + \dots$, i.e., by the value at the Fermi level $\omega' = 0$ of the equilibrium ground state. This is because the Keldysh vertex functions, $\Gamma_{\sigma\sigma';\sigma'\sigma}^{-\nu_2;\nu_3+}(\omega, \omega'; \omega', \omega)$ and $\Gamma_{\sigma\sigma';\sigma'\sigma}^{+\nu_2;\nu_3-}(\omega, \omega'; \omega', \omega)$ vanish at $\omega = \omega' = eV = T = 0$ and thus the leading-order terms of the imaginary part of Eqs. (5.24a) and (5.32a) for $\nu_1 = -\nu_4$ emerge through these vertex components in the integrands.

1. The ω derivative of $\Sigma_{U,\sigma}^{+-}$ and $\Sigma_{U,\sigma}^{-+}$

We first of all examine the level diagonal $\sigma = \sigma'$ part of Eq. (5.24a) for the greater and lesser self-energies, i.e. $\nu_1 = -\nu_4$, using the low-energy asymptotic forms given in Eqs. (7.3) and (7.4). Since the quadratic dependence of the lesser and greater self-energies on ω, eV , and T are determined by the fermionic collision integrals $\mathcal{I}^{+-}(\omega)$ and $\mathcal{I}^{-+}(\omega)$, the ω -linear term of the Ward identities Eq. (5.24a) for $\sigma = \sigma'$ can be extracted by taking the derivative of these functions with respect to ω .

For the greater self-energy $\Sigma_{U,\sigma}^{+-}(\omega)$, it can be calcu-

TABLE VII. Low-energy expansion of the Keldysh vertex corrections for the same levels $\sigma = \sigma'$, which is asymptotically exact up to linear order terms with respect eV , T , and frequencies ϵ and ϵ' . The leading-order terms of the $\sigma = \sigma'$ components are pure imaginary and is determined by the collision $\mathcal{W}_K^{\text{ph}}(\omega)$, defined in Eq. (7.23). The components with three identical Keldysh indexes such as $\Gamma_{\sigma\sigma;\sigma\sigma}^{--;--}$ and $\Gamma_{\sigma\sigma;\sigma\sigma}^{++;--}$ vanish in the leading order.

$$\begin{aligned}
& \Gamma_{\sigma\sigma;\sigma\sigma}^{--;++}(\epsilon, \epsilon'; \epsilon', \epsilon) + \Gamma_{\sigma\sigma;\sigma\sigma}^{++;--}(\epsilon, \epsilon'; \epsilon', \epsilon) = -i \frac{2\pi}{\{\rho_{d\sigma}\}^2} \sum_{\sigma''(\neq\sigma)} \chi_{\sigma\sigma''}^2 \mathcal{W}_K^{\text{ph}}(\epsilon - \epsilon') + \dots \\
& \Gamma_{\sigma\sigma;\sigma\sigma}^{--;++}(\epsilon, \epsilon'; \epsilon', \epsilon) - \Gamma_{\sigma\sigma;\sigma\sigma}^{++;--}(\epsilon, \epsilon'; \epsilon', \epsilon) = -i \frac{2\pi}{\{\rho_{d\sigma}\}^2} \sum_{\sigma''(\neq\sigma)} \chi_{\sigma\sigma''}^2 [\epsilon - \epsilon'] + \dots \\
& \Gamma_{\sigma\sigma;\sigma\sigma}^{--;+-}(\epsilon, \epsilon'; \epsilon', \epsilon) + \Gamma_{\sigma\sigma;\sigma\sigma}^{+-;--}(\epsilon, \epsilon'; \epsilon', \epsilon) = i \frac{2\pi}{\{\rho_{d\sigma}\}^2} \sum_{\sigma''(\neq\sigma)} \chi_{\sigma\sigma''}^2 \mathcal{W}_K^{\text{ph}}(0) + \dots \\
& \Gamma_{\sigma\sigma;\sigma\sigma}^{--;+-}(\epsilon, \epsilon'; \epsilon', \epsilon) - \Gamma_{\sigma\sigma;\sigma\sigma}^{+-;--}(\epsilon, \epsilon'; \epsilon', \epsilon) = 0 + \dots \\
& \Gamma_{\sigma\sigma;\sigma\sigma}^{+-;--}(\epsilon, \epsilon'; \epsilon', \epsilon) = 0 + \dots, \quad \Gamma_{\sigma\sigma;\sigma\sigma}^{+-;+-}(\epsilon, \epsilon'; \epsilon', \epsilon) = 0 + \dots \\
& \Gamma_{\sigma\sigma;\sigma\sigma}^{--;--}(\epsilon, \epsilon'; \epsilon', \epsilon) = i \frac{\pi}{\{\rho_{d\sigma}\}^2} \sum_{\sigma''(\neq\sigma)} \chi_{\sigma\sigma''}^2 \left[\mathcal{W}_K^{\text{ph}}(\epsilon - \epsilon') - \mathcal{W}_K^{\text{ph}}(0) \right] + \dots, \quad \Gamma_{\sigma\sigma;\sigma\sigma}^{++;++}(\epsilon, \epsilon'; \epsilon', \epsilon) = -\{\Gamma_{\sigma\sigma;\sigma\sigma}^{--;--}(\epsilon, \epsilon'; \epsilon', \epsilon)\}^*
\end{aligned}$$

lated up to linear-order terms, using Eq. (7.4),

$$\begin{aligned}
& \left(\frac{\partial}{\partial\omega} + \frac{\partial}{\partial\epsilon_{d\sigma}} \right) \Sigma_{U,\sigma}^{+-}(\omega) \\
& = i \frac{2\pi}{\rho_{d\sigma}} \sum_{\sigma''(\neq\sigma)} \chi_{\sigma\sigma''} \frac{\partial \mathcal{I}^{+-}(\omega)}{\partial\omega} + \mathcal{O}(\omega^2, (eV)^2, T^2),
\end{aligned} \tag{8.3}$$

and the derivative of the fermionic collision integral takes the form,

$$\begin{aligned}
\frac{\partial \mathcal{I}^{+-}(\omega)}{\partial\omega} & = \int d\varepsilon_1 \int d\varepsilon_2 \frac{\partial}{\partial\omega} \left[1 - f_{\text{eff}}(\varepsilon_1 + \omega) \right] \\
& \quad \times \left[1 - f_{\text{eff}}(\varepsilon_2) \right] f_{\text{eff}}(\varepsilon_1 + \varepsilon_2) \\
& = \int d\omega' \mathcal{W}^{\text{ph}}(\omega - \omega') \left\{ -\frac{\partial f_{\text{eff}}(\omega')}{\partial\omega'} \right\} \\
& \xrightarrow{T \rightarrow 0} \sum_{\substack{j,k,\ell \\ =L,R}} \frac{\Gamma_j \Gamma_k \Gamma_\ell}{\Delta^3} \mathcal{W}_{\text{eq}}(\omega + \mu_j - \mu_k - \mu_\ell).
\end{aligned} \tag{8.4}$$

Here, the bosonic one $\mathcal{W}^{\text{ph}}(\omega - \omega')$ appearing in the second line can be related to the low-energy asymptotic form of the vertex function $\Gamma_{\sigma\sigma;\sigma\sigma}^{--;++}(\omega, \omega'; \omega', \omega) \rho_{d\sigma}^2 = -i2\pi \sum_{\sigma''(\neq\sigma)} \chi_{\sigma\sigma''}^2 \mathcal{W}^{\text{ph}}(\omega - \omega') + \dots$, which is one the results shown in TABLE VII. This vertex component is determined by the collision process described in Fig. 8 (a) for $(\mu, \nu) = (-, +)$ and is calculated as Eq. (C12a). Therefore, Eq. (8.4) shows that in the Fermi-liquid regime the Ward identity Eq. (5.24a) for $(\nu_4, \nu_1) = (+, -)$ is satisfied through this relation between $\partial \mathcal{I}^{+-}(\omega)/\partial\omega$ and $\mathcal{W}^{\text{ph}}(\omega - \omega')$, specifically at $T \rightarrow 0$ the bosonic collision integral in the right-hand side takes the form $\mathcal{W}_{\text{eq}}(\varepsilon) \rightarrow |\varepsilon| \theta(\varepsilon)$.

Similarly, the derivative of the lesser self-energy $\Sigma_{U,\sigma}^{+-}(\omega)$ can be described by the collision integral $\mathcal{I}^{-+}(\omega)$

up to linear order terms with respect to ω , eV , and T , using Eqs. (7.3) and (7.6),

$$\begin{aligned}
& \left(\frac{\partial}{\partial\omega} + \frac{\partial}{\partial\epsilon_{d\sigma}} \right) \Sigma_{U,\sigma}^{-+}(\omega) \\
& = -i \frac{2\pi}{\rho_{d\sigma}} \sum_{\sigma''(\neq\sigma)} \chi_{\sigma\sigma''} \frac{\partial \mathcal{I}^{-+}(\omega)}{\partial\omega} + \mathcal{O}(\omega^2, (eV)^2, T^2),
\end{aligned} \tag{8.5}$$

$$\begin{aligned}
\frac{\partial \mathcal{I}^{-+}(\omega)}{\partial\omega} & = \int d\varepsilon_1 \int d\varepsilon_2 \frac{\partial}{\partial\omega} f_{\text{eff}}(\varepsilon_1 + \omega) \\
& \quad \times f_{\text{eff}}(\varepsilon_2) \left[1 - f_{\text{eff}}(\varepsilon_1 + \varepsilon_2) \right] \\
& = - \int d\omega' \mathcal{W}^{\text{ph}}(\omega' - \omega) \left\{ -\frac{\partial f_{\text{eff}}(\omega')}{\partial\omega'} \right\} \\
& \xrightarrow{T \rightarrow 0} - \sum_{\substack{j,k,\ell \\ =L,R}} \frac{\Gamma_j \Gamma_k \Gamma_\ell}{\Delta^3} \mathcal{W}_{\text{eq}}(-\omega + \mu_k - \mu_j + \mu_\ell).
\end{aligned} \tag{8.6}$$

Here, the bosonic collision integral $\mathcal{W}^{\text{ph}}(\omega' - \omega)$ is related to the low-energy asymptotic form of the vertex function $\Gamma_{\sigma\sigma;\sigma\sigma}^{+-;--}(\omega, \omega'; \omega', \omega) \rho_{d\sigma}^2 = -i2\pi \sum_{\sigma''(\neq\sigma)} \chi_{\sigma\sigma''}^2 \mathcal{W}^{\text{ph}}(\omega' - \omega) + \dots$, which is determined by the collision process described in Fig. 8 (a) for $(\mu, \nu) = (+, -)$. It can be calculated as Eq. (C12b) and the result is also listed in TABLE VII. Therefore, the last line of Eq. (8.6) also shows that in the Fermi-liquid regime the Ward identity Eq. (5.24a) for $\sigma = \sigma'$ and $(\nu_4, \nu_1) = (-, +)$ is satisfied through this relation between $\partial \mathcal{I}^{-+}(\omega)/\partial\omega$ and $\mathcal{W}^{\text{ph}}(\omega' - \omega)$.

TABLE VIII. Low-energy expansion of the Keldysh vertex corrections for different levels $\sigma \neq \sigma'$, which asymptotically exact up to linear order terms with respect eV , T , and frequencies ϵ and ϵ' . The imaginary part of the $\sigma \neq \sigma'$ components is determined by the bosonic collision integrals $\mathcal{W}_K^{\text{ph}}(\omega)$, $\mathcal{W}_K^{\text{pp}}(\omega)$, $\mathcal{W}_{\text{dif}}^{\text{pp}}(\omega)$, and also $\mathcal{W}_{\text{dif}}^{\text{ph}}(\omega) = \omega$, defined in Eqs. (7.22)–(7.25). The components with three identical Keldysh indexes such as $\Gamma_{\sigma\sigma';\sigma'\sigma}^{--;--+}$ and $\Gamma_{\sigma\sigma';\sigma'\sigma}^{++;--}$ do not appear in the leading order at low energies. Note that the counter part of the component is given by $\Gamma_{\sigma\sigma';\sigma'\sigma}^{++;++}(\epsilon, \epsilon'; \epsilon', \epsilon) = -\left\{ \Gamma_{\sigma\sigma';\sigma'\sigma}^{--;--}(\epsilon, \epsilon'; \epsilon', \epsilon) \right\}^*$, and $\tilde{\chi}_{\sigma\sigma'} = \chi_{\sigma\sigma'}/\rho_{d\sigma}$.

$$\begin{aligned} \Gamma_{\sigma\sigma';\sigma'\sigma}^{--;++}(\epsilon, \epsilon'; \epsilon', \epsilon) + \Gamma_{\sigma\sigma';\sigma'\sigma}^{++;--}(\epsilon, \epsilon'; \epsilon', \epsilon) &= -i \frac{2\pi}{\rho_{d\sigma}\rho_{d\sigma'}} \chi_{\sigma\sigma'}^2 \mathcal{W}_K^{\text{ph}}(\epsilon - \epsilon') + \dots \\ \Gamma_{\sigma\sigma';\sigma'\sigma}^{--;++}(\epsilon, \epsilon'; \epsilon', \epsilon) - \Gamma_{\sigma\sigma';\sigma'\sigma}^{++;--}(\epsilon, \epsilon'; \epsilon', \epsilon) &= -i \frac{2\pi}{\rho_{d\sigma}\rho_{d\sigma'}} \chi_{\sigma\sigma'}^2 [\epsilon - \epsilon'] + \dots \\ \Gamma_{\sigma\sigma';\sigma'\sigma}^{--;+-}(\epsilon, \epsilon'; \epsilon', \epsilon) + \Gamma_{\sigma\sigma';\sigma'\sigma}^{+-;--}(\epsilon, \epsilon'; \epsilon', \epsilon) &= i \frac{2\pi}{\rho_{d\sigma}\rho_{d\sigma'}} \chi_{\sigma\sigma'}^2 \mathcal{W}_K^{\text{pp}}(\epsilon + \epsilon') + \dots \\ \Gamma_{\sigma\sigma';\sigma'\sigma}^{--;+-}(\epsilon, \epsilon'; \epsilon', \epsilon) - \Gamma_{\sigma\sigma';\sigma'\sigma}^{+-;--}(\epsilon, \epsilon'; \epsilon', \epsilon) &= i \frac{2\pi}{\rho_{d\sigma}\rho_{d\sigma'}} \chi_{\sigma\sigma'}^2 \mathcal{W}_{\text{dif}}^{\text{pp}}(\epsilon + \epsilon') + \dots \\ \Gamma_{\sigma\sigma';\sigma'\sigma}^{--;+-}(\epsilon, \epsilon'; \epsilon', \epsilon) + \Gamma_{\sigma\sigma';\sigma'\sigma}^{+-;--}(\epsilon, \epsilon'; \epsilon', \epsilon) &= i \frac{2\pi}{\rho_{d\sigma}\rho_{d\sigma'}} \sum_{\sigma''(\neq\sigma, \sigma')} \chi_{\sigma\sigma''} \chi_{\sigma''\sigma'} \mathcal{W}_K^{\text{ph}}(0) + \dots \\ \Gamma_{\sigma\sigma';\sigma'\sigma}^{--;+-}(\epsilon, \epsilon'; \epsilon', \epsilon) - \Gamma_{\sigma\sigma';\sigma'\sigma}^{+-;--}(\epsilon, \epsilon'; \epsilon', \epsilon) &= 0 + \dots \\ \text{Im} \Gamma_{\sigma\sigma';\sigma'\sigma}^{--;--}(\epsilon, \epsilon'; \epsilon', \epsilon) &= \frac{\pi}{\rho_{d\sigma}\rho_{d\sigma'}} \left[\chi_{\sigma\sigma'}^2 \left\{ \mathcal{W}_K^{\text{ph}}(\epsilon - \epsilon') - \mathcal{W}_K^{\text{pp}}(\epsilon + \epsilon') \right\} - \sum_{\sigma''(\neq\sigma, \sigma')} \chi_{\sigma\sigma''} \chi_{\sigma''\sigma'} \mathcal{W}_K^{\text{ph}}(0) \right] + \dots \\ \text{Re} \Gamma_{\sigma\sigma';\sigma'\sigma}^{--;--}(\epsilon, \epsilon'; \epsilon', \epsilon) &= \frac{1}{\rho_{d\sigma}\rho_{d\sigma'}} \left[-\chi_{\sigma\sigma'} + \rho_{d\sigma} \frac{\partial \tilde{\chi}_{\sigma\sigma'}}{\partial \epsilon_{d\sigma}} \epsilon + \rho_{d\sigma'} \frac{\partial \tilde{\chi}_{\sigma'\sigma}}{\partial \epsilon_{d\sigma'}} \epsilon' + \beta_{\sigma\sigma'} \alpha_{\text{sh}} eV \right] + \dots \\ \beta_{\sigma\sigma'} &\equiv -\frac{\partial \rho_{d\sigma}}{\partial \epsilon_{d\sigma'}} \sum_{\sigma''(\neq\sigma)} \tilde{\chi}_{\sigma\sigma''} - \frac{\partial \rho_{d\sigma'}}{\partial \epsilon_{d\sigma'}} \sum_{\sigma''(\neq\sigma')} \tilde{\chi}_{\sigma'\sigma''} + \sum_{\sigma'''(\neq\sigma, \sigma')} \frac{\partial \chi_{\sigma\sigma'}}{\partial \epsilon_{d\sigma'''}} \end{aligned}$$

2. The $\epsilon_{d\sigma'}$ derivative of $\Sigma_{U,\sigma}^{+-}$ and $\Sigma_{U,\sigma}^{+-}$

We next consider the off-diagonal $\sigma' \neq \sigma$ components of Eq. (5.24a), i.e. the Ward identities for $\partial \Sigma_{U,\sigma}^{+-}(\omega)/\partial \epsilon_{d\sigma'}$ and $\partial \Sigma_{U,\sigma}^{+-}(\omega)/\partial \epsilon_{d\sigma'}$, which show quadratic dependences on ω , eV , and T at low energies,

$$\frac{\partial \Sigma_{U,\sigma}^{\nu,-\nu}(\omega)}{\partial \epsilon_{d\sigma'}} = 0 + \mathcal{O}(\omega^2, (eV)^2, T^2). \quad (8.7)$$

It can be confirmed directly that the asymptotic forms of vertex functions obtained in Appendix C satisfy the Ward identities for $\sigma' \neq \sigma$ up to linear-order terms with respect to ω , eV , and T ; substituting the results shown in TABLE VIII into Eq. (5.24a), we find that the constant and linear-order terms of the right-hand side vanish. Here we describe an alternative way to verify this consistency with the current conservation in terms of the collision integrals.

These Ward identities for $\sigma' \neq \sigma$ have been derived in Sec. V, using Eq. (5.25) which represents the property that the value of the self-energy is unchanged if the internal frequencies of the Green's functions along a closed-loop of level σ' are shifted by an arbitrary amount ω_0 . The current conservation in the Fermi-liquid regime can be verified, applying this procedure to the collision pro-

cess shown in Fig. 7. For the greater self-energy, it takes the form

$$\begin{aligned} \frac{\partial \Sigma_{U,\sigma}^{+-}(\omega)}{\partial \epsilon_{d\sigma'}} &= \left(\frac{\partial}{\partial \omega_0} + \frac{\partial}{\partial \epsilon_{d\sigma'}} \right) \Sigma_{U,\sigma}^{+-}(\omega) \\ &= \left(\frac{\partial}{\partial \omega_0} + \frac{\partial}{\partial \epsilon_{d\sigma'}} \right) i \frac{2\pi \chi_{\sigma\sigma'}}{\rho_{d\sigma}} \mathcal{I}^{+-}(\omega) + \dots \\ &= i \frac{2\pi \chi_{\sigma\sigma'}}{\rho_{d\sigma}} \frac{\partial \mathcal{I}^{+-}(\omega)}{\partial \omega_0} + \mathcal{O}(\omega^2, (eV)^2, T^2). \end{aligned} \quad (8.8)$$

Note that the fermionic collision integral $\mathcal{I}^{+-}(\omega)$ can be written in the form, shifting the loop frequency by ω_0 from the one described in Eq. (7.2),

$$\begin{aligned} \mathcal{I}^{+-}(\omega) &= \int d\varepsilon_1 \int d\varepsilon_2 \left[1 - f_{\text{eff}}(\varepsilon_1) \right] \\ &\quad \times \left[1 - f_{\text{eff}}(\varepsilon_2 + \omega_0) \right] f_{\text{eff}}(\varepsilon_1 + \varepsilon_2 + \omega_0 - \omega). \end{aligned} \quad (8.9)$$

Although the derivative $\partial \mathcal{I}^{+-}(\omega)/\partial \omega_0$ itself vanishes, it can be expressed in terms of the bosonic collision inte-

grals, as

$$\begin{aligned}
& \int d\varepsilon_1 \int d\varepsilon_2 [1 - f_{\text{eff}}(\varepsilon_1)] \frac{\partial}{\partial \varepsilon_2} [1 - f_{\text{eff}}(\varepsilon_2)] f_{\text{eff}}(\varepsilon_1 + \varepsilon_2 - \omega) \\
&= \int d\omega' \left[\mathcal{W}^{\text{ph}}(\omega - \omega') - \mathcal{W}^{\text{pp}}(\omega + \omega') \right] \left\{ -\frac{\partial f_{\text{eff}}(\omega')}{\partial \omega'} \right\} \\
&\xrightarrow{T \rightarrow 0} \sum_{j,k,\ell=L,R} \frac{\Gamma_j \Gamma_k \Gamma_\ell}{\Delta^3} \left[\mathcal{W}_{\text{eq}}(\omega - \mu_\ell - \mu_k + \mu_j) \right. \\
&\quad \left. - \mathcal{W}_{\text{eq}}(\omega + \mu_\ell - \mu_k - \mu_j) \right] = 0. \tag{8.10}
\end{aligned}$$

Here, the bosonic collision integrals $\mathcal{W}^{\text{ph}}(\omega - \omega')$ and $\mathcal{W}^{\text{pp}}(\omega + \omega')$ that emerged in the second line can be regarded as the contributions of the vertex corrections $\Gamma_{\sigma\sigma';\sigma'\sigma}^{-+;++}(\omega, \omega'; \omega', \omega) \rho_{d\sigma} \rho_{d\sigma'} = -i 2\pi \chi_{\sigma\sigma'}^2 \mathcal{W}^{\text{ph}}(\omega - \omega')$, and $\Gamma_{\sigma\sigma';\sigma'\sigma}^{-+;-+}(\omega, \omega'; \omega', \omega) \rho_{d\sigma} \rho_{d\sigma'} = i 2\pi \chi_{\sigma\sigma'}^2 \mathcal{W}^{\text{pp}}(\omega + \omega')$, shown in TABLE VIII up to linear-order terms. These two vertex contributions are caused by the collision processes, described in Figs. 8 (b) and (c) for $(\mu, \nu) = (-, +)$, and are calculated in Eqs. (C27a) and (C31a). Therefore, Eqs. (8.8)–(8.10) show that the vertex function that is obtained in Appendix C and the greater self-energy satisfy the Ward identity Eq. (5.24a) for $\sigma \neq \sigma'$ in the Fermi-liquid regime through the relation between the fermionic and bosonic collision integrals.

Similarly, for the lesser self-energy, $\partial \Sigma_{U,\sigma}^{-+}(\omega)/\partial \epsilon_{d\sigma'}$ can be expressed in terms of $\partial \mathcal{I}^{-+}(\omega)/\partial \omega_0$ which takes the following form,

$$\begin{aligned}
& \int d\varepsilon_1 \int d\varepsilon_2 f_{\text{eff}}(\varepsilon_1) \frac{\partial}{\partial \varepsilon_2} f_{\text{eff}}(\varepsilon_2) [1 - f_{\text{eff}}(\varepsilon_1 + \varepsilon_2 - \omega)] \\
&= \int d\omega' \left[\mathcal{W}^{\text{ph}}(\omega' - \omega) - \mathcal{W}^{\text{hh}}(\omega + \omega') \right] \left\{ -\frac{\partial f_{\text{eff}}(\omega')}{\partial \omega'} \right\} \\
&\xrightarrow{T \rightarrow 0} \sum_{j,k,\ell=L,R} \frac{\Gamma_j \Gamma_k \Gamma_\ell}{\Delta^3} \left[\mathcal{W}_{\text{eq}}(-\omega + \mu_\ell - \mu_k + \mu_j) \right. \\
&\quad \left. - \mathcal{W}_{\text{eq}}(-\omega - \mu_\ell + \mu_k + \mu_j) \right] = 0. \tag{8.11}
\end{aligned}$$

The bosonic collision integrals $\mathcal{W}^{\text{ph}}(\omega' - \omega)$ and $\mathcal{W}^{\text{hh}}(\omega + \omega')$ in the second line correspond to the vertex functions $\Gamma_{\sigma\sigma';\sigma'\sigma}^{++;--}(\omega, \omega'; \omega', \omega) \rho_{d\sigma} \rho_{d\sigma'} = -i 2\pi \chi_{\sigma\sigma'}^2 \mathcal{W}^{\text{ph}}(\omega' - \omega)$ and $\Gamma_{\sigma\sigma';\sigma'\sigma}^{+-;-+}(\omega, \omega'; \omega', \omega) \rho_{d\sigma} \rho_{d\sigma'} = i 2\pi \chi_{\sigma\sigma'}^2 \mathcal{W}^{\text{hh}}(\omega + \omega')$ that emerge in the right-hand side of Ward identity Eq. (5.24a). These two vertex components represent the contributions of the collision processes, described in Figs. 8 (b) and (c), and are calculated in Eqs. (C27b) and (C31b).

3. The eV derivative of $\Sigma_{U,\sigma}^{+-}$ and $\Sigma_{U,\sigma}^{-+}$

We show here that the low-energy asymptotic forms of the vertex functions, given in TABLES VII and VIII, satisfy the Ward identity Eq. (5.32) with $\partial \Sigma_{U,\sigma}^{+-}(\omega)/\partial (eV)$

and $\partial \Sigma_{U,\sigma}^{-+}(\omega)/\partial (eV)$. Since the quadratic ω^2 , $(eV)^2$, and T^2 dependences of $\Sigma_{U,\sigma}^{+-}(\omega)$ and $\Sigma_{U,\sigma}^{-+}(\omega)$ are described by the fermionic collision integrals $\mathcal{I}^{+-}(\omega)$ and $\mathcal{I}^{-+}(\omega)$, the linear order terms of these derivatives can be calculated by using Eqs. (7.3) and (7.4),

$$\frac{\partial \Sigma_{U,\sigma}^{+-}(\omega)}{\partial eV} = i \frac{2\pi}{\rho_{d\sigma}} \sum_{\sigma'(\neq\sigma)} \chi_{\sigma\sigma'}^2 \frac{\partial \mathcal{I}^{+-}(\omega)}{\partial eV} + \dots, \tag{8.12}$$

$$\frac{\partial \Sigma_{U,\sigma}^{-+}(\omega)}{\partial eV} = -i \frac{2\pi}{\rho_{d\sigma}} \sum_{\sigma'(\neq\sigma)} \chi_{\sigma\sigma'}^2 \frac{\partial \mathcal{I}^{-+}(\omega)}{\partial eV} + \dots. \tag{8.13}$$

For the greater self-energy, $\partial \mathcal{I}^{+-}(\omega)/\partial (eV)$ can be expressed in the following form, taking the derivative of the three nonequilibrium distribution functions f_{eff} in the integrand in Eq. (7.2),

$$\begin{aligned}
\frac{\partial \mathcal{I}^{+-}(\omega)}{\partial eV} &= \int d\omega' \left[2\mathcal{W}^{\text{ph}}(\omega - \omega') - \mathcal{W}^{\text{pp}}(\omega + \omega') \right] \\
&\quad \times \left\{ -\frac{\partial f_{\text{eff}}(\omega')}{\partial eV} \right\} \\
&\xrightarrow{T \rightarrow 0} \sum_{\substack{j,k,\ell \\ =L,R}} \frac{\Gamma_j \Gamma_k \Gamma_\ell}{\Delta^3} \left(\frac{\mu_\ell - \mu_j - \mu_k}{eV} \right) \\
&\quad \times \mathcal{W}_{\text{eq}}(\omega + \mu_\ell - \mu_j - \mu_k). \tag{8.14}
\end{aligned}$$

Here, two \mathcal{W}^{ph} 's and \mathcal{W}^{pp} in the integrand correspond to the vertex contributions $\Gamma_{\sigma\sigma';\sigma\sigma}^{-+;++}(\omega, \omega'; \omega', \omega)$, $\Gamma_{\sigma\sigma';\sigma'\sigma}^{-+;--}(\omega, \omega'; \omega', \omega)$, and $\Gamma_{\sigma\sigma';\sigma'\sigma}^{-+;-+}(\omega, \omega'; \omega', \omega)$ up to linear-order terms, shown in TABLES VII and VIII. These vertex contributions are caused by the collision processes described in Figs. 8 (a), (b), and (c) for $(\mu, \nu) = (-, +)$, and are calculated in Appendix C. Furthermore, the last line of Eq. (8.14), in which $\mathcal{W}_{\text{eq}}(\varepsilon) \xrightarrow{T \rightarrow 0} |\varepsilon| \theta(\varepsilon)$, explicitly shows that these contributions coincide with the that of the right hand of the Ward identity Eq. (5.32b).

Similarly, the low-energy behavior of $\partial \Sigma_{U,\sigma}^{-+}(\omega)/\partial eV$ is determined by the derivative of $\mathcal{I}^{-+}(\omega)$,

$$\begin{aligned}
\frac{\partial \mathcal{I}^{-+}(\omega)}{\partial eV} &= - \int d\omega' \left[2\mathcal{W}^{\text{ph}}(\omega' - \omega) - \mathcal{W}^{\text{hh}}(\omega + \omega') \right] \\
&\quad \times \left\{ -\frac{\partial f_{\text{eff}}(\omega')}{\partial eV} \right\} \\
&\xrightarrow{T \rightarrow 0} - \sum_{\substack{j,k,\ell \\ =L,R}} \frac{\Gamma_j \Gamma_k \Gamma_\ell}{\Delta^3} \left(\frac{\mu_\ell - \mu_j - \mu_k}{eV} \right) \\
&\quad \times \mathcal{W}_{\text{eq}}(-\mu_\ell + \mu_j + \mu_k - \omega). \tag{8.15}
\end{aligned}$$

In this case, two \mathcal{W}^{ph} 's and one \mathcal{W}^{hh} in the integrand correspond to vertex contributions $\Gamma_{\sigma\sigma';\sigma\sigma}^{++;--}(\omega, \omega'; \omega', \omega)$, $\Gamma_{\sigma\sigma';\sigma'\sigma}^{+-;-+}(\omega, \omega'; \omega', \omega)$, and $\Gamma_{\sigma\sigma';\sigma'\sigma}^{-+;-+}(\omega, \omega'; \omega', \omega)$ up to linear-order terms, shown in TABLES VII and VIII.

These vertex components are caused by the collision processes described in Figs. 8 (a), (b), and (c) for $(\mu, \nu) = (+, -)$, and are calculated in Appendix C. In particular, the last line of Eq. (8.15) shows that at $T = 0$ these contributions coincide with that of the right hand of the Ward identity Eq. (5.32b).

B. Real part of the vertex function at finite eV

We next show that the asymptotic form of the real part of the vertex function at finite bias voltages can also be deduced from the Ward identity Eq. (5.24b). That is the explicit expression of the eV -linear real part of $\Gamma_{\sigma\sigma';\sigma'\sigma}^{--;--}(0, 0; 0, 0)$, which has not been taken into account in Eq. (3.19). To be specific, we consider nonequilibrium behaviors at $T = 0$ in this subsection.

The Keldysh vertex components other than the causal one and its counter part are pure imaginary, as shown explicitly in TABLES VII and VIII, up terms of order ω , ω' , and eV . Thus, only $\Gamma_{\sigma\sigma';\sigma'\sigma}^{--;--}(\omega, \omega'; \omega', \omega)$ and $\Gamma_{\sigma\sigma';\sigma'\sigma}^{++;++}(\omega, \omega'; \omega', \omega)$ have the real parts in the Fermi-liquid regime, which can be related to the the real part of the retarded self-energy which is identical to the real part of the causal one $\text{Re } \Sigma_{U,\sigma}^r(\omega) \equiv \text{Re } \Sigma_{U,\sigma}^{--}(\omega)$ through the Ward identity Eq. (5.24b):

$$\begin{aligned} & \left(\delta_{\sigma\sigma'} \frac{\partial}{\partial \omega} + \frac{\partial}{\partial \epsilon_{d\sigma'}} \right) \text{Re } \Sigma_{U,\sigma}^r(\omega) \\ &= - \sum_{j=L,R} \text{Re } \Gamma_{\sigma\sigma';\sigma'\sigma}^{--;--}(\omega, \mu_j; \mu_j, \omega) A_{d\sigma'}^{(1)}(\mu_j) \frac{\Gamma_j}{\Delta} \\ & \quad + O(\omega^2, (eV)^2). \end{aligned} \quad (8.16)$$

Here, the product of the two Green's that appeared in the right-hand side of Eq. (5.24b) has been rewritten into the form $\Delta G_{\sigma}^r(\omega) G_{\sigma}^a(\omega)/\pi = A_{d\sigma}^{(1)}(\omega) + O(\omega^2, (eV)^2)$, using the spectral function $A_{d\sigma}^{(1)}(\omega)$ which takes into account the self-energy corrections up to linear-order terms in ω and eV :

$$\begin{aligned} A_{d\sigma}^{(1)}(\omega) &\equiv \frac{1}{\pi} \frac{\Delta}{\left(\tilde{\chi}_{\sigma\sigma} \omega - \epsilon_{d\sigma}^* + \sum_{\sigma''(\neq\sigma)} \tilde{\chi}_{\sigma\sigma''} \alpha_{\text{sh}} eV \right)^2 + \Delta^2} \\ &= \rho_{d\sigma} + \rho'_{d\sigma} \left[\omega + \sum_{\sigma''(\neq\sigma)} \frac{\tilde{\chi}_{\sigma\sigma''}}{\tilde{\chi}_{\sigma\sigma}} \alpha_{\text{sh}} eV \right] + \dots \end{aligned} \quad (8.17)$$

Here, $\rho'_{d\sigma}$ is the derivative of the equilibrium density of state, defined in Eq. (3.8). The spectral function $A_{d\sigma}^{(1)}(\omega)$ includes the order eV energy shift emerging for asymmetric junctions with $\alpha_{\text{sh}} \neq 0$ in addition to the equilibrium energy shift $\epsilon_{d\sigma}^* \equiv \epsilon_{d\sigma} + \Sigma_{\text{eq},\sigma}^r(0)$.

As we already know the low-energy asymptotic form of the retarded self-energy as shown in Eq. (3.23a), the derivatives in the left-hand side of Eq. (8.16) can be cal-

culated explicitly up to terms of order ω and eV : it vanishes for $\sigma = \sigma'$,

$$\left(\frac{\partial}{\partial \omega} + \frac{\partial}{\partial \epsilon_{d\sigma}} \right) \text{Re } \Sigma_{U,\sigma}^r(\omega) = 0 + O(\omega^2, (eV)^2), \quad (8.18)$$

and it takes the following form for $\sigma \neq \sigma'$,

$$\begin{aligned} & \frac{\partial}{\partial \epsilon_{d\sigma'}} \text{Re } \Sigma_{U,\sigma}^r(\omega) \\ &= \tilde{\chi}_{\sigma\sigma'} - \frac{\partial \tilde{\chi}_{\sigma\sigma}}{\partial \epsilon_{d\sigma'}} \omega - \sum_{\sigma''(\neq\sigma)} \frac{\partial \tilde{\chi}_{\sigma\sigma''}}{\partial \epsilon_{d\sigma'}} \alpha_{\text{sh}} eV + \dots \end{aligned} \quad (8.19)$$

Therefore, $\text{Re } \Gamma_{\sigma\sigma';\sigma'\sigma}^{--;--}(\omega, \omega'; \omega', \omega)$ in left-hand side of Eq. (8.16) can be deduced from these expressions using also Eq. (8.17). As shown in Eq. (3.18), the real part of causal vertex function for $\sigma = \sigma'$, does not have a constant and linear-order terms with respect ω and ω' at $eV = 0$. This does not change up to order eV ,

$$\text{Re } \Gamma_{\sigma\sigma';\sigma'\sigma}^{--;--}(\omega, \omega'; \omega', \omega) = 0 + O(\omega^2, \omega'^2, (eV)^2). \quad (8.20)$$

We also find that the real part of the causal vertex function for $\sigma \neq \sigma'$ captures the eV -linear term when the inversion symmetry is broken in a way such that $\alpha_{\text{sh}} \neq 0$,

$$\begin{aligned} & \text{Re } \Gamma_{\sigma\sigma';\sigma'\sigma}^{--;--}(\omega, \omega'; \omega', \omega) \rho_{d\sigma} \rho_{d\sigma'} \\ &= -\chi_{\sigma\sigma'} + \rho_{d\sigma} \frac{\partial \tilde{\chi}_{\sigma\sigma'}}{\partial \epsilon_{d\sigma}} \omega + \rho_{d\sigma'} \frac{\partial \tilde{\chi}_{\sigma'\sigma}}{\partial \epsilon_{d\sigma'}} \omega' + \beta_{\sigma\sigma'} \alpha_{\text{sh}} eV \\ & \quad + O(\omega^2, \omega'^2, (eV)^2) \end{aligned} \quad (8.21)$$

$$\begin{aligned} \beta_{\sigma\sigma'} &\equiv - \frac{\partial \rho_{d\sigma}}{\partial \epsilon_{d\sigma'}} \sum_{\sigma''(\neq\sigma)} \tilde{\chi}_{\sigma\sigma''} - \frac{\partial \rho_{d\sigma'}}{\partial \epsilon_{d\sigma}} \sum_{\sigma''(\neq\sigma')} \tilde{\chi}_{\sigma'\sigma''} \\ & \quad + \sum_{\sigma'''(\neq\sigma,\sigma')} \frac{\partial \chi_{\sigma\sigma'}}{\partial \epsilon_{d\sigma'''}}. \end{aligned} \quad (8.22)$$

We have also confirmed that these results for the real parts of the vertex functions Eqs. (8.20) and (8.21) satisfy the Ward identity for the eV derivative given in Eq. (5.32b), which takes the following form for the real part,

$$\begin{aligned} & \frac{\partial}{\partial eV} \text{Re } \Sigma_{U,\sigma}^r(\omega) \\ &= - \sum_{\sigma'} \sum_{j=L,R} \text{Re } \Gamma_{\sigma\sigma';\sigma'\sigma}^{--;--}(\omega, \mu_j; \mu_j, \omega) A_{d\sigma'}^{(1)}(\mu_j) \left(\frac{-\Gamma_j \mu_j}{\Delta eV} \right) \\ & \quad + O(\omega^2, (eV)^2). \end{aligned} \quad (8.23)$$

Namely, the right-hand side of this identity Eq. (8.23) coincides with the derivative of $\text{Re } \Sigma_{U,\sigma}^r(\omega)$ on the left-hand

side that can be calculated directly using Eq. (3.23a),

$$\begin{aligned} \frac{\partial \text{Re} \Sigma_{U,\sigma}^r(\omega)}{\partial eV} = & - \sum_{\sigma''(\neq\sigma)} \left[\tilde{\chi}_{\sigma\sigma''} - \frac{\partial \tilde{\chi}_{\sigma\sigma''}}{\partial \epsilon_{d\sigma}} \omega \right] \alpha_{\text{sh}} \\ & + \frac{\Gamma_L \Gamma_R}{\Delta^2} \sum_{\sigma''(\neq\sigma)} \frac{1}{\rho_{d\sigma}} \frac{\partial \chi_{\sigma\sigma''}}{\partial \epsilon_{d\sigma}} eV \\ & + \sum_{\sigma'(\neq\sigma)} \sum_{\sigma''(\neq\sigma)} \frac{\partial \tilde{\chi}_{\sigma\sigma'}}{\partial \epsilon_{d\sigma''}} \alpha_{\text{sh}}^2 eV + \dots \end{aligned} \quad (8.24)$$

IX. CURRENT NOISE FORMULA IN THE FERMI-LIQUID REGIME

We are now at the stage of being able to calculate the current noise $S_{\text{noise}}^{\text{QD}}$ at finite bias voltages up to order $(eV)^3$. It is defined in terms of the current-current correlation function $\mathcal{K}_{\sigma'\sigma}^{\alpha'\alpha}$,

$$S_{\text{noise}}^{\text{QD}} = e^2 \int_{-\infty}^{\infty} dt \sum_{\sigma\sigma'} i \left[\mathcal{K}_{\sigma'\sigma}^{+-}(t,0) + \mathcal{K}_{\sigma'\sigma}^{-+}(t,0) \right]. \quad (9.1)$$

Here, $\mathcal{K}_{\sigma'\sigma}^{+-}(t,0) \equiv -i \langle \delta \hat{J}_{\sigma'}(t) \delta \hat{J}_{\sigma}(0) \rangle$, $\mathcal{K}_{\sigma'\sigma}^{-+}(t,0) \equiv -i \langle \delta \hat{J}_{\sigma}(0) \delta \hat{J}_{\sigma'}(t) \rangle$. The symmetrized current operator \hat{J}_{σ} is defined in Eq. (2.4). In the Keldysh-Feynman diagrammatic representation, this operator can be treated as a matrix current vertex $\lambda_{\text{sym}}^{\alpha}(\epsilon, \epsilon + \omega)$ defined in Eq. (6.12) in the frequency domain, and in Fig. 2 it is illustrated as a black diamond (\blacklozenge). In particular, at $\omega = 0$, the current vertex for the constant noise can be expressed

in the following form using the Pauli matrix τ_2 ,

$$\lambda_{\text{sym}}^{\alpha}(\epsilon, \epsilon) = \frac{-2\Gamma_L \Gamma_R [f_L(\epsilon) - f_R(\epsilon)]}{\Gamma_L + \Gamma_R} i\tau_2, \quad (9.2)$$

and becomes independent of whether $\alpha = -$ or $+$. At $T = 0$, this current vertex $\lambda_{\text{sym}}^{\alpha}(\epsilon, \epsilon)$ takes a finite value just at the bias-window region $\mu_R \leq \epsilon \leq \mu_L$, and it identically vanishes at equilibrium $eV = 0$.

We calculate $S_{\text{noise}}^{\text{QD}}$ separating it into four parts,

$$\begin{aligned} S_{\text{noise}}^{\text{QD}} = & \left(\frac{\Gamma_L}{\Gamma_L + \Gamma_R} \right)^2 \delta S_{RR} + \left(\frac{\Gamma_R}{\Gamma_L + \Gamma_R} \right)^2 \delta S_{LL} \\ & + S_{\text{sym}}^{\text{qp}} + S_{\text{sym}}^{\text{coll}}. \end{aligned} \quad (9.3)$$

The first two terms δS_{RR} and δS_{LL} represent the contributions of the processes, illustrated in the bottom row of Fig. 2, and can be expressed in the form,

$$\delta S_{jj} = \frac{e^2}{\hbar} i 4\Gamma_j \sum_{\sigma} \int_{-\infty}^{\infty} \frac{d\epsilon}{2\pi} \left[f_j G_{\sigma}^{+-} - (1 - f_j) G_{\sigma}^{-+} \right], \quad (9.4)$$

for $j = L, R$. In the Feynman diagrams for these processes, the dashed line represents the bare conduction-electron Green's function \mathbf{g}_j of the isolated leads on $j = L$ and R , defined in Eq. (5.13). The solid line represents the full impurity-electron Green's function \mathbf{G}_{σ} . The contributions of δS_{RR} and δS_{LL} on the total noise $S_{\text{noise}}^{\text{QD}}$ can also be expressed in the following form, rewriting the lesser and greater Green's functions in Eq. (9.4) by using Eq. (5.19),

$$\begin{aligned} & \left(\frac{\Gamma_L}{\Gamma_L + \Gamma_R} \right)^2 \delta S_{RR} + \left(\frac{\Gamma_R}{\Gamma_L + \Gamma_R} \right)^2 \delta S_{LL} \\ & = \frac{2e^2}{\hbar} 4\Gamma_L \Gamma_R \sum_{\sigma} \int_{-\infty}^{\infty} d\epsilon G_{\sigma}^r G_{\sigma}^a \left[f_R(1 - f_R) + f_L(1 - f_L) + \left\{ 1 - \frac{2\Gamma_L \Gamma_R}{(\Gamma_R + \Gamma_L)^2} \right\} (f_L - f_R)^2 \right. \\ & \quad \left. + \frac{\Gamma_R f_L + \Gamma_L f_R}{(\Gamma_L + \Gamma_R)^2} \frac{\Sigma_{U,\sigma}^{+-}}{2i} - \frac{\Gamma_R(1 - f_L) + \Gamma_L(1 - f_R)}{(\Gamma_L + \Gamma_R)^2} \frac{\Sigma_{U,\sigma}^{-+}}{2i} \right]. \end{aligned} \quad (9.5)$$

The remaining two parts, $S_{\text{sym}}^{\text{qp}}$ and $S_{\text{sym}}^{\text{coll}}$ of Eq. (9.3), represent the contributions of the diagrams shown in the top

row of Fig. 2, i.e. the bubble diagram on the left and the one with vertex corrections on the right,

$$\begin{aligned} S_{\text{sym}}^{\text{qp}} &= \frac{e^2}{\hbar} \sum_{\alpha=+,-} \sum_{\sigma} \int_{-\infty}^{\infty} \frac{d\epsilon}{2\pi} \text{Tr} \left[\lambda_{\text{sym}}^{\alpha}(\epsilon, \epsilon) \mathbf{G}_{\sigma}(\epsilon) \lambda_{\text{sym}}^{-\alpha}(\epsilon, \epsilon) \mathbf{G}_{\sigma}(\epsilon) \right] \\ &= \frac{2e^2}{\hbar} \left[\frac{2\Gamma_L \Gamma_R}{\Gamma_L + \Gamma_R} \right]^2 \sum_{\sigma} \int_{-\infty}^{\infty} d\epsilon [f_L(\epsilon) - f_R(\epsilon)]^2 \left[\{G_{\sigma}^r(\epsilon) - G_{\sigma}^a(\epsilon)\}^2 + 2G_{\sigma}^r(\epsilon) G_{\sigma}^a(\epsilon) \right], \end{aligned} \quad (9.6)$$

$$S_{\text{sym}}^{\text{coll}} = \frac{e^2}{\hbar} \left[\frac{2\Gamma_L \Gamma_R}{\Gamma_L + \Gamma_R} \right]^2 \sum_{\alpha=+,-} \int_{-\infty}^{\infty} \frac{d\epsilon}{2\pi} \int_{-\infty}^{\infty} \frac{d\epsilon'}{2\pi} [f_L(\epsilon) - f_R(\epsilon)] [f_L(\epsilon') - f_R(\epsilon')] \mathcal{Q}(\epsilon, \epsilon'), \quad (9.7)$$

$$\mathcal{Q}(\epsilon, \epsilon') \equiv (-i) \sum_{\sigma\sigma'} \sum_{\substack{\mu\mu' \\ \nu\nu'}} \Gamma_{\sigma\sigma';\sigma'\sigma}^{\mu\mu';\nu\nu'}(\epsilon, \epsilon'; \epsilon', \epsilon) \{ \mathbf{G}_{\sigma}(\epsilon) i\tau_2 \mathbf{G}_{\sigma}(\epsilon) \}_{\mu\nu} \{ \mathbf{G}_{\sigma'}(\epsilon') i\tau_2 \mathbf{G}_{\sigma'}(\epsilon') \}_{\nu'\mu'}. \quad (9.8)$$

In order to obtain Eq. (9.6), we have decomposed the product of the Green's function into the three parts, using the basis set, described in Eq. (5.3), as

$$\mathbf{G}_{\sigma} i\tau_2 \mathbf{G}_{\sigma} = a_{1\sigma} (\mathbf{1} + \tau_1) + a_{3\sigma} \tau_3 - a_{2\sigma} i\tau_2. \quad (9.9)$$

The coefficients can be determined, for instance, in a way such that $\text{Tr} [i\tau_2 \mathbf{G}_{\sigma} i\tau_2 \mathbf{G}_{\sigma}] = 2a_{2\sigma}$, as

$$a_{1\sigma} = \frac{(G_{\sigma}^{+-} + G_{\sigma}^{-+})(G_{\sigma}^r - G_{\sigma}^a)}{2}, \quad (9.10a)$$

$$a_{3\sigma} = \frac{\{G_{\sigma}^r\}^2 - \{G_{\sigma}^a\}^2}{2}, \quad (9.10b)$$

$$a_{2\sigma} = \frac{\{G_{\sigma}^r\}^2 + \{G_{\sigma}^a\}^2}{2}. \quad (9.10c)$$

The free-quasiparticle part, i.e. $S_{\text{sym}}^{\text{qp}}$ of Eq. (9.6), vanishes at equilibrium $eV = 0$ and shows an $|eV|$ -linear dependence at small bias voltages since the distribution function $(f_L - f_R)^2$ restricts the region of the integration to the inside of the bias window $\mu_R \leq \epsilon \leq \mu_L$.

The fourth part, $S_{\text{sym}}^{\text{coll}}$ of Eq. (9.7), represents the contributions of collisions between quasiparticles, which enter through the vertex functions in the kernel $\mathcal{Q}(\epsilon, \epsilon')$ defined as Eq. (9.8). The domains of integrations with respect to ϵ and ϵ' are also restricted by the distribution functions $f_L(\epsilon) - f_R(\epsilon)$ and $f_L(\epsilon') - f_R(\epsilon')$. Therefore, this part $S_{\text{sym}}^{\text{coll}}$ does not show an $|eV|$ -linear dependence, and the restrictions due to the bias window themselves cause a contribution of order $|eV|^2$ at small bias voltages.

A. Thermal noise at equilibrium $eV = 0$

Here we briefly show how the previous result for the thermal noise at equilibrium can be reproduced in our formulation. At $eV = 0$, the contributions of $S_{\text{sym}}^{\text{qp}}$ and $S_{\text{sym}}^{\text{coll}}$ vanish among the four parts of the current noise, described in Eq. (9.3). Furthermore, the lesser and greater Green's functions that determine δS_{RR} and

δS_{LL} through Eq. (9.4) can be written in terms of the retarded Green's function $(-1/\pi) \text{Im} G_{\text{eq},\sigma}^r$, using Eq. (5.21). Therefore, the well-known thermal noise formula is derived from Eqs. (9.3) and (9.4), as

$$\begin{aligned} S_{\text{noise}}^{\text{QD}} &\xrightarrow{eV \rightarrow 0} \left(\frac{\Gamma_L}{\Gamma_L + \Gamma_R} \right)^2 \delta S_{RR} + \left(\frac{\Gamma_R}{\Gamma_L + \Gamma_R} \right)^2 \delta S_{LL} \\ &= 4T \frac{e^2}{\hbar} \sum_{\sigma} \int_{-\infty}^{\infty} d\epsilon \left(-\frac{\partial f(\epsilon)}{\partial \epsilon} \right) \mathcal{T}_{\text{eq},\sigma}(\epsilon). \end{aligned} \quad (9.11)$$

Here, $\mathcal{T}_{\text{eq},\sigma}(\epsilon) \equiv \mathcal{T}_{\sigma}(\epsilon)|_{eV=0}$ is the transmission probability, defined in Eq. (2.6). We have also used the relation $T(-\partial f/\partial \epsilon) = f(1-f)$ of the Fermi function part. In low-temperature Fermi-liquid regime, the thermal noise can be deduced up to terms of order T^3 by using the low-temperature expansion of the linear conductance, given in Eq. (4.3).

B. The $|eV|$ -linear current noise at $T = 0$

We next consider the $|eV|$ -linear contributions of the current noise $S_{\text{noise}}^{\text{QD}}$ that can be determined by the first three terms of Eq. (9.3). The order $|eV|$ contributions of $S_{\text{sym}}^{\text{qp}}$ can be calculated, taking the frequency argument for the Green's functions in Eq. (9.6) to be $\epsilon = 0$ as the linear dependence is determined by the width of the bias window. For the weighted sum of δS_{RR} and δS_{LL} in Eq. (9.5), the lesser or greater self-energy that appeared in the right-hand side do not yield order $|eV|$ contributions. This is because these two self-energies $\Sigma_{U,\sigma}^{-+}(\epsilon)$ and $\Sigma_{U,\sigma}^{+-}(\epsilon)$ in the integrand show the ϵ^2 and $|eV|^2$ behaviors, as described in Eqs. (7.3) and (7.4), and yield high-order terms which we consider later in next subsection. Therefore, the sum of these contributions determine the linear

current noise at $T = 0$, as

$$\begin{aligned} S_{\text{noise}}^{\text{QD}} &\xrightarrow{T \rightarrow 0} \left(\frac{\Gamma_L}{\Gamma_L + \Gamma_R} \right)^2 \delta S_{RR} + \left(\frac{\Gamma_R}{\Gamma_L + \Gamma_R} \right)^2 \delta S_{LL} \\ &\quad + S_{\text{sym}}^{\text{qp}} + O(|eV|^2) \\ &= \frac{2e^2}{h} |eV| \sum_{\sigma} \mathcal{T}_{\text{eq},\sigma}(0) \left[1 - \mathcal{T}_{\text{eq},\sigma}(0) \right] + \dots \end{aligned} \quad (9.12)$$

It reproduces the well-established linear-noise formula, which is determined by the transmission probability at the Fermi level $\mathcal{T}_{\text{eq},\sigma}(0) = \sin^2 \delta_{\sigma}$.

C. Order $|eV|^3$ terms of current noise $S_{\text{noise}}^{\text{QD}}$

We calculate order $|eV|^3$ terms of the current noise $S_{\text{noise}}^{\text{QD}}$ in the rest of this section, specifically for symmetric junctions $\Gamma_L = \Gamma_R$ and $\mu_L = -\mu_R = eV/2$, at $T = 0$. To this end, we consider first of all the contributions of the first three parts of Eq. (9.3), for which effects of the Coulomb interaction enter only through the Green's function $G_{\sigma}^{\mu\nu}(\epsilon)$, or the self-energy $\Sigma_{U,\sigma}^{\mu\nu}(\epsilon)$, as shown in Eqs. (9.5) and (9.6). Then, we calculate the remaining part $S_{\text{sym}}^{\text{coll}}$, which includes effects vertex corrections as shown in Eq. (9.7), later in this subsection.

1. Contributions of bubble diagrams

The free quasiparticle contributions without vertex corrections are described by the first three parts of Eq. (9.3), as mentioned. The sum of these contributions take a simplified form for symmetric junctions $\Gamma_L = \Gamma_R$ and $\mu_L = -\mu_R = eV/2$, at $T = 0$,

$$\begin{aligned} &\left(\frac{\Gamma_L}{\Gamma_L + \Gamma_R} \right)^2 \delta S_{RR} + \left(\frac{\Gamma_R}{\Gamma_L + \Gamma_R} \right)^2 \delta S_{LL} + S_{\text{sym}}^{\text{qp}} \\ &= \frac{2e^2}{h} \sum_{\sigma} \int_{-\infty}^{\infty} d\epsilon (f_L - f_R)^2 \Delta^2 \left[\left(\frac{G_{\sigma}^r - G_{\sigma}^a}{2} \right)^2 + G_{\sigma}^r G_{\sigma}^a \right] \\ &\quad + \frac{2e^2}{h} \sum_{\sigma} \int_{-\infty}^{\infty} d\epsilon \Delta G_{\sigma}^r G_{\sigma}^a \\ &\quad \times \left[\frac{f_L + f_R}{4i} \Sigma_{U,\sigma}^{+-} - \frac{(1-f_L) + (1-f_R)}{4i} \Sigma_{U,\sigma}^{-+} \right]. \end{aligned} \quad (9.13)$$

In order to extract order $|eV|^3$ terms from this equation, the lesser and greater self-energies in the last line can be replaced by the low-energy asymptotic forms, given in Eqs. (7.3) and (7.4) which exactly describe the ϵ^2 and $(eV)^2$ dependences of $\Sigma_{U,\sigma}^{-+}(\epsilon)$ and $\Sigma_{U,\sigma}^{+-}(\epsilon)$. Thus, it can

be rewritten into the form,

$$\begin{aligned} &\left(\frac{\Gamma_L}{\Gamma_L + \Gamma_R} \right)^2 \delta S_{RR} + \left(\frac{\Gamma_R}{\Gamma_L + \Gamma_R} \right)^2 \delta S_{LL} + S_{\text{sym}}^{\text{qp}} \\ &= \frac{2e^2}{h} \sum_{\sigma} \int_{-\frac{|eV|}{2}}^{\frac{|eV|}{2}} d\epsilon \Delta^2 \left[\left\{ \frac{G_{\sigma}^r(\epsilon) - G_{\sigma}^a(\epsilon)}{2} \right\}^2 + G_{\sigma}^r(\epsilon) G_{\sigma}^a(\epsilon) \right] \\ &\quad + \frac{2e^2}{h} \sum_{\sigma} \frac{\pi \Delta G_{\sigma}^r(0) G_{\sigma}^a(0)}{\rho_{d\sigma}} \sum_{\sigma'' (\neq \sigma)} \chi_{\sigma\sigma''}^2 \\ &\quad \times \int_{-\infty}^{\infty} d\epsilon \left[\frac{f_L + f_R}{2} \mathcal{I}^{+-} + \frac{(1-f_L) + (1-f_R)}{2} \mathcal{I}^{-+} \right] \\ &\quad + \dots \end{aligned} \quad (9.14)$$

The contributions of the first integral in Eq. (9.14) can be calculated, expanding $G_{\sigma}^r(\epsilon)$ and $G_{\sigma}^a(\epsilon)$ in the integrand up to order ϵ^2 and $|eV|^2$ using the asymptotic form of the self-energy summarized in TABLE V. Note that $\Delta G_{\sigma}^r(0) G_{\sigma}^a(0) = \pi \rho_{d\sigma}$, and the low-energy expansion of $G_{\sigma}^r(\epsilon) - G_{\sigma}^a(\epsilon)$ for symmetric junctions is given in Eq. (4.1). The product of the retarded and advanced Green's functions $G_{\sigma}^r(\epsilon) G_{\sigma}^a(\epsilon)$ can also be expanded in a similar way. The second integral in Eq. (9.14) can be carried out, using the explicit form of the collision integrals $\mathcal{I}^{-+}(\epsilon)$ and $\mathcal{I}^{+-}(\epsilon)$ given in Eq. (7.2), as

$$\begin{aligned} &\int_{-\infty}^{\infty} d\epsilon \left[\frac{f_L + f_R}{2} \mathcal{I}^{+-} + \frac{(1-f_L) + (1-f_R)}{2} \mathcal{I}^{-+} \right] \\ &= \int_{-\frac{3|eV|}{2}}^{-\frac{|eV|}{2}} d\epsilon \frac{\left(\epsilon + \frac{3|eV|}{2} \right)^2}{32} + \int_{-\frac{3|eV|}{2}}^{\frac{|eV|}{2}} d\epsilon \frac{\left(\epsilon + \frac{3|eV|}{2} \right)^2}{32} \\ &\quad + 3 \int_{-\frac{|eV|}{2}}^{\frac{|eV|}{2}} d\epsilon \frac{\left(\epsilon + \frac{|eV|}{2} \right)^2}{32} + 3 \int_{-\frac{|eV|}{2}}^{\frac{|eV|}{2}} d\epsilon \frac{\left(\epsilon - \frac{|eV|}{2} \right)^2}{32} \\ &\quad + \int_{-\frac{|eV|}{2}}^{\frac{3|eV|}{2}} d\epsilon \frac{\left(\epsilon - \frac{3|eV|}{2} \right)^2}{32} + \int_{\frac{|eV|}{2}}^{\frac{3|eV|}{2}} d\epsilon \frac{\left(\epsilon - \frac{3|eV|}{2} \right)^2}{32} \\ &= \frac{|eV|^3}{4}. \end{aligned} \quad (9.15)$$

Therefore, the sum of the first three parts of Eq. (9.3) can be expressed in the following form, which is exact up to terms of order $|eV|^3$ for symmetric junctions at $T = 0$,

$$\begin{aligned} &S_{\text{sym}}^{\text{qp}} + \left(\frac{\Gamma_L}{\Gamma_L + \Gamma_R} \right)^2 \delta S_{RR} + \left(\frac{\Gamma_R}{\Gamma_L + \Gamma_R} \right)^2 \delta S_{LL} \\ &= \frac{2e^2}{h} |eV| \sum_{\sigma} \frac{\sin^2 2\delta_{\sigma}}{4} \\ &\quad - \frac{2e^2}{h} \frac{|eV|^3}{3} \sum_{\sigma} \left[c_{V,\sigma} \cos 2\delta_{\sigma} + \frac{\pi^2}{4} \sin^2 2\delta_{\sigma} \chi_{\sigma\sigma}^2 \right. \\ &\quad \left. + \frac{\pi^2}{2} \sum_{\sigma' (\neq \sigma)} \chi_{\sigma\sigma'}^2 \right] + \dots \end{aligned} \quad (9.16)$$

Here, $c_{V,\sigma}$ is the coefficient for the order $(eV)^2$ term of the differential conductance dJ/dV , given in Eq. (4.2) and TABLE I.

2. Contributions of vertex corrections $S_{\text{sym}}^{\text{coll}}$

The remaining term, $S_{\text{sym}}^{\text{coll}}$ of Eq. (9.3), represents the contributions of the two-quasiparticle collision processes, which corresponds to the second diagram in the first row of Fig. 2. The equation (9.7) takes a simplified form, for symmetric junctions $\Gamma_L = \Gamma_R = \Delta/2$ and $\mu_L = -\mu_R = eV/2$, especially at $T = 0$,

$$S_{\text{sym}}^{\text{coll}} = \frac{2e^2 \Delta^2}{h 8\pi} \int_{-\frac{|eV|}{2}}^{\frac{|eV|}{2}} d\epsilon \int_{-\frac{|eV|}{2}}^{\frac{|eV|}{2}} d\epsilon' \mathcal{Q}(\epsilon, \epsilon'). \quad (9.17)$$

The domains of the integrals with respect to ϵ and ϵ' are restricted to the inside of the bias window. Therefore, in order to calculate $S_{\text{sym}}^{\text{coll}}$ up to order $|eV|^3$, the kernel $\mathcal{Q}(\epsilon, \epsilon')$ should be expanded up to linear order in ϵ, ϵ' , and $|eV|$. To this end, we rewrite $\mathcal{Q}(\epsilon, \epsilon')$ into the following form by substituting Eq. (9.9) into Eq. (9.8),

$$\mathcal{Q}(\epsilon, \epsilon') = \sum_{\sigma\sigma'} \sum_{l=1}^3 \sum_{m=1}^3 a_{l\sigma}(\epsilon) a_{m\sigma'}(\epsilon') \overline{\mathcal{Q}}_{\sigma\sigma'}^{lm}(\epsilon, \epsilon'). \quad (9.18)$$

Here, $\overline{\mathcal{Q}}_{\sigma\sigma'}^{lm}(\epsilon, \epsilon')$ corresponds to the vertex contributions, for which the summations over the Keldysh-branch indexes $(\mu, \mu'; \nu', \nu)$ in Eq. (9.8) have been carried out with matrix set $\mathbf{1} + \boldsymbol{\tau}_1$, $\boldsymbol{\tau}_3$, and $i\boldsymbol{\tau}_2$. Specifically, for symmetric junctions $\Gamma_L = \Gamma_R = \Delta/2$ and $\mu_L = -\mu_R = eV/2$, only the two components $\overline{\mathcal{Q}}_{\sigma\sigma'}^{33}(\epsilon, \epsilon')$ and $\overline{\mathcal{Q}}_{\sigma\sigma'}^{22}(\epsilon, \epsilon')$ among nine possible (l, m) configurations have linear-order terms with respect to ϵ, ϵ' and $|eV|$, and thus Eq. (9.18) takes a simplified form,

$$\mathcal{Q}(\epsilon, \epsilon') = \sum_{\sigma\sigma'} \left[a_{3\sigma}(\epsilon) a_{3\sigma'}(\epsilon') \overline{\mathcal{Q}}_{\sigma\sigma'}^{33}(\epsilon, \epsilon') + a_{2\sigma}(\epsilon) a_{2\sigma'}(\epsilon') \overline{\mathcal{Q}}_{\sigma\sigma'}^{22}(\epsilon, \epsilon') \right] + \dots \quad (9.19)$$

One of the reasons for this is that the coefficient $a_{1\sigma}(\epsilon)$, defined in Eq. (9.10), vanishes identically inside the bias-window region $|\epsilon| \leq |eV|/2$. It follows from the low-energy properties of the lesser and greater Green's function, described in Eq. (7.5),

$$G_{\sigma}^{+-}(\epsilon) + G_{\sigma}^{-+}(\epsilon) \simeq -2i\Delta [1 - 2f_{\text{eff}}(\epsilon)] G_{\sigma}^r(\epsilon) G_{\sigma}^a(\epsilon). \quad (9.20)$$

Thus, the components which are accompanied by $a_{1\sigma}(\epsilon)$ or $a_{1\sigma'}(\epsilon')$ vanish in the right-hand side of Eq. (9.18) since $1 - 2f_{\text{eff}}(\epsilon) \equiv 0$ at $|\epsilon| < |eV|/2$ for symmetric junctions. Another reason is that two other components $\overline{\mathcal{Q}}_{\sigma\sigma'}^{32}(\epsilon, \epsilon')$

and $\overline{\mathcal{Q}}_{\sigma\sigma'}^{23}(\epsilon, \epsilon')$ do not have linear-order terms in ϵ, ϵ' and $|eV|$:

$$\begin{aligned} \overline{\mathcal{Q}}_{\sigma\sigma'}^{32}(\epsilon, \epsilon') &= i \sum_{\mu\nu} \sum_{\mu'\nu'} \{ \boldsymbol{\tau}_3 \}_{\mu\nu} \Gamma_{\sigma\sigma';\sigma'\sigma}^{\mu\mu';\nu'\nu}(\epsilon, \epsilon'; \epsilon', \epsilon) \{ i\boldsymbol{\tau}_2 \}_{\nu'\mu'} \\ &= i \left[\Gamma_{\sigma\sigma';\sigma'\sigma}^{-+;-} + \Gamma_{\sigma\sigma';\sigma'\sigma}^{+-;+-} - \Gamma_{\sigma\sigma';\sigma'\sigma}^{-+;+-} - \Gamma_{\sigma\sigma';\sigma'\sigma}^{+-;-} \right] \\ &= 0 + O(\epsilon^2, \epsilon'^2, |eV|^2), \end{aligned} \quad (9.21)$$

and also $\overline{\mathcal{Q}}_{\sigma\sigma'}^{23}(\epsilon, \epsilon') = 0 + O(\epsilon^2, \epsilon'^2, |eV|^2)$. This is because each one of the Keldysh vertex components with three identical branch indexes, such as $\Gamma_{\sigma\sigma';\sigma\sigma}^{+-;+-}$ and $\Gamma_{\sigma\sigma';\sigma\sigma}^{-+;-}$, does not have a constant and linear order terms with respect to ϵ, ϵ' , and eV .

The two components $\overline{\mathcal{Q}}_{\sigma\sigma'}^{33}(\epsilon, \epsilon')$ and $\overline{\mathcal{Q}}_{\sigma\sigma'}^{22}(\epsilon, \epsilon')$ in Eq. (9.19) can be calculated, using the low-energy expansion of the vertex functions, given in TABLES VII and VIII. These components for $\sigma = \sigma'$ can be expressed in the following form at $|\epsilon| < |eV|/2$ and $|\epsilon'| < |eV|/2$,

$$\begin{aligned} \overline{\mathcal{Q}}_{\sigma\sigma}^{33}(\epsilon, \epsilon') &= -i \sum_{\mu\nu} \sum_{\mu'\nu'} \{ \boldsymbol{\tau}_3 \}_{\mu\nu} \Gamma_{\sigma\sigma;\sigma\sigma}^{\mu\mu';\nu'\nu}(\epsilon, \epsilon'; \epsilon', \epsilon) \{ \boldsymbol{\tau}_3 \}_{\nu'\mu'} \\ &= -i \left[\Gamma_{\sigma\sigma;\sigma\sigma}^{-+;-} + \Gamma_{\sigma\sigma;\sigma\sigma}^{+-;+-} - \Gamma_{\sigma\sigma;\sigma\sigma}^{-+;+-} - \Gamma_{\sigma\sigma;\sigma\sigma}^{+-;-} \right] \\ &= \frac{\pi}{\rho_{d\sigma}^2} \sum_{\sigma''(\neq\sigma)} \chi_{\sigma\sigma''}^2 \left[|\epsilon - \epsilon'| - |eV| \right] + \dots, \end{aligned} \quad (9.22)$$

and

$$\begin{aligned} \overline{\mathcal{Q}}_{\sigma\sigma}^{22}(\epsilon, \epsilon') &= -i \sum_{\mu\nu} \sum_{\mu'\nu'} \{ i\boldsymbol{\tau}_2 \}_{\mu\nu} \Gamma_{\sigma\sigma;\sigma\sigma}^{\mu\mu';\nu'\nu}(\epsilon, \epsilon'; \epsilon', \epsilon) \{ i\boldsymbol{\tau}_2 \}_{\nu'\mu'} \\ &= -i \left[\Gamma_{\sigma\sigma;\sigma\sigma}^{-+;-} + \Gamma_{\sigma\sigma;\sigma\sigma}^{+-;+-} - \Gamma_{\sigma\sigma;\sigma\sigma}^{-+;+-} - \Gamma_{\sigma\sigma;\sigma\sigma}^{+-;-} \right] \\ &= \frac{\pi}{\rho_{d\sigma}^2} \sum_{\sigma''(\neq\sigma)} \chi_{\sigma\sigma''}^2 \left[|\epsilon - \epsilon'| + |eV| \right] + \dots. \end{aligned} \quad (9.23)$$

Similarly, at $|\epsilon| < |eV|/2$ and $|\epsilon'| < |eV|/2$, the components for $\sigma \neq \sigma'$ are given by

$$\begin{aligned} \overline{\mathcal{Q}}_{\sigma\sigma'}^{33}(\epsilon, \epsilon') &= -i \sum_{\mu\nu} \sum_{\mu'\nu'} \{ \boldsymbol{\tau}_3 \}_{\mu\nu} \Gamma_{\sigma\sigma';\sigma'\sigma}^{\mu\mu';\nu'\nu}(\epsilon, \epsilon'; \epsilon', \epsilon) \{ \boldsymbol{\tau}_3 \}_{\nu'\mu'} \\ &= -i \left[\Gamma_{\sigma\sigma';\sigma'\sigma}^{-+;-} + \Gamma_{\sigma\sigma';\sigma'\sigma}^{+-;+-} - \Gamma_{\sigma\sigma';\sigma'\sigma}^{-+;+-} - \Gamma_{\sigma\sigma';\sigma'\sigma}^{+-;-} \right] \\ &= \frac{\pi}{\rho_{d\sigma} \rho_{d\sigma'}} \left[\chi_{\sigma\sigma'}^2 \left(|\epsilon - \epsilon'| - |\epsilon + \epsilon'| \right) \right. \\ &\quad \left. - 2|eV| \sum_{\sigma_3(\neq\sigma, \sigma')} \chi_{\sigma\sigma_3} \chi_{\sigma_3\sigma'} \right] + \dots, \end{aligned} \quad (9.24)$$

and

$$\begin{aligned}
\overline{\mathcal{Q}}_{\sigma\sigma'}^{22}(\epsilon, \epsilon') &= -i \sum_{\mu\nu} \sum_{\mu'\nu'} \{i\tau_2\}_{\mu\nu} \Gamma_{\sigma\sigma';\sigma'\sigma}^{\mu\mu';\nu'\nu}(\epsilon, \epsilon'; \epsilon', \epsilon) \{i\tau_2\}_{\nu'\nu'} \\
&= -i \left[\Gamma_{\sigma\sigma';\sigma'\sigma}^{-+-; -+} + \Gamma_{\sigma\sigma';\sigma'\sigma}^{+-; ++} - \Gamma_{\sigma\sigma';\sigma'\sigma}^{--; ++} - \Gamma_{\sigma\sigma';\sigma'\sigma}^{++; --} \right] \\
&= \frac{\pi}{\rho_{d\sigma}\rho_{d\sigma'}} \chi_{\sigma\sigma'}^2 \left[|\epsilon - \epsilon'| + |\epsilon + \epsilon'| + 2|eV| \right] \\
&\quad + \dots
\end{aligned} \tag{9.25}$$

In order to obtain these expressions, we have used the properties of the bosonic collision integrals, described in Eqs. (7.26) and (7.27). Note that $a_{3\sigma}(\epsilon)$ and $a_{2\sigma}(\epsilon)$ in Eq. (9.19) can be replaced by their zero-frequency values

$$a_{3\sigma}(0) = i \frac{\pi\rho_{d\sigma}}{\Delta} \sin 2\delta_\sigma, \quad a_{2\sigma}(0) = \frac{\pi\rho_{d\sigma}}{\Delta} \cos 2\delta_\sigma, \tag{9.26}$$

since their ϵ dependence yields the higher-order corrections than the order $|eV|^3$ ones.

We can now calculate the vertex contributions $S_{\text{sym}}^{\text{coll}}$ by substituting Eqs. (9.22) and (9.25) into Eq. (9.19), and then carrying out the double integral in Eq. (9.17) that is given by

$$\int_{-\frac{|eV|}{2}}^{\frac{|eV|}{2}} d\epsilon \int_{-\frac{|eV|}{2}}^{\frac{|eV|}{2}} d\epsilon' |\epsilon \pm \epsilon'| = \frac{1}{3} |eV|^3. \tag{9.27}$$

Consequently, the vertex contributions to the nonlinear current noise $S_{\text{sym}}^{\text{coll}}$ are obtained exactly up to order $|eV|^3$ at $T = 0$,

$$\begin{aligned}
S_{\text{sym}}^{\text{coll}} &= \frac{2e^2 \pi^2 |eV|^3}{h} \sum_{\sigma} \sum_{\sigma'(\neq\sigma)} \\
&\times \left[\left(\sin^2 2\delta_\sigma + 2 \cos^2 2\delta_\sigma \right) \chi_{\sigma\sigma'}^2 \right. \\
&\quad + 4 \cos 2\delta_\sigma \cos 2\delta_{\sigma'} \chi_{\sigma\sigma'}^2 \\
&\quad \left. + 3 \sin 2\delta_\sigma \sin 2\delta_{\sigma'} \sum_{\sigma''(\neq\sigma, \sigma')} \chi_{\sigma\sigma''} \chi_{\sigma''\sigma'} \right] + \dots
\end{aligned} \tag{9.28}$$

D. Total current noise $S_{\text{noise}}^{\text{QD}}$ up to order $|eV|^3$

We have calculated the nonlinear current noise in the above, separating it into four parts as shown in Eq. (9.3). The contributions of the first three parts which are described by the bubble diagrams are given in Eq. (9.16), and the remaining part that represents contributions of the vertex corrections are given in Eq. (9.28). Adding all contributions, we obtain the following formula for the nonlinear current noise that is exact up to order $|eV|^3$ at $T = 0$ for symmetric junctions $\Gamma_L = \Gamma_R$ and

$$\mu_L = -\mu_R = eV/2,$$

$$S_{\text{noise}}^{\text{QD}} = \frac{2e^2}{h} |eV| \sum_{\sigma} \left[\frac{\sin^2 2\delta_\sigma}{4} + c_{S,\sigma} (eV)^2 + \dots \right]. \tag{9.29}$$

The coefficient $c_{S,\sigma}$ is given by

$$\begin{aligned}
c_{S,\sigma} &= \frac{\pi^2}{12} \left[\cos 4\delta_\sigma \chi_{\sigma\sigma}^2 + (2 + 3 \cos 4\delta_\sigma) \sum_{\sigma'(\neq\sigma)} \chi_{\sigma\sigma'}^2 \right. \\
&\quad + 4 \sum_{\sigma'(\neq\sigma)} \cos 2\delta_\sigma \cos 2\delta_{\sigma'} \chi_{\sigma\sigma'}^2 \\
&\quad + 3 \sum_{\sigma'(\neq\sigma)} \sum_{\sigma''(\neq\sigma, \sigma')} \sin 2\delta_\sigma \sin 2\delta_{\sigma'} \chi_{\sigma\sigma''} \chi_{\sigma''\sigma'} \\
&\quad \left. - \left(\chi_{\sigma\sigma\sigma}^{[3]} + 3 \sum_{\sigma'(\neq\sigma)} \chi_{\sigma\sigma'\sigma'}^{[3]} \right) \frac{\sin 4\delta_\sigma}{4\pi} \right].
\end{aligned} \tag{9.30}$$

This is also one of the most important results of this paper and is described in Sec. IV.

X. SUMMARY

In summary, we have investigated thoroughly low-energy behaviors of the Keldysh vertex functions $\Gamma_{\sigma\sigma';\sigma'\sigma}^{\nu_1\nu_2;\nu_3\nu_4}(\omega, \omega'; \omega', \omega)$ of the Anderson impurity model in a nonequilibrium steady state under a finite bias voltage eV . This information is essential to determine the next-to-leading order transport of the nonlinear current noise through quantum dots in the Fermi-liquid regime.

We have provided a Feynman-diagrammatic derivation of the Ward identities, which describes the relations between the Keldysh vertex functions and the self-energies $\Sigma_{U,\sigma}^{\nu_4\nu_1}(\omega)$. In the perturbation theory in U , effects of the bias voltage eV and temperature T enter through the nonequilibrium distribution function $f_{\text{eff}}(\omega)$ that is contained in the noninteracting propagators $G_{0\sigma}^{\nu_4\nu_1}(\omega)$, given in Eq. (5.8). It appears in the right-hand side of the Ward identities Eqs. (5.24) and (5.32), and each of the derivatives $\partial f_{\text{eff}}(\omega)/\partial\omega$ and $\partial f_{\text{eff}}(\omega)/\partial(eV)$ evolves into the two Dirac delta functions at $\omega = \mu_L$ and μ_R in the limit $T \rightarrow 0$.

We have also verified that these relations can be derived from more general Ward-Takahashi identities for the three-point Keldysh correlations functions $\Phi_{\gamma,\sigma\sigma'}^\alpha(\epsilon, \epsilon + \omega)$, or the corresponding three-point vertex functions $\Lambda_{\gamma,\sigma\sigma'}^\alpha(\epsilon, \epsilon + \omega)$ for $\gamma = L, R, d$ and $\alpha = +, -$, given in Eqs. (6.17) and (6.18). These equations explicitly show that the Ward identity Eq. (5.24) reflects the local current conservation between the impurity site and the conduction bands holding for each σ component.

Thus, the current conservation plays an essential role to the next-to-leading order transport in the Fermi-liquid regime since a quasiparticle shows the damping of order ω^2 , $(eV)^2$ and T^2 . It is determined the scattering processes illustrated in Fig. 7, and its precise dependences on

ω , eV and T can be described in terms of the fermionic collision integrals $\mathcal{I}^{+-}(\omega)$ and $\mathcal{I}^{-+}(\omega)$, defined in Sec. VII. Correspondingly, the imaginary part of the vertex functions are determined by the scattering processes illustrated in Fig. 8 at low energies up to linear-order terms with respect to ω , eV and T ; the results are summarized in TABLES VII and VIII. The imaginary part of the vertex functions can be expressed in terms of the bosonic collision integrals $\mathcal{W}^{\text{ph}}(\omega)$, $\mathcal{W}^{\text{pp}}(\omega)$, and $\mathcal{W}^{\text{hh}}(\omega)$ which represent the single particle-hole, particle-particle, and hole-hole propagating processes.

The imaginary parts of the Ward identities are full filled in the Fermi-liquid regime through the relations between these bosonic collision integrals and the fermionic ones, as shown in Sec. VIII. Furthermore, from the Ward identities, we have also deduced the eV -linear real part which emerges for the causal vertex component, i.e. $\text{Re}\Gamma_{\sigma\sigma';\sigma'\sigma}^{--}(\omega, \omega'; \omega', \omega)$ for $\sigma \neq \sigma'$. This real part becomes finite when the inversion symmetry of the tunnel junction is broken in a way such that $\Gamma_L \mu_L + \Gamma_R \mu_R \neq 0$, and its value is determined by the nonlinear three-body susceptibilities and the derivative of the density of states.

Using these exact low-energy asymptotic forms of the Keldysh vertex functions and Green's functions, we have calculated the current noise $S_{\text{noise}}^{\text{QD}}$ up to terms of order $|eV|^3$, and have applied it to some typical cases: the $\text{SU}(N)$ Anderson model, and the $S = 1/2$ Anderson model in a magnetic field b . Our formula is applicable to a wide class of quantum dots without particle-hole or time-reversal symmetry, for any value of the impurity-electron filling $\langle n_{d\sigma} \rangle$ which varies with parameters U , $\epsilon_{d\sigma}$, and Δ . In this paper, the order $|eV|^3$ current noise has been obtained specifically for symmetric tunnel junctions satisfying the conditions $\Gamma_L = \Gamma_R = \Delta/2$ and $\mu_L = -\mu_R = eV/2$, just for simplicity. Nevertheless, calculations carried out in Sec. IX can be extended straightforwardly to quantum dots with no such junction symmetries, and it is left for a future work. The necessary information for carrying it out, namely the low-energy asymptotic form of the Keldysh vertex functions in the Fermi-liquid regime, has already been obtained in this paper without assuming these symmetries for tunnel junctions.

ACKNOWLEDGMENTS

We would like to thank K. Kobayashi, T. Hata, M. Ferrier, and A. C. Hewson for valuable discussions. This work was supported by JSPS KAKENHI Grant Numbers JP18J10205, JP18K03495, JP21K03415, JST CREST Grant No. JPMJCR1876, and the Sasakawa Scientific Research Grant from the Japan Science Society No. 2021-2009.

Appendix A: Linear dependency of the Keldysh correlation functions

We describe here briefly the linear dependence among the components of the Keldysh correlation functions. To this end, we quickly look back the situation for the single-particle Green's function.

By definition given in Eq. (5.1), the components of $G_{\sigma}^{\mu\nu}$ are linearly dependent, as

$$\sum_{\mu\nu} \text{sgn}(\mu\nu) G_{\sigma}^{\mu\nu} = G_{\sigma}^{--} + G_{\sigma}^{++} - G_{\sigma}^{+-} - G_{\sigma}^{-+} = 0. \quad (\text{A1})$$

Corresponding relation between the self-energy components can be deduced from this relations. It can be carried out, substituting the expressions of $G_{\sigma}^{\mu\nu}$ in the right-hand side of the Dyson equation, $\mathbf{G}_{\sigma} = \mathbf{G}_{0\sigma} + \mathbf{G}_{0\sigma} \Sigma_{U,\sigma} \mathbf{G}_{\sigma}$, into Eq. (A1), and using also Eq. (5.3) to rewrite $G_{\sigma}^{\mu\nu}$ further in terms of G_{σ}^r , G_{σ}^a , and G_{σ}^K , as

$$\sum_{\mu\nu} \text{sgn}(\mu\nu) G_{0\sigma}^{\mu\nu} + G_{0\sigma}^a G_{\sigma}^r \sum_{\mu'\nu'} \Sigma_{U,\sigma}^{\mu'\nu'} = 0. \quad (\text{A2})$$

The first term in the left-hand side vanishes because the noninteracting Green's function $G_{0\sigma}^{\mu\nu}$ also satisfies the same linear-dependent relation as Eq. (A1). Furthermore, as the product $G_{0\sigma}^a G_{\sigma}^r$ in the left-hand side of Eq. (A2) does not identically vanish, it follows that

$$\Sigma_{U,\sigma}^{--} + \Sigma_{U,\sigma}^{++} + \Sigma_{U,\sigma}^{+-} + \Sigma_{U,\sigma}^{-+} = 0. \quad (\text{A3})$$

In the next two subsections, we examine the linear dependency of $\Lambda_{\gamma,\sigma\sigma'}^{\alpha;\mu\nu}$ and $\Gamma_{\sigma_1\sigma_2;\sigma_3\sigma_4}^{\nu_1\nu_2;\nu_3\nu_4}$, following along the similar line.

1. Linear dependence of $\Lambda_{\gamma,\sigma\sigma'}^{\alpha;\mu\nu}$

The three-point function $\Phi_{\gamma,\sigma\sigma'}^{\alpha;\mu\nu}$ for $\gamma = L, R, d$ are also linearly dependent as it can be verified directly from the definition given in Eq. (6.1),

$$\begin{aligned} & \left(\Phi_{\gamma,\sigma\sigma'}^{-;-} + \Phi_{\gamma,\sigma\sigma'}^{-;+-} - \Phi_{\gamma,\sigma\sigma'}^{-;+} - \Phi_{\gamma,\sigma\sigma'}^{-;-} \right) \\ & - \left(\Phi_{\gamma,\sigma\sigma'}^{+;+-} + \Phi_{\gamma,\sigma\sigma'}^{+;+} - \Phi_{\gamma,\sigma\sigma'}^{+;-} - \Phi_{\gamma,\sigma\sigma'}^{+;-} \right) = 0. \end{aligned} \quad (\text{A4})$$

Therefore, the components of the vertex $\Lambda_{\gamma,\sigma\sigma'}^{\alpha;\mu\nu}(\epsilon, \epsilon + \omega)$, defined in Eq. (6.3) such that $\Phi_{\gamma,\sigma\sigma'}^{\alpha} = \mathbf{G}_{\sigma}^{\alpha} \Lambda_{\gamma,\sigma\sigma'}^{\alpha} \mathbf{G}_{\sigma}$ in the frequency domain, are also linearly dependent. The left-hand side of Eq. (A4) can be rewritten in terms of $\Lambda_{\gamma,\sigma\sigma'}^{\alpha;\mu\nu}$, G_{σ}^r , G_{σ}^a , and G_{σ}^K , using also Eq. (5.3), as

$$\begin{aligned} & G_{\sigma}^a(\epsilon) G_{\sigma}^r(\epsilon + \omega) \left[\Lambda_{\gamma,\sigma\sigma'}^{-;-} + \Lambda_{\gamma,\sigma\sigma'}^{-;+-} + \Lambda_{\gamma,\sigma\sigma'}^{-;+} + \Lambda_{\gamma,\sigma\sigma'}^{-;-} \right. \\ & \left. - \Lambda_{\gamma,\sigma\sigma'}^{+;+-} - \Lambda_{\gamma,\sigma\sigma'}^{+;+} - \Lambda_{\gamma,\sigma\sigma'}^{+;-} - \Lambda_{\gamma,\sigma\sigma'}^{+;-} \right] = 0. \end{aligned} \quad (\text{A5})$$

Thus, from this, it follows that

$$\sum_{\alpha=\pm} \sum_{\mu\nu} \text{sgn}(\alpha) \Lambda_{\gamma,\sigma\sigma'}^{\alpha;\mu\nu}(\epsilon, \epsilon + \omega) = 0. \quad (\text{A6})$$

2. Linear dependence of $\Gamma_{\sigma_1\sigma_2;\sigma_3\sigma_4}^{\nu_1\nu_2;\nu_3\nu_4}$

We next consider the four-point correlation function, defined by

$$\begin{aligned} & \mathcal{G}_{\sigma_4,\sigma_2;\sigma_3,\sigma_1}^{\mu_4\mu_2;\mu_3\mu_1}(t_4, t_2; t_3, t_1) \\ & \equiv i \langle T_C d_{\sigma_4}(t_4^{\mu_4}) d_{\sigma_2}(t_2^{\mu_2}) d_{\sigma_3}^\dagger(t_3^{\mu_3}) d_{\sigma_1}^\dagger(t_1^{\mu_1}) \rangle. \end{aligned} \quad (\text{A7})$$

It can be expressed in terms of the four-point vertex corrections, as

$$\begin{aligned} & \mathcal{G}_{\sigma_4,\sigma_2,\sigma_3,\sigma_1}^{\mu_4\mu_2;\mu_3\mu_1}(t_4, t_2; t_3, t_1) \\ & = -i G_{\sigma_1}^{\mu_4\mu_1}(t_4, t_1) G_{\sigma_2}^{\mu_2\mu_3}(t_2, t_3) \delta_{\sigma_4\sigma_1} \delta_{\sigma_2\sigma_3} \\ & \quad + i G_{\sigma_4}^{\mu_4\mu_3}(t_4, t_3) G_{\sigma_1}^{\mu_2\mu_1}(t_2, t_1) \delta_{\sigma_2\sigma_1} \delta_{\sigma_4\sigma_3} \\ & \quad + \int \prod_{k=1}^4 dt'_k \sum_{\substack{\nu_1\nu_2 \\ \nu_3\nu_4}} \Gamma_{\sigma_1\sigma_2;\sigma_3\sigma_4}^{\nu_1\nu_2;\nu_3\nu_4}(t'_1, t'_2; t'_3, t'_4) \\ & \quad \times G_{\sigma_4}^{\nu_1\mu_1}(t'_1, t_1) G_{\sigma_2}^{\mu_2\nu_2}(t_2, t'_2) G_{\sigma_3}^{\nu_3\mu_3}(t'_3, t_3) G_{\sigma_1}^{\mu_4\nu_4}(t_4, t'_4). \end{aligned} \quad (\text{A8})$$

By definition, sixteen Keldysh components of $\mathcal{G}_{\sigma_4,\sigma_2;\sigma_3,\sigma_1}^{\mu_4\mu_2;\mu_3\mu_1}$ are linear dependent, and the relation among them is given by

$$\begin{aligned} & \sum_{\substack{\mu_4\mu_2 \\ \mu_3\mu_1}} \text{sgn}(\mu_4\mu_2\mu_3\mu_1) \mathcal{G}_{\sigma_4,\sigma_2;\sigma_3,\sigma_1}^{\mu_4\mu_2;\mu_3\mu_1} \\ & \equiv \mathcal{G}_{\sigma_4,\sigma_2;\sigma_3,\sigma_1}^{--;--} + \mathcal{G}_{\sigma_4,\sigma_2;\sigma_3,\sigma_1}^{++;++} + \mathcal{G}_{\sigma_4,\sigma_2;\sigma_3,\sigma_1}^{-+;-} + \mathcal{G}_{\sigma_4,\sigma_2;\sigma_3,\sigma_1}^{+-;-} \\ & \quad + \mathcal{G}_{\sigma_4,\sigma_2;\sigma_3,\sigma_1}^{+-;+-} + \mathcal{G}_{\sigma_4,\sigma_2;\sigma_3,\sigma_1}^{-+;-+} + \mathcal{G}_{\sigma_4,\sigma_2;\sigma_3,\sigma_1}^{++;-} + \mathcal{G}_{\sigma_4,\sigma_2;\sigma_3,\sigma_1}^{--;+-} \\ & \quad - \mathcal{G}_{\sigma_4,\sigma_2;\sigma_3,\sigma_1}^{+-;-} - \mathcal{G}_{\sigma_4,\sigma_2;\sigma_3,\sigma_1}^{-+;-} - \mathcal{G}_{\sigma_4,\sigma_2;\sigma_3,\sigma_1}^{--;-} - \mathcal{G}_{\sigma_4,\sigma_2;\sigma_3,\sigma_1}^{+-;-} \\ & \quad - \mathcal{G}_{\sigma_4,\sigma_2;\sigma_3,\sigma_1}^{-+;+-} - \mathcal{G}_{\sigma_4,\sigma_2;\sigma_3,\sigma_1}^{++;-} - \mathcal{G}_{\sigma_4,\sigma_2;\sigma_3,\sigma_1}^{--;+-} - \mathcal{G}_{\sigma_4,\sigma_2;\sigma_3,\sigma_1}^{+-;-} \\ & = 0. \end{aligned} \quad (\text{A9})$$

This relation can be rewritten in terms of $\Gamma_{\sigma_1\sigma_2;\sigma_3\sigma_4}^{\nu_1\nu_2;\nu_3\nu_4}$, G_{σ}^r , G_{σ}^a , and G_{σ}^K , by substituting Eq. (A8) into the left-hand side of Eq. (A9), and using Eq. (5.3), as

$$\begin{aligned} & \sum_{\substack{\mu_4\mu_2 \\ \mu_3\mu_1}} \text{sgn}(\mu_4\mu_2\mu_3\mu_1) \mathcal{G}_{\sigma_4,\sigma_2;\sigma_3,\sigma_1}^{\mu_4\mu_2;\mu_3\mu_1}(t_4, t_2; t_3, t_1) \\ & = \int \prod_{k=1}^4 dt'_k \sum_{\substack{\nu_1\nu_2 \\ \nu_3\nu_4}} \Gamma_{\sigma_1\sigma_2;\sigma_3\sigma_4}^{\nu_1\nu_2;\nu_3\nu_4}(t'_1, t'_2; t'_3, t'_4) \\ & \quad \times G_{\sigma_1}^r(t'_1, t_1) G_{\sigma_2}^a(t_2, t'_2) G_{\sigma_3}^r(t'_3, t_3) G_{\sigma_4}^a(t_4, t'_4) = 0. \end{aligned} \quad (\text{A10})$$

Note that the contributions of the disconnected parts, which correspond to the first two terms in the right-hand side of Eq. (A8), vanish in this summation,

$$\sum_{\substack{\mu_1\mu_2 \\ \mu_3\mu_4}} \text{sgn}(\mu_4\mu_2\mu_3\mu_1) G_{\sigma_1}^{\mu_4\mu_1} G_{\sigma_2}^{\mu_2\mu_3} = 0. \quad (\text{A11})$$

This can be verified, using Eq. (A1), or directly from Eq. (5.3).

The relation obtained in Eq. (A10) holds for arbitrary t_1 , t_2 , t_3 , and t_4 , and thus

$$\sum_{\substack{\nu_1\nu_2 \\ \nu_3\nu_4}} \Gamma_{\sigma_1\sigma_2;\sigma_3\sigma_4}^{\nu_1\nu_2;\nu_3\nu_4}(t'_1, t'_2; t'_3, t'_4) = 0. \quad (\text{A12})$$

The linear dependence among the Fourier transformed functions $\Gamma_{\sigma_1\sigma_2;\sigma_3\sigma_4}^{\nu_1\nu_2;\nu_3\nu_4}(\omega_1, \omega_2; \omega_3, \omega_4)$ can also be expressed in the same form as Eq. (A12), in the frequency domain:

$$\begin{aligned} & \int \prod_{k=1}^4 dt_k e^{i(\omega_4 t_4 + \omega_2 t_2 - \omega_3 t_3 - \omega_1 t_1)} \Gamma_{\sigma_1\sigma_2;\sigma_3\sigma_4}^{\nu_1\nu_2;\nu_3\nu_4}(t_1, t_2; t_3, t_4) \\ & = 2\pi \delta(\omega_1 + \omega_3 - \omega_2 - \omega_4) \Gamma_{\sigma_1\sigma_2;\sigma_3\sigma_4}^{\nu_1\nu_2;\nu_3\nu_4}(\omega_1, \omega_2; \omega_3, \omega_4). \end{aligned} \quad (\text{A13})$$

Appendix B: Derivation of Ward-Takahashi identity for finite eV and T

In this Appendix, we provide a derivation of the Ward-Takahashi identity for the Keldysh three-point functions defined in Sec. VI:

$$\begin{aligned} & i \frac{\partial}{\partial t} \Phi_{d,\sigma\sigma'}^\alpha(t; t_1, t_2) + i \Phi_{R,\sigma\sigma'}^\alpha(t; t_1, t_2) - i \Phi_{L,\sigma\sigma'}^\alpha(t; t_1, t_2) \\ & = -\delta_{\sigma\sigma'} \delta(t - t_1) \rho_3^\alpha \tau_3 \mathbf{G}_\sigma(t, t_2) \\ & \quad + \delta_{\sigma\sigma'} \delta(t_2 - t) \mathbf{G}_\sigma(t_1, t) \tau_3 \rho_3^\alpha. \end{aligned} \quad (\text{B1})$$

This identity, which is also given Eq. (6.16), reflects the conservation of the current flowing between the dot and leads,

$$\frac{\partial}{\partial t} \delta n_{d,\sigma}(t) + \delta J_{R,\sigma} - \delta J_{L,\sigma} = 0. \quad (\text{B2})$$

It can be deduced from the equation of motion for $\Phi_{d,\sigma\sigma'}^\alpha$ along the forward $\alpha = -$ and backward $\alpha = +$ branches of the Keldysh time-loop contour. In the following two subsections, Eq. (B1) is derived separately for these two subsections, Eq. (B1) is derived separately for these two branches as Eqs. (B3) and (B11). Note that ρ_3^α , defined in Eq. (6.6), is the projection operator into the subspace of the α branch, and it has the properties $\rho_3^\alpha \tau_3 = \tau_3 \rho_3^\alpha = \eta_\alpha \rho_3^\alpha$ with $\eta_- = +1$ and $\eta_+ = -1$.

1. Forward-branch time evolution of $\Phi_{d,\sigma\sigma'}^-(t; t_1, t_2)$

We consider first the forward branch $\alpha = -$, and show that the equation of motion of $\{\Phi_{d,\sigma\sigma'}^-\}^{\mu\nu} = \Phi_{d,\sigma\sigma'}^{-;\mu\nu}$ can be expressed in the following form,

$$\begin{aligned} & \frac{\partial}{\partial t} \Phi_{d,\sigma\sigma'}^-(t; t_1, t_2) + \Phi_{R,\sigma\sigma'}^-(t; t_1, t_2) - \Phi_{L,\sigma\sigma'}^-(t; t_1, t_2) \\ & = \delta_{\sigma\sigma'} \left[\delta(t - t_1) \rho_3^- i \mathbf{G}_\sigma(t, t_2) - \delta(t_2 - t) i \mathbf{G}_\sigma(t_1, t) \rho_3^- \right]. \end{aligned} \quad (\text{B3})$$

One of the four matrix elements of $\Phi_{d,\sigma\sigma'}^-$, is the causal function, i.e., $\Phi_{d,\sigma\sigma'}^{-;\mu\nu}$ for $\mu = \nu = -$. The time derivative

of this function can be calculated, following the standard approach for the causal three-point functions, described, for instance, in Ref. 61,

$$\begin{aligned}
& \frac{\partial}{\partial t} \Phi_{d,\sigma\sigma'}^{-;-}(t; t_1, t_2) + \Phi_{R,\sigma\sigma'}^{-;-}(t; t_1, t_2) - \Phi_{L,\sigma\sigma'}^{-;-}(t; t_1, t_2) \\
&= -\delta(t-t_1) \langle T[\delta n_{d,\sigma'}(t_1), d_\sigma(t_1)] d_\sigma^\dagger(t_2) \rangle \\
&\quad - \delta(t_2-t) \langle T d_\sigma(t_1) [\delta n_{d,\sigma'}(t_2), d_\sigma^\dagger(t_2)] \rangle \\
&= \delta_{\sigma\sigma'} \left[\delta(t-t_1) iG_\sigma^{-}(t, t_2) - \delta(t_2-t) iG_\sigma^{-}(t_1, t) \right].
\end{aligned} \tag{B4}$$

Here, we have used the current conservation law Eq. (B2) and the equal-time commutation relations $[n_{d\sigma'}, d_\sigma] = -\delta_{\sigma\sigma'} d_\sigma$, and $[n_{d\sigma'}, d_\sigma^\dagger] = \delta_{\sigma\sigma'} d_\sigma^\dagger$. Note that the Dirac delta functions arise from the derivatives of the Heaviside step functions, $\theta(t)$'s, that specify the time-ordering of t_1 , t_2 , and t .

We next consider the component with $\mu = \nu = +$, for which the time ordering is much simpler,

$$\begin{aligned}
-\Phi_{d,\sigma\sigma'}^{-;++}(t; t_1, t_2) &= -\theta(t_1-t_2) \langle d_\sigma^\dagger(t_2) d_\sigma(t_1) \delta n_{d,\sigma'}(t) \rangle \\
&\quad + \theta(t_2-t_1) \langle d_\sigma(t_1) d_\sigma^\dagger(t_2) \delta n_{d,\sigma'}(t) \rangle.
\end{aligned} \tag{B5}$$

Since the t -dependence enters only through the charge fluctuation operator $\delta n_{d,\sigma'}(t)$ in the right-hand side, the equation of motion of this component is determined simply by $\partial \delta n_{d,\sigma'}(t) / \partial t$ that satisfies Eq. (B2). Therefore,

$$\begin{aligned}
& \frac{\partial}{\partial t} \Phi_{d,\sigma\sigma'}^{-;++}(t; t_1, t_2) + \Phi_{R,\sigma\sigma'}^{-;++}(t; t_1, t_2) - \Phi_{L,\sigma\sigma'}^{-;++}(t; t_1, t_2) \\
&= 0.
\end{aligned} \tag{B6}$$

The other component with $\mu = +$ and $\nu = -$ can also be expressed, using the step function for time-ordering, as

$$\begin{aligned}
-\Phi_{d,\sigma\sigma'}^{-;+-}(t; t_1, t_2) &= \theta(t-t_2) \langle d_\sigma(t_1) \delta n_{d,\sigma'}(t) d_\sigma^\dagger(t_2) \rangle \\
&\quad + \theta(t_2-t) \langle d_\sigma(t_1) d_\sigma^\dagger(t_2) \delta n_{d,\sigma'}(t) \rangle.
\end{aligned} \tag{B7}$$

Thus, the time-derivative of this function is given by

$$\begin{aligned}
& \frac{\partial}{\partial t} \Phi_{d,\sigma\sigma'}^{-;+-}(t; t_1, t_2) + \Phi_{R,\sigma\sigma'}^{-;+-}(t; t_1, t_2) - \Phi_{L,\sigma\sigma'}^{-;+-}(t; t_1, t_2) \\
&= -\delta(t-t_2) \langle d_\sigma(t_1) [\delta n_{d,\sigma'}(t_2), d_\sigma^\dagger(t_2)] \rangle \\
&= -\delta_{\sigma\sigma'} \delta(t-t_2) iG_\sigma^{+-}(t_1, t).
\end{aligned} \tag{B8}$$

Similarly, the time-ordering of the last one of four forward-branch components, i.e., the one with $\mu = -$ and $\nu = +$, can be expressed in the form,

$$\begin{aligned}
-\Phi_{d,\sigma\sigma'}^{-;+-(t; t_1, t_2) &= -\theta(t-t_1) \langle d_\sigma^\dagger(t_2) \delta n_{d,\sigma'}(t) d_\sigma(t_1) \rangle \\
&\quad - \theta(t_1-t) \langle d_\sigma^\dagger(t_2) d_\sigma(t_1) \delta n_{d,\sigma'}(t) \rangle.
\end{aligned} \tag{B9}$$

Taking the derivative with respect to t , we obtain

$$\begin{aligned}
& \frac{\partial}{\partial t} \Phi_{d,\sigma\sigma'}^{-;-+}(t; t_1, t_2) + \Phi_{R,\sigma\sigma'}^{-;-+}(t; t_1, t_2) - \Phi_{L,\sigma\sigma'}^{-;-+}(t; t_1, t_2) \\
&= \delta(t-t_1) \langle d_\sigma^\dagger(t_2) [\delta n_{d,\sigma'}(t), d_\sigma(t_1)] \rangle \\
&= \delta_{\sigma\sigma'} \delta(t-t_1) iG_\sigma^{-+}(t, t_2).
\end{aligned} \tag{B10}$$

The four equations (B4), (B6), (B8), and (B10) can be expressed as one matrix equation, as described in Eq. (B3).

2. Backward-branch time evolution of $\Phi_{d,\sigma\sigma'}^+(t; t_1, t_2)$

Time evolution of the three-point function $\Phi_{d,\sigma\sigma'}^{\alpha;\mu\nu}$ along the backward branch $\alpha = +$ can also be deduced from the equation of continuity Eq. (B2), in a similar way that is described in the above to obtain Eq. (B3). The results can be written in the form,

$$\begin{aligned}
& \frac{\partial}{\partial t} \Phi_{d,\sigma\sigma'}^+(t; t_1, t_2) + \Phi_{R,\sigma\sigma'}^+(t; t_1, t_2) - \Phi_{L,\sigma\sigma'}^+(t; t_1, t_2) \\
&= \delta_{\sigma\sigma'} \left[-\delta(t-t_1) \rho_3^+ i\mathbf{G}_\sigma(t, t_2) + \delta(t_2-t) i\mathbf{G}_\sigma(t_1, t) \rho_3^+ \right].
\end{aligned} \tag{B11}$$

Here we provide the derivation of each element of this matrix equation in the following.

The three-point function for $\mu = \nu = +$ corresponds to the counterpart of the causal function described in Eq. (B4). Therefore, the time derivative of this function can also be calculated, following the same standard approach,⁶¹ as

$$\begin{aligned}
& \frac{\partial}{\partial t} \Phi_{d,\sigma\sigma'}^{+;++}(t; t_1, t_2) + \Phi_{R,\sigma\sigma'}^{+;++}(t; t_1, t_2) - \Phi_{L,\sigma\sigma'}^{+;++}(t; t_1, t_2) \\
&= \delta(t-t_1) \langle \tilde{T}[\delta n_{d,\sigma'}(t_1), d_\sigma(t_1)] d_\sigma^\dagger(t_2) \rangle \\
&\quad + \delta(t_2-t) \langle \tilde{T} d_\sigma(t_1) [\delta n_{d,\sigma'}(t_2), d_\sigma^\dagger(t_2)] \rangle \\
&= \delta_{\sigma\sigma'} \left[-\delta(t-t_1) iG_\sigma^{++}(t, t_2) + \delta(t_2-t) iG_\sigma^{++}(t_1, t) \right].
\end{aligned} \tag{B12}$$

For the component of $\mu = \nu = -$, the time-ordering can explicitly be written in the form,

$$\begin{aligned}
-\Phi_{d,\sigma\sigma'}^{+;-}(t; t_1, t_2) &= \theta(t_1-t_2) \langle \delta n_{d,\sigma'}(t) d_\sigma(t_1) d_\sigma^\dagger(t_2) \rangle \\
&\quad - \theta(t_2-t_1) \langle \delta n_{d,\sigma'}(t) d_\sigma^\dagger(t_2) d_\sigma(t_1) \rangle.
\end{aligned} \tag{B13}$$

Since the step functions do not depend on t in this case, the equation of motion does not have a source term,

$$\begin{aligned}
& \frac{\partial}{\partial t} \Phi_{d,\sigma\sigma'}^{+;-}(t; t_1, t_2) + \Phi_{R,\sigma\sigma'}^{+;-}(t; t_1, t_2) - \Phi_{L,\sigma\sigma'}^{+;-}(t; t_1, t_2) \\
&= 0.
\end{aligned} \tag{B14}$$

In contrast, the time-ordering of the component with $\mu = -$ and $\nu = +$ depends on t ,

$$-\Phi_{d,\sigma\sigma'}^{+;-+}(t; t_1, t_2) = -\theta(t - t_2) \langle d_\sigma^\dagger(t_2) \delta n_{d,\sigma'}(t) d_\sigma(t_1) \rangle \\ - \theta(t_2 - t) \langle \delta n_{d,\sigma'}(t) d_\sigma^\dagger(t_2) d_\sigma(t_1) \rangle. \quad (\text{B15})$$

Thus, the equation of motion has a source term in the right-hand side, as

$$\frac{\partial}{\partial t} \Phi_{d,\sigma\sigma'}^{+;-+}(t; t_1, t_2) + \Phi_{R,\sigma\sigma'}^{+;-+}(t; t_1, t_2) - \Phi_{L,\sigma\sigma'}^{+;-+}(t; t_1, t_2) \\ = \delta(t - t_2) \langle [d_\sigma^\dagger(t), \delta n_{d,\sigma'}(t)] d_\sigma(t_1) \rangle \\ = \delta_{\sigma\sigma'} \delta(t - t_2) iG_\sigma^{+-}(t_1, t). \quad (\text{B16})$$

Similarly, the component with $\mu = +$ and $\nu = -$ can be written in the following form,

$$-\Phi_{d,\sigma\sigma'}^{+;-+}(t; t_1, t_2) = \theta(t - t_1) \langle d_\sigma(t_1) \delta n_{d,\sigma'}(t) d_\sigma^\dagger(t_2) \rangle \\ + \theta(t_1 - t) \langle \delta n_{d,\sigma'}(t) d_\sigma(t_1) d_\sigma^\dagger(t_2) \rangle. \quad (\text{B17})$$

The equation of motion of this component is given by

$$\frac{\partial}{\partial t} \Phi_{d,\sigma\sigma'}^{+;-+}(t; t_1, t_2) + \Phi_{R,\sigma\sigma'}^{+;-+}(t; t_1, t_2) - \Phi_{L,\sigma\sigma'}^{+;-+}(t; t_1, t_2) \\ = -\delta(t - t_1) \langle [d_\sigma(t), \delta n_{d,\sigma'}(t)] d_\sigma^\dagger(t_2) \rangle \\ = -\delta_{\sigma\sigma'} \delta(t - t_1) iG_\sigma^{+-}(t, t_2). \quad (\text{B18})$$

Therefore, the equation of motions for the four backward-branch components, Eqs. (B12), (B14), (B16), and (B18), can also be expressed as the matrix equation that is shown in Eq. (B11).

Appendix C: Low-energy expansion of the Keldysh vertex functions

In this appendix, we calculate the low-energy expansion of the Keldysh vertex functions $\Gamma_{\sigma\sigma';\sigma'\sigma}^{\mu\mu';\nu'\nu}(\epsilon, \epsilon'; \epsilon', \epsilon)$ up to linear-order terms with respect to ϵ , ϵ' , eV , and T , using the Feynman diagrammatic technique. Calculations are carried out for all Keldysh-branch components $(\mu, \mu'; \nu', \nu)$ and internal degrees of freedoms σ, σ' . The results are summarized in TABLES VII and VIII. It has already been shown in Sec. VIII that these results of $\Gamma_{\sigma\sigma';\sigma'\sigma}^{\mu\mu';\nu'\nu}(\epsilon, \epsilon'; \epsilon', \epsilon)$ satisfy the current conservation law consistently with the the low-energy behavior of the Keldysh self-energies $\Sigma_{\sigma\sigma'}^{\nu\mu}(\epsilon)$ in the Fermi-liquid regime, which are also summarized in TABLE V. These results also explicitly show that all the vertex components other than the causal component $\Gamma_{\sigma\sigma';\sigma'\sigma}^{-;-}(\epsilon, \epsilon'; \epsilon', \epsilon)$ and its counterpart $\Gamma_{\sigma\sigma';\sigma'\sigma}^{+;+}(\epsilon, \epsilon'; \epsilon', \epsilon)$ are pure imaginary in the Fermi-liquid regime. Furthermore, the real part of the causal component and the counterpart can be deduced up to order eV from the nonequilibrium Ward

identity in Sec. VIII B, as shown in Sec. VIII B and TABLE VIII.

We start with a few remarks on the general properties of the Keldysh vertex function. First of all, the sixteen branch components are linearly dependent, as shown in Eq. (5.30) and explained more precisely in Appendix A.⁶² The vertex functions also have the symmetrical property $\Gamma_{\sigma\sigma';\sigma'\sigma}^{\mu\mu';\nu'\nu}(\epsilon, \epsilon'; \epsilon', \epsilon) = \Gamma_{\sigma'\sigma;\sigma\sigma'}^{\nu'\nu;\mu\mu'}(\epsilon', \epsilon; \epsilon, \epsilon')$ under the interchange of the variables for incoming and outgoing particles. Furthermore, the causal vertex function and its counterpart for $\sigma = \sigma'$ identically vanish at zero frequencies $\epsilon = \epsilon' = 0$, as a result of the Pauli exclusion principle,

$$\Gamma_{\sigma,\sigma;\sigma,\sigma}^{-;-}(0, 0; 0, 0) = 0, \quad \Gamma_{\sigma,\sigma;\sigma,\sigma}^{+;+}(0, 0; 0, 0) = 0. \quad (\text{C1})$$

In contrast, for different levels $\sigma \neq \sigma'$, the zero-frequency value of the causal vertex function is finite and is determined by the off-diagonal susceptibility $\chi_{\sigma\sigma'}$, specifically at $eV = T = 0$,

$$\Gamma_{\sigma\sigma';\sigma'\sigma}^{-;-}(0, 0; 0, 0) \rho_{d\sigma} \rho_{d\sigma'} = -\Gamma_{\sigma\sigma';\sigma'\sigma}^{+;+}(0, 0; 0, 0) \rho_{d\sigma} \rho_{d\sigma'} \\ = -\chi_{\sigma\sigma'}. \quad (\text{C2})$$

In the following, we calculate the imaginary part of Keldysh vertex functions $\Gamma_{\sigma\sigma';\sigma'\sigma}^{\mu\mu';\nu'\nu}(\epsilon, \epsilon'; \epsilon', \epsilon)$ up to terms of order ϵ , ϵ' , eV , and T . To this end, we demonstrate how the imaginary part arises first in the second order perturbation theory in U , and then take into account the contributions of multiple scattering to all orders in U .

1. Perturbation expansion of the Keldysh vertex function

Here we briefly summarize the Feynman rules for the Keldysh vertex corrections. In the perturbation theory with respect to the Coulomb interactions, the sign of an order U^n Feynman diagram of a vertex component is given by

$$(-i)^n (i)^{2n} (-1)^m (-1)^{F'} \{i\} U^n = (-1)^m (-1)^{F'} i^{n+1} U^n. \quad (\text{C3})$$

Here, $(-i)^n$ and $(i)^{2n}$ in the left-hand side are associated with U^n which emerges through the time-evolution operator and the $2n$ internal Green's functions, respectively.⁵⁶ Another sign factor $(-1)^m$ appears in the Keldysh formalism, where m is the number of U 's arising from the time-evolution along the backward branch ($m \leq n$) [see, for instance, Figs. 9 and 10]. The factor $(-1)^{F'}$ is determined by the number of fermion loops F' , which include an additional closed loop that may be created when the two external Green's functions with σ' on the right side of the vertex diagrams are connected with each other to construct a three-point correlation function, as shown in Fig. 6. The remaining factor $\{i\}$ in the left-side of Eq. (C3) corresponds to the coefficient that is assigned in the definitions of $\Phi_{\gamma,\sigma\sigma'}^\alpha$ and $\Gamma_{\sigma\sigma';\sigma'\sigma}^{\mu\mu';\nu'\nu}$, described in Eq. (6.23).

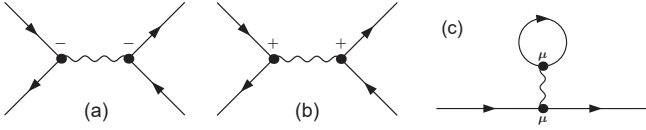


FIG. 9. Feynman diagrams for order U contributions, with $\mu = +, -$ the Keldysh index.

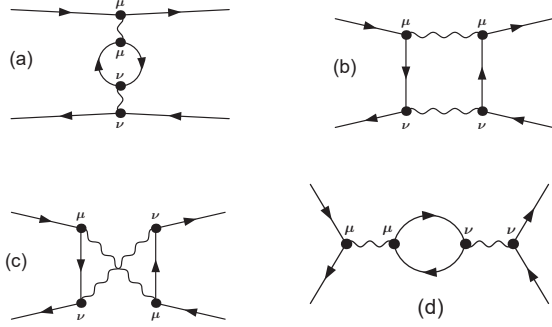


FIG. 10. Order U^2 vertex function $\Gamma_{\sigma\sigma';\sigma'\sigma}^{\mu_1\mu_2;\mu_3;\mu_4}$. The diagram (a) is for $\sigma = \sigma'$, and (b) and (c) are for $\sigma \neq \sigma'$, where σ and σ' are the level indexes for the propagators on the left and right, respectively. The diagram (d) also contributes to $\sigma \neq \sigma'$ components for multi-level case $N > 2$ as well as $\sigma = \sigma'$ components.

Figures 9 (a) and (b) describe the Feynman diagrams for the first-order vertex corrections with different levels $\sigma \neq \sigma'$. The sign for each of these two diagrams is determined, substituting $n = 1$, $F^l = 1$, and (a) $m = 0$ and (b) $m = 1$, into the right-hand side of Eq. (C3),

$$\Gamma_{\sigma\sigma';\sigma'\sigma}^{(1)---} = (-1)^0 (-1)^1 i^{1+1} U = U, \quad (\text{C4a})$$

$$\Gamma_{\sigma\sigma';\sigma'\sigma}^{(1)+++} = (-1)^1 (-1)^1 i^{1+1} U = -U. \quad (\text{C4b})$$

Similarly, the order U self-energy, described diagrammatically in Fig. 9 (c), is given by

$$\begin{aligned} \Sigma_{\sigma}^{(1)---} &= U \int \frac{d\epsilon'}{2\pi i} e^{i\epsilon'0^+} \sum_{\sigma'(\neq\sigma)} G_{\sigma'}^{--}(\epsilon') \\ &= \int \frac{d\epsilon'}{2\pi i} e^{i\epsilon'0^+} \sum_{\sigma'(\neq\sigma)} \Gamma_{\sigma\sigma';\sigma'\sigma}^{(1)---} G_{\sigma'}^{--}(\epsilon'), \end{aligned} \quad (\text{C5a})$$

$$\begin{aligned} \Sigma_{\sigma}^{(1)+++} &= -U \int \frac{d\epsilon'}{2\pi i} e^{-i\epsilon'0^+} \sum_{\sigma'(\neq\sigma)} G_{\sigma'}^{++}(\epsilon') \\ &= \int \frac{d\epsilon'}{2\pi i} e^{-i\epsilon'0^+} \sum_{\sigma'(\neq\sigma)} \Gamma_{\sigma\sigma';\sigma'\sigma}^{(1)+++} G_{\sigma'}^{++}(\epsilon'). \end{aligned} \quad (\text{C5b})$$

Note that these self-energies can also be regarded as the lowest-order terms of the skeleton-diagram expansion, in which the exact Green's functions G instead of the non-interacting ones G_0 are assigned to the internal lines of the Feynman diagrams.

2. $\Gamma_{\sigma\sigma';\sigma'\sigma}^{\nu_1\nu_2;\nu_3\nu_4}(\epsilon, \epsilon'; \epsilon', \epsilon)$ for $\sigma = \sigma'$ up to linear-order terms in ϵ, ϵ', eV , and T

We next consider low-energy asymptotic form of the vertex corrections for electrons with $\sigma = \sigma'$. The imaginary part arises first from the order U^2 scattering processes for $\Gamma_{\sigma\sigma';\sigma'\sigma}^{\mu\mu';\nu\nu'}(\epsilon, \epsilon'; \epsilon', \epsilon)$, shown in Figs. 10 (a) and (d). For each of these two diagrams, there are six different branch configurations, $\Gamma_{\sigma\sigma';\sigma'\sigma}^{---;---}$, $\Gamma_{\sigma\sigma';\sigma'\sigma}^{+++;+++}$, $\Gamma_{\sigma\sigma';\sigma'\sigma}^{---;+++}$, $\Gamma_{\sigma\sigma';\sigma'\sigma}^{+++;---}$, $\Gamma_{\sigma\sigma';\sigma'\sigma}^{+-;+-}$, $\Gamma_{\sigma\sigma';\sigma'\sigma}^{+--;+--}$. In the following, we demonstrate how the imaginary part emerges in the second-order skeleton diagrams. Then, taking into account multiple scatterings to all orders in U , we calculate the low-energy asymptotic form of the vertex full functions up to terms of order ϵ, ϵ', eV , and T .

a. Low-energy expansion of $\Gamma_{\sigma\sigma';\sigma'\sigma}^{---;---}$ & $\Gamma_{\sigma\sigma';\sigma'\sigma}^{+++;+++}$

In the second-order perturbation theory in U , the causal component ($---;---$) of the vertex function with $\sigma = \sigma'$ is described by the Feynman diagrams shown in Figs. 10 (a) and (d) which have $F'_a = 1$ and $F'_d = 2$ closed loops, respectively. Since $m = 0$ and $n = 2$ for these processes the corresponding vertex functions are given by

$$\begin{aligned} \Gamma_{\sigma\sigma';\sigma'\sigma}^{(2a)---;---}(\epsilon, \epsilon'; \epsilon', \epsilon) &= (-1)^0 i^{2+1} (-1)^{F'_a} \\ &\times \sum_{\sigma''(\neq\sigma)} U^2 \int \frac{d\epsilon_1}{2\pi} G_{\sigma''}^{--}(\epsilon_1 + \epsilon - \epsilon') G_{\sigma''}^{--}(\epsilon_1), \end{aligned} \quad (\text{C6a})$$

$$\begin{aligned} \Gamma_{\sigma\sigma';\sigma'\sigma}^{(2d)---;---}(\epsilon, \epsilon'; \epsilon', \epsilon) &= (-1)^0 i^{2+1} (-1)^{F'_d} \\ &\times \sum_{\sigma''(\neq\sigma)} U^2 \int \frac{d\epsilon_1}{2\pi} G_{\sigma''}^{--}(\epsilon_1) G_{\sigma''}^{--}(\epsilon_1). \end{aligned} \quad (\text{C6b})$$

The sum $\Gamma_{\sigma\sigma';\sigma'\sigma}^{(2)---;---} \equiv \Gamma_{\sigma\sigma';\sigma'\sigma}^{(2a)---;---} + \Gamma_{\sigma\sigma';\sigma'\sigma}^{(2d)---;---}$ can be written in terms of the particle-hole propagator $X_{\sigma\sigma'}^{--}$, defined in Eq. (7.16),

$$\begin{aligned} \Gamma_{\sigma\sigma';\sigma'\sigma}^{(2)---;---}(\epsilon, \epsilon'; \epsilon', \epsilon) &= \sum_{\sigma''(\neq\sigma)} U^2 \left[X_{\sigma''\sigma''}^{--}(\epsilon - \epsilon') - X_{\sigma''\sigma''}^{--}(0) \right]. \end{aligned} \quad (\text{C7})$$

The corresponding ($+++;+++$) component of Figs. 10 (a) and (d), can be obtained, replacing $G_{\sigma''}^{--}$ in Eq. (C6) by $G_{\sigma''}^{++}$ and taking $m = 2$, as

$$\begin{aligned} \Gamma_{\sigma\sigma';\sigma'\sigma}^{(2)+++;+++}(\epsilon, \epsilon'; \epsilon', \epsilon) &= \sum_{\sigma''(\neq\sigma)} U^2 \left[X_{\sigma''\sigma''}^{++}(\epsilon - \epsilon') - X_{\sigma''\sigma''}^{++}(0) \right]. \end{aligned} \quad (\text{C8})$$

Therefore, the low-energy behavior of these two components are determined by the particle-hole pair propagator $X_{\sigma''\sigma''}^{\mu\nu}$. Furthermore, these results explicitly show that $\Gamma_{\sigma\sigma';\sigma'\sigma}^{(2)+++;+++} = - \left\{ \Gamma_{\sigma\sigma';\sigma'\sigma}^{(2)---;---} \right\}^*$.

To obtain the full vertex function $\Gamma_{\sigma\sigma;\sigma\sigma}^{--;--}(\epsilon, \epsilon'; \epsilon', \epsilon)$, all contributions of multiple quasiparticle collision processes are needed to be taken into account. For the imaginary part, it can be carried out by replacing bare U by the full vertex $\Gamma_{\sigma\sigma';\sigma''\sigma}^{--;--}(0, 0; 0, 0)$ for $\sigma \neq \sigma''$, defined at $eV = T = 0$.^{14,16,49,56} This is because the damping of a quasiparticle in the low-energy Fermi-liquid regime is determined by the scattering processes in which a single particle-hole or particle-particle pair is excited in the intermediate states, and the scattering matrix element is given by the zero-frequency value of the full vertex function that includes all possible higher-order corrections. Therefore, the imaginary part of $\Gamma_{\sigma\sigma;\sigma\sigma}^{--;--}(\epsilon, \epsilon'; \epsilon', \epsilon)$ is determined by the single particle-hole pair excitation shown in Figs. 8 (a) and (d) up to linear-order terms with respect to $\epsilon - \epsilon'$, eV , and T ,

$$\begin{aligned}
& \text{Im} \Gamma_{\sigma\sigma;\sigma\sigma}^{--;--}(\epsilon, \epsilon'; \epsilon', \epsilon) \\
&= \text{Im} \int \frac{d\varepsilon_1}{2\pi i} \sum_{\sigma''(\neq\sigma)} \Gamma_{\sigma\sigma';\sigma''\sigma}^{--;--}(0, 0; 0, 0) \Gamma_{\sigma''\sigma;\sigma\sigma''}^{--;--}(0, 0; 0, 0) \\
&\quad \times \left[-G_{\sigma''}^{--}(\varepsilon_1 + \epsilon - \epsilon') G_{\sigma''}^{--}(\varepsilon_1) + G_{\sigma''}^{--}(\varepsilon_1) G_{\sigma''}^{--}(\varepsilon_1) \right] \\
&\quad + \dots \\
&= \sum_{\sigma''(\neq\sigma)} \left| \Gamma_{\sigma\sigma';\sigma''\sigma}^{--;--}(0, 0; 0, 0) \right|^2 \\
&\quad \times \text{Im} \left[X_{\sigma''\sigma''}^{--}(\epsilon - \epsilon') - X_{\sigma''\sigma''}^{--}(0) \right] + \dots \\
&= \frac{\pi}{\{\rho_{d\sigma}\}^2} \sum_{\sigma''(\neq\sigma)} \chi_{\sigma\sigma''}^2 \left[\mathcal{W}_K^{\text{ph}}(\epsilon - \epsilon') - \mathcal{W}_K^{\text{ph}}(0) \right] + \dots.
\end{aligned} \tag{C9}$$

To obtain the last line we have used properties of the particle-hole propagator $X_{\sigma\sigma'}^{\mu\nu}$ and the collision integral $\mathcal{W}_K^{\text{ph}}(\omega) \equiv \mathcal{W}^{\text{ph}}(\omega) + \mathcal{W}^{\text{ph}}(-\omega)$, described in Sec. VII B and TABLE VI. Note that the susceptibility for $\sigma'' \neq \sigma$ is given by $\chi_{\sigma\sigma''} = -\Gamma_{\sigma\sigma';\sigma''\sigma}^{--;--}(0, 0; 0, 0) \rho_{d\sigma} \rho_{d\sigma''}$.

The real part of the causal vertex function for the same level $\sigma = \sigma'$ vanishes at low-energies up to linear order terms in ϵ and ϵ' due to the fermionic antisymmetrical properties:^{28,29} $\text{Re} \Gamma_{\sigma\sigma;\sigma\sigma}^{--;--}(\epsilon, \epsilon'; \epsilon', \epsilon) = 0 + O(\epsilon^2, \epsilon'^2)$. Therefore, the causal component for $\sigma = \sigma'$ is pure imaginary up to linear order terms with respect to $\epsilon - \epsilon'$, eV , and T ,

$$\begin{aligned}
& \{\rho_{d\sigma}\}^2 \Gamma_{\sigma\sigma;\sigma\sigma}^{--;--}(\epsilon, \epsilon'; \epsilon', \epsilon) \\
&= i\pi \sum_{\sigma''(\neq\sigma)} \chi_{\sigma\sigma''}^2 \left[\mathcal{W}_K^{\text{ph}}(\epsilon - \epsilon') - \mathcal{W}_K^{\text{ph}}(0) \right] + \dots. \tag{C10}
\end{aligned}$$

Correspondingly, the $(++;++)$ component is given by $\Gamma_{\sigma\sigma;\sigma\sigma}^{++;++}(\epsilon, \epsilon'; \epsilon', \epsilon) = -\{\Gamma_{\sigma\sigma;\sigma\sigma}^{--;--}(\epsilon, \epsilon'; \epsilon', \epsilon)\}^*$.

b. Low-energy expansion of $\Gamma_{\sigma\sigma;\sigma\sigma}^{--;++}$ & $\Gamma_{\sigma\sigma;\sigma\sigma}^{++;--}$

We next consider the $(--;++)$ component, for which order U^2 contributions arise from the diagram Fig. 10 (a). In this case, $\mu = -$, $\nu = +$, and thus $m = 1$, and it has one fermion loop $F'_2 = 1$,

$$\begin{aligned}
& \Gamma_{\sigma\sigma;\sigma\sigma}^{(2)--;++}(\epsilon, \epsilon'; \epsilon', \epsilon) \\
&= (-1)^1 i^{2+1} (-1)^{F'_2} \\
&\quad \times \sum_{\sigma''(\neq\sigma)} U^2 \int \frac{d\varepsilon_1}{2\pi} G_{\sigma''}^{+-}(\varepsilon_1 + \epsilon - \epsilon') G_{\sigma''}^{+-}(\varepsilon_1) \\
&= - \sum_{\sigma''(\neq\sigma)} U^2 X_{\sigma''\sigma''}^{+-}(\epsilon - \epsilon'). \tag{C11a}
\end{aligned}$$

Similarly, the diagram Fig. 10 (a) for $\mu = +$ and $\nu = -$ describes the $(++;--)$ component of the order U^2 vertex function, which takes the form,

$$\begin{aligned}
& \Gamma_{\sigma\sigma;\sigma\sigma}^{(2)++;--}(\epsilon, \epsilon'; \epsilon', \epsilon) \\
&= (-1)^1 i^{2+1} (-1)^{F'_2} \\
&\quad \times \sum_{\sigma''(\neq\sigma)} U^2 \int \frac{d\varepsilon_1}{2\pi} G_{\sigma''}^{+-}(\varepsilon_1 + \epsilon - \epsilon') G_{\sigma''}^{+-}(\varepsilon_1) \\
&= - \sum_{\sigma''(\neq\sigma)} U^2 X_{\sigma''\sigma''}^{+-}(\epsilon - \epsilon'). \tag{C11b}
\end{aligned}$$

Note that these two vertex components are pure imaginary. Therefore, the fully renormalized vertex functions corresponding to these ones are determined by a single particle-hole pair excitation described in the diagram Fig. 8 (a) up to linear order terms with respect to $\epsilon - \epsilon'$, eV and T ,

$$\begin{aligned}
& \Gamma_{\sigma\sigma;\sigma\sigma}^{--;++}(\epsilon, \epsilon'; \epsilon', \epsilon) \\
&= - \int \frac{d\varepsilon_1}{2\pi i} \sum_{\sigma''(\neq\sigma)} \Gamma_{\sigma\sigma';\sigma''\sigma}^{--;--}(0, 0; 0, 0) \Gamma_{\sigma''\sigma;\sigma\sigma''}^{++;++}(0, 0; 0, 0) \\
&\quad \times G_{\sigma''}^{+-}(\varepsilon_1 + \epsilon - \epsilon') G_{\sigma''}^{+-}(\varepsilon_1) + \dots \\
&= - \sum_{\sigma''(\neq\sigma)} \left| \Gamma_{\sigma\sigma';\sigma''\sigma}^{--;--}(0, 0; 0, 0) \right|^2 X_{\sigma''\sigma''}^{+-}(\epsilon - \epsilon') + \dots, \tag{C12a}
\end{aligned}$$

$$\begin{aligned}
& \Gamma_{\sigma\sigma;\sigma\sigma}^{++;--}(\epsilon, \epsilon'; \epsilon', \epsilon) \\
&= - \int \frac{d\varepsilon_1}{2\pi i} \sum_{\sigma''(\neq\sigma)} \Gamma_{\sigma\sigma';\sigma''\sigma}^{++;++}(0, 0; 0, 0) \Gamma_{\sigma''\sigma;\sigma\sigma''}^{--;--}(0, 0; 0, 0) \\
&\quad \times G_{\sigma''}^{+-}(\varepsilon_1 + \epsilon - \epsilon') G_{\sigma''}^{+-}(\varepsilon_1) + \dots \\
&= - \sum_{\sigma''(\neq\sigma)} \left| \Gamma_{\sigma\sigma';\sigma''\sigma}^{--;--}(0, 0; 0, 0) \right|^2 X_{\sigma''\sigma''}^{+-}(\epsilon - \epsilon') + \dots. \tag{C12b}
\end{aligned}$$

These two full vertex components can be rearranged into the symmetric and antisymmetric parts,

$$\begin{aligned} & \{\rho_{d\sigma}\}^2 \left[\Gamma_{\sigma\sigma;\sigma\sigma}^{--;+-}(\epsilon, \epsilon'; \epsilon', \epsilon) + \Gamma_{\sigma\sigma;\sigma\sigma}^{++;-}(\epsilon, \epsilon'; \epsilon', \epsilon) \right] \\ &= -i2\pi \sum_{\sigma''(\neq\sigma)} \chi_{\sigma\sigma''}^2 \mathcal{W}_K^{\text{ph}}(\epsilon - \epsilon') + \dots, \quad (\text{C13}) \end{aligned}$$

$$\begin{aligned} & \{\rho_{d\sigma}\}^2 \left[\Gamma_{\sigma\sigma;\sigma\sigma}^{--;+-}(\epsilon, \epsilon'; \epsilon', \epsilon) - \Gamma_{\sigma\sigma;\sigma\sigma}^{++;-}(\epsilon, \epsilon'; \epsilon', \epsilon) \right] \\ &= -i2\pi \sum_{\sigma''(\neq\sigma)} \chi_{\sigma\sigma''}^2 [\epsilon - \epsilon'] + \dots. \quad (\text{C14}) \end{aligned}$$

Note that $\mathcal{W}^{\text{ph}}(\omega) - \mathcal{W}^{\text{ph}}(-\omega) = \omega$ as mentioned in Sec. VII B. The explicit expression of $\mathcal{W}_K^{\text{ph}}(\omega)$ is shown in TABLE VI.

c. Low-energy expansion of $\Gamma_{\sigma\sigma;\sigma\sigma}^{-+;+-}$ & $\Gamma_{\sigma\sigma;\sigma\sigma}^{+-;-}$

For $\sigma = \sigma'$ components, there are two other types of order U^2 vertex corrections, $\Gamma_{\sigma\sigma;\sigma\sigma}^{-+;+-}$ and $\Gamma_{\sigma\sigma;\sigma\sigma}^{+-;-}$, which emerge from the scattering process illustrated in Fig. 10 (d). In this case, the number of loops is $F'_d = 2$, and these vertex components can be expressed in the following form,

$$\begin{aligned} & \Gamma_{\sigma\sigma;\sigma\sigma}^{(2)-+;+-}(\epsilon, \epsilon'; \epsilon', \epsilon) \\ &= (-1)^1 i^{2+1} (-1)^{F'_d} \sum_{\sigma''(\neq\sigma)} U^2 \int \frac{d\varepsilon_1}{2\pi} G_{\sigma''}^{+-}(\varepsilon_1) G_{\sigma''}^{+}(\varepsilon_1) \\ &= \sum_{\sigma''(\neq\sigma)} U^2 X_{\sigma''\sigma''}^{+-}(0), \quad (\text{C15a}) \end{aligned}$$

$$\begin{aligned} & \Gamma_{\sigma\sigma;\sigma\sigma}^{(2)+-;-}(\epsilon, \epsilon'; \epsilon', \epsilon) \\ &= (-1)^1 i^{2+1} (-1)^{F'_d} \sum_{\sigma''(\neq\sigma)} U^2 \int \frac{d\varepsilon_1}{2\pi} G_{\sigma''}^{+-}(\varepsilon_1) G_{\sigma''}^{+}(\varepsilon_1) \\ &= \sum_{\sigma''(\neq\sigma)} U^2 X_{\sigma''\sigma''}^{-+}(0). \quad (\text{C15b}) \end{aligned}$$

These components are pure imaginary, and the corresponding full vertex are determined by the multiple scattering processes described in Fig. 8 (d), up to linear order terms in eV , T , and frequencies ϵ and ϵ' ,

$$\begin{aligned} & \Gamma_{\sigma\sigma;\sigma\sigma}^{-+;+-}(\epsilon, \epsilon'; \epsilon', \epsilon) \\ &= \int \frac{d\varepsilon_1}{2\pi i} \sum_{\sigma''(\neq\sigma)} \Gamma_{\sigma\sigma'';\sigma''\sigma}^{--;--}(0, 0; 0, 0) \Gamma_{\sigma''\sigma;\sigma\sigma''}^{++;++}(0, 0; 0, 0) \\ & \quad \times G_{\sigma''}^{+-}(\varepsilon_1) G_{\sigma''}^{+}(\varepsilon_1) + \dots \\ &= \sum_{\sigma''(\neq\sigma)} \left| \Gamma_{\sigma\sigma'';\sigma''\sigma}^{--;--}(0, 0; 0, 0) \right|^2 X_{\sigma''\sigma''}^{+-}(0) + \dots, \quad (\text{C16a}) \end{aligned}$$

$$\begin{aligned} & \Gamma_{\sigma\sigma;\sigma\sigma}^{+-;-}(\epsilon, \epsilon'; \epsilon', \epsilon) \\ &= \int \frac{d\varepsilon_1}{2\pi i} \sum_{\sigma''(\neq\sigma)} \Gamma_{\sigma\sigma'';\sigma''\sigma}^{++;++}(0, 0; 0, 0) \Gamma_{\sigma''\sigma;\sigma\sigma''}^{--;--}(0, 0; 0, 0) \\ & \quad \times G_{\sigma''}^{+-}(\varepsilon_1) G_{\sigma''}^{+}(\varepsilon_1) + \dots \\ &= \sum_{\sigma''(\neq\sigma)} \left| \Gamma_{\sigma\sigma'';\sigma''\sigma}^{--;--}(0, 0; 0, 0) \right|^2 X_{\sigma''\sigma''}^{-+}(0) + \dots. \quad (\text{C16b}) \end{aligned}$$

Note that $X_{\sigma''\sigma''}^{+-}(0) = X_{\sigma''\sigma''}^{-+}(0)$ at zero frequency. These two vertex components can also be expressed in the symmetrized form,

$$\begin{aligned} & \{\rho_{d\sigma}\}^2 \left[\Gamma_{\sigma\sigma;\sigma\sigma}^{-+;+-}(\epsilon, \epsilon'; \epsilon', \epsilon) + \Gamma_{\sigma\sigma;\sigma\sigma}^{+-;-}(\epsilon, \epsilon'; \epsilon', \epsilon) \right] \\ &= i2\pi \sum_{\sigma''(\neq\sigma)} \chi_{\sigma\sigma''}^2 \mathcal{W}_K^{\text{ph}}(0) + \dots, \quad (\text{C17}) \end{aligned}$$

$$\begin{aligned} & \{\rho_{d\sigma}\}^2 \left[\Gamma_{\sigma\sigma;\sigma\sigma}^{-+;+-}(\epsilon, \epsilon'; \epsilon', \epsilon) - \Gamma_{\sigma\sigma;\sigma\sigma}^{+-;-}(\epsilon, \epsilon'; \epsilon', \epsilon) \right] \\ &= 0 + O((eV)^2, T^2). \quad (\text{C18}) \end{aligned}$$

3. $\Gamma_{\sigma\sigma';\sigma'\sigma}^{\nu_1\nu_2;\nu_3\nu_4}(\epsilon, \epsilon'; \epsilon', \epsilon)$ for $\sigma \neq \sigma'$ up to linear-order terms in ϵ, ϵ', eV , and T

We next consider low-energy behavior of the vertex corrections between electrons in different levels $\sigma \neq \sigma'$ in the Fermi-liquid regime. For the vertex functions of $\sigma \neq \sigma'$, two other Keldysh components $\Gamma_{\sigma\sigma';\sigma'\sigma}^{-+;+-}$ and $\Gamma_{\sigma\sigma';\sigma'\sigma}^{+-;-}$ contribute to the linear order terms with respect to ϵ, ϵ', eV and T , in addition to the ones that appear for $\sigma = \sigma'$ in the above, i.e., $\Gamma_{\sigma\sigma';\sigma'\sigma}^{--;--}$, $\Gamma_{\sigma\sigma';\sigma'\sigma}^{++;++}$, $\Gamma_{\sigma\sigma';\sigma'\sigma}^{--;+-}$, $\Gamma_{\sigma\sigma';\sigma'\sigma}^{+-;-}$, $\Gamma_{\sigma\sigma';\sigma'\sigma}^{+-;-}$. We calculate low-energy expansion of all these components in this subsection.

a. Low-energy expansion of $\Gamma_{\sigma\sigma';\sigma'\sigma}^{--;--}$ & $\Gamma_{\sigma\sigma';\sigma'\sigma}^{+-;-}$

For the causal ($--;--$) component, the imaginary part arises from the order U^2 scattering processes shown in Figs. 10 (b), (c), and (d) for $\sigma \neq \sigma'$. At low energies, leading-order terms of the imaginary part are determined by a single particle-hole-pair excitations in (b) and (d), and the particle-particle-pair excitations in (c). Contributions of each of these three diagrams can be written in the following form, taking $F'_b = F'_c = 1$ and $F'_d = 2$,

$$\begin{aligned} & \Gamma_{\sigma\sigma';\sigma'\sigma}^{(2b)--;--}(\epsilon, \epsilon'; \epsilon', \epsilon) \\ &= (-1)^0 i^{2+1} (-1)^{F'_b} U^2 \int \frac{d\varepsilon_1}{2\pi} G_{\sigma'}^{--}(\varepsilon_1 + \epsilon - \epsilon') G_{\sigma'}^{--}(\varepsilon_1) \\ &= U^2 X_{\sigma\sigma'}^{--}(\epsilon - \epsilon'), \quad (\text{C19a}) \end{aligned}$$

$$\begin{aligned}
& \Gamma_{\sigma\sigma';\sigma'\sigma}^{(2c)---;--}(\epsilon, \epsilon'; \epsilon', \epsilon) \\
&= (-1)^0 i^{2+1} (-1)^{F'_c} U^2 \int \frac{d\varepsilon_1}{2\pi} G_{\sigma}^{--}(\epsilon + \epsilon' - \varepsilon_1) G_{\sigma'}^{--}(\varepsilon_1) \\
&= U^2 Y_{\sigma\sigma'}^{--}(\epsilon + \epsilon'), \tag{C19b}
\end{aligned}$$

$$\begin{aligned}
& \Gamma_{\sigma\sigma';\sigma'\sigma}^{(2d)---;--}(\epsilon, \epsilon'; \epsilon', \epsilon) \\
&= (-1)^0 i^{2+1} (-1)^{F'_d} U^2 \int \frac{d\varepsilon_1}{2\pi} \sum_{\sigma''(\neq\sigma, \sigma')} G_{\sigma''}^{--}(\varepsilon_1) G_{\sigma''}^{--}(\varepsilon_1) \\
&= -U^2 \sum_{\sigma''(\neq\sigma, \sigma')} X_{\sigma''\sigma''}^{--}(0). \tag{C19c}
\end{aligned}$$

Thus, the total of order U^2 causal component is given by $\Gamma_{\sigma\sigma';\sigma'\sigma}^{(2)---;--} \equiv \Gamma_{\sigma\sigma';\sigma'\sigma}^{(2b)---;--} + \Gamma_{\sigma\sigma';\sigma'\sigma}^{(2c)---;--} + \Gamma_{\sigma\sigma';\sigma'\sigma}^{(2d)---;--}$. The contribution of the diagram Fig. 10 (d) appears for $N > 2$ as the summation for σ'' runs over $N - 2 > 0$ possible intermediate states other than σ and σ' . Similarly, for the corresponding $(++;++)$ components, order U^2 contributions of the diagrams Figs. 10 (b), (c), and (d) can be calculated, replacing G^{--} in Eq. (C19) by G^{++} , as

$$\begin{aligned}
& \Gamma_{\sigma\sigma';\sigma'\sigma}^{(2)++;++}(\epsilon, \epsilon'; \epsilon', \epsilon) = - \left\{ \Gamma_{\sigma\sigma';\sigma'\sigma}^{(2)---;--}(\epsilon, \epsilon'; \epsilon', \epsilon) \right\}^* \\
&= U^2 \left[X_{\sigma\sigma'}^{++}(\epsilon - \epsilon') + Y_{\sigma\sigma'}^{++}(\epsilon + \epsilon') - \sum_{\sigma''(\neq\sigma, \sigma')} X_{\sigma''\sigma''}^{++}(0) \right]. \tag{C20}
\end{aligned}$$

The imaginary part of the full vertex function that includes multiple scatterings of all order in U can be calculated up to linear order terms with respect to ϵ , ϵ' , eV , and T , from the diagrams show in Figs. 8 (b), (c), and (d). The leading-order behaviors are determined by the single particle-hole pair or the particle-particle pair, excitation in the intermediate states. Therefore, the imaginary part of the full causal vertex function is given by

$$\begin{aligned}
& \text{Im} \Gamma_{\sigma\sigma';\sigma'\sigma}^{(b)---;--}(\epsilon, \epsilon'; \epsilon', \epsilon) \\
&= -\text{Im} \int \frac{d\varepsilon_1}{2\pi i} G_{\sigma}^{--}(\varepsilon_1 + \epsilon - \epsilon') G_{\sigma'}^{--}(\varepsilon_1) \\
&\quad \times \Gamma_{\sigma\sigma';\sigma'\sigma}^{---;--}(0, 0; 0, 0) \Gamma_{\sigma'\sigma';\sigma\sigma'}^{---;--}(0, 0; 0, 0) + \dots \\
&= \left| \Gamma_{\sigma\sigma';\sigma'\sigma}^{---;--}(0, 0; 0, 0) \right|^2 \text{Im} X_{\sigma\sigma'}^{--}(\epsilon - \epsilon') + \dots, \tag{C21}
\end{aligned}$$

$$\begin{aligned}
& \text{Im} \Gamma_{\sigma\sigma';\sigma'\sigma}^{(c)---;--}(\epsilon, \epsilon'; \epsilon', \epsilon) \\
&= -\text{Im} \int \frac{d\varepsilon_1}{2\pi i} G_{\sigma}^{--}(\epsilon + \epsilon' - \varepsilon_1) G_{\sigma'}^{--}(\varepsilon_1) \\
&\quad \times \Gamma_{\sigma\sigma';\sigma'\sigma}^{---;--}(0, 0; 0, 0) \Gamma_{\sigma'\sigma';\sigma\sigma'}^{---;--}(0, 0; 0, 0) + \dots \\
&= \left| \Gamma_{\sigma\sigma';\sigma'\sigma}^{---;--}(0, 0; 0, 0) \right|^2 \text{Im} Y_{\sigma\sigma'}^{--}(\epsilon + \epsilon') + \dots, \tag{C22}
\end{aligned}$$

$$\begin{aligned}
& \text{Im} \Gamma_{\sigma\sigma';\sigma'\sigma}^{(d)---;--}(\epsilon, \epsilon'; \epsilon', \epsilon) \\
&= \text{Im} \int \frac{d\varepsilon_1}{2\pi i} \sum_{\sigma''(\neq\sigma, \sigma')} G_{\sigma''}^{--}(\varepsilon_1) G_{\sigma''}^{--}(\varepsilon_1) \tag{C23}
\end{aligned}$$

$$\begin{aligned}
& \quad \times \Gamma_{\sigma\sigma'';\sigma''\sigma}^{---;--}(0, 0; 0, 0) \Gamma_{\sigma''\sigma';\sigma'\sigma''}^{---;--}(0, 0; 0, 0) + \dots \\
&= - \sum_{\sigma''(\neq\sigma, \sigma')} \Gamma_{\sigma\sigma'';\sigma''\sigma}^{---;--}(0, 0; 0, 0) \Gamma_{\sigma''\sigma';\sigma'\sigma''}^{---;--}(0, 0; 0, 0) \\
& \quad \times \text{Im} X_{\sigma''\sigma''}^{--}(0) + \dots. \tag{C24}
\end{aligned}$$

The sum $\Gamma_{\sigma\sigma';\sigma'\sigma}^{---;--} \equiv \Gamma_{\sigma\sigma';\sigma'\sigma}^{(b)---;--} + \Gamma_{\sigma\sigma';\sigma'\sigma}^{(c)---;--} + \Gamma_{\sigma\sigma';\sigma'\sigma}^{(d)---;--}$ can also be expressed in the following form, in terms of the collision integrals,

$$\begin{aligned}
& \text{Im} \Gamma_{\sigma\sigma';\sigma'\sigma}^{---;--}(\epsilon, \epsilon'; \epsilon', \epsilon) \\
&= \frac{\pi}{\rho_{d\sigma} \rho_{d\sigma'}} \left\{ \chi_{\sigma\sigma'}^2 \left[\mathcal{W}_{\text{K}}^{\text{ph}}(\epsilon - \epsilon') - \mathcal{W}_{\text{K}}^{\text{pp}}(\epsilon + \epsilon') \right] \right. \\
& \quad \left. - \sum_{\sigma''(\neq\sigma, \sigma')} \chi_{\sigma\sigma''} \chi_{\sigma''\sigma'} \mathcal{W}_{\text{K}}^{\text{ph}}(0) \right\} + \dots. \tag{C25}
\end{aligned}$$

The properties of the PH propagator $X_{\sigma\sigma'}^{\mu\nu}$, and PP propagator $Y_{\sigma\sigma'}^{\mu\nu}$, and also the collision integrals $\mathcal{W}_{\text{K}}^{\text{ph}}(\omega)$ and $\mathcal{W}_{\text{K}}^{\text{pp}}(\omega)$, are described in Sec. VII B.

Note that the causal vertex function for $\sigma \neq \sigma'$ also has the eV -linear real part $\text{Re} \Gamma_{\sigma\sigma';\sigma'\sigma}^{---;--}(\epsilon, \epsilon'; \epsilon', \epsilon)$, and it is deduced from the Ward identity in Sec. VIII B and is shown in TABLE VIII.

b. Low-energy expansion of $\Gamma_{\sigma\sigma';\sigma'\sigma}^{---;++}$ & $\Gamma_{\sigma\sigma';\sigma'\sigma}^{++;--}$

We next consider $\Gamma_{\sigma\sigma';\sigma'\sigma}^{---;++}$ and $\Gamma_{\sigma\sigma';\sigma'\sigma}^{++;--}$ which arise first from order U^2 particle-hole ladder diagram Fig. 10 (b). The contributions of this process can be calculated, taking $F' = 1$, as

$$\begin{aligned}
& \Gamma_{\sigma\sigma';\sigma'\sigma}^{(2)---;++}(\epsilon, \epsilon'; \epsilon', \epsilon) \\
&= (-1)^1 i^{2+1} (-1)^{F'} U^2 \int \frac{d\varepsilon_1}{2\pi} G_{\sigma}^{+-}(\varepsilon_1 + \epsilon - \epsilon') G_{\sigma'}^{-+}(\varepsilon_1) \\
&= -U^2 X_{\sigma\sigma'}^{+-}(\epsilon - \epsilon'), \tag{C26a}
\end{aligned}$$

$$\begin{aligned}
& \Gamma_{\sigma\sigma';\sigma'\sigma}^{(2)++;--}(\epsilon, \epsilon'; \epsilon', \epsilon) \\
&= (-1)^1 i^{2+1} (-1)^{F'} U^2 \int \frac{d\varepsilon_1}{2\pi} G_{\sigma}^{-+}(\varepsilon_1 + \epsilon - \epsilon') G_{\sigma'}^{+-}(\varepsilon_1) \\
&= -U^2 X_{\sigma\sigma'}^{-+}(\epsilon - \epsilon'). \tag{C26b}
\end{aligned}$$

These two components are pure imaginary. The low-energy asymptotic forms of the corresponding full vertex functions can be deduced from the diagram Fig. 8 (b) which include multiple-scattering processes of all orders

in U ,

$$\begin{aligned} & \Gamma_{\sigma\sigma';\sigma'\sigma}^{-+;-+}(\epsilon, \epsilon'; \epsilon', \epsilon) \\ &= - \int \frac{d\varepsilon_1}{2\pi i} \Gamma_{\sigma\sigma';\sigma'\sigma}^{-+;-+}(0, 0; 0, 0) \Gamma_{\sigma\sigma';\sigma'\sigma}^{++;++}(0, 0; 0, 0) \\ & \quad \times G_{\sigma}^{+-}(\varepsilon_1 + \epsilon - \epsilon') G_{\sigma'}^{+-}(\varepsilon_1) + \dots \\ &= - \left| \Gamma_{\sigma\sigma';\sigma'\sigma}^{-+;-+}(0, 0; 0, 0) \right|^2 X_{\sigma\sigma'}^{+-}(\epsilon - \epsilon') + \dots, \quad (\text{C27a}) \end{aligned}$$

$$\begin{aligned} & \Gamma_{\sigma\sigma';\sigma'\sigma}^{++;-+}(\epsilon, \epsilon'; \epsilon', \epsilon) \\ &= - \int \frac{d\varepsilon_1}{2\pi i} \Gamma_{\sigma\sigma';\sigma'\sigma}^{++;++}(0, 0; 0, 0) \Gamma_{\sigma\sigma';\sigma'\sigma}^{-+;-+}(0, 0; 0, 0) \\ & \quad \times G_{\sigma}^{-+}(\varepsilon_1 + \epsilon - \epsilon') G_{\sigma'}^{+-}(\varepsilon_1) + \dots, \\ &= - \left| \Gamma_{\sigma\sigma';\sigma'\sigma}^{-+;-+}(0, 0; 0, 0) \right|^2 X_{\sigma\sigma'}^{-+}(\epsilon - \epsilon') + \dots, \quad (\text{C27b}) \end{aligned}$$

Therefore, the symmetrized and antisymmetrized parts of these two full vertex functions can be written, as

$$\begin{aligned} & \rho_{d\sigma} \rho_{d\sigma'} \left[\Gamma_{\sigma\sigma';\sigma'\sigma}^{-+;-+}(\epsilon, \epsilon'; \epsilon', \epsilon) + \Gamma_{\sigma\sigma';\sigma'\sigma}^{-+;-+}(\epsilon, \epsilon'; \epsilon', \epsilon) \right] \\ &= -i 2\pi \chi_{\sigma\sigma'}^2 \mathcal{W}_{\text{K}}^{\text{ph}}(\epsilon - \epsilon') + \dots, \quad (\text{C28}) \end{aligned}$$

$$\begin{aligned} & \rho_{d\sigma} \rho_{d\sigma'} \left[\Gamma_{\sigma\sigma';\sigma'\sigma}^{-+;-+}(\epsilon, \epsilon'; \epsilon', \epsilon) - \Gamma_{\sigma\sigma';\sigma'\sigma}^{-+;-+}(\epsilon, \epsilon'; \epsilon', \epsilon) \right] \\ &= -i 2\pi \chi_{\sigma\sigma'}^2 [\epsilon - \epsilon'] + \dots. \quad (\text{C29}) \end{aligned}$$

Note that $\mathcal{W}^{\text{ph}}(\omega) - \mathcal{W}^{\text{ph}}(-\omega) = \omega$, and the explicit expression of $\mathcal{W}_{\text{K}}^{\text{ph}}(\epsilon - \epsilon')$ is shown in TABLE VI.

c. Low-energy expansion of $\Gamma_{\sigma\sigma';\sigma'\sigma}^{-+;-+}$ & $\Gamma_{\sigma\sigma';\sigma'\sigma}^{++;-+}$

The following two vertex components, $\Gamma_{\sigma\sigma';\sigma'\sigma}^{-+;-+}$ and $\Gamma_{\sigma\sigma';\sigma'\sigma}^{++;-+}$ for $\sigma \neq \sigma'$, arise first from the order U^2 diagram Fig. 10 (c). These vertex functions are determined by intermediate particle-particle-pair excitation are pure imaginary, which can be verified taking $F' = 1$, as

$$\begin{aligned} & \Gamma_{\sigma\sigma';\sigma'\sigma}^{(2)-+;-+}(\epsilon, \epsilon'; \epsilon', \epsilon) \\ &= (-1)^1 i^{2+1} (-1)^{F'} U^2 \int \frac{d\varepsilon_1}{2\pi} G_{\sigma}^{+-}(\epsilon + \epsilon' - \varepsilon_1) G_{\sigma'}^{+-}(\varepsilon_1) \\ &= -U^2 Y_{\sigma\sigma'}^{+-}(\epsilon + \epsilon'), \quad (\text{C30a}) \end{aligned}$$

$$\begin{aligned} & \Gamma_{\sigma\sigma';\sigma'\sigma}^{(2)++;-+}(\epsilon, \epsilon'; \epsilon', \epsilon) \\ &= (-1)^1 i^{2+1} (-1)^{F'} U^2 \int \frac{d\varepsilon_1}{2\pi} G_{\sigma}^{-+}(\epsilon + \epsilon' - \varepsilon_1) G_{\sigma'}^{-+}(\varepsilon_1) \\ &= -U^2 Y_{\sigma\sigma'}^{-+}(\epsilon + \epsilon'). \quad (\text{C30b}) \end{aligned}$$

For these two components, contributions of multiple scatterings of all orders in U can also be deduced up to linear-order terms with respect to $|\epsilon - \epsilon'|$, eV , and T from the

diagram Fig. 8 (c),

$$\begin{aligned} & \Gamma_{\sigma\sigma';\sigma'\sigma}^{-+;-+}(\epsilon, \epsilon'; \epsilon', \epsilon) \\ &= - \int \frac{d\varepsilon_1}{2\pi i} \Gamma_{\sigma\sigma';\sigma'\sigma}^{-+;-+}(0, 0; 0, 0) \Gamma_{\sigma\sigma';\sigma'\sigma}^{++;++}(0, 0; 0, 0) \\ & \quad \times G_{\sigma}^{+-}(\epsilon + \epsilon' - \varepsilon_1) G_{\sigma'}^{+-}(\varepsilon_1) + \dots \\ &= - \left| \Gamma_{\sigma\sigma';\sigma'\sigma}^{-+;-+}(0, 0; 0, 0) \right|^2 Y_{\sigma\sigma'}^{+-}(\epsilon + \epsilon') + \dots, \quad (\text{C31a}) \end{aligned}$$

$$\begin{aligned} & \Gamma_{\sigma\sigma';\sigma'\sigma}^{++;-+}(\epsilon, \epsilon'; \epsilon', \epsilon) \\ &= - \int \frac{d\varepsilon_1}{2\pi i} \Gamma_{\sigma\sigma';\sigma'\sigma}^{++;++}(0, 0; 0, 0) \Gamma_{\sigma\sigma';\sigma'\sigma}^{-+;-+}(0, 0; 0, 0) \\ & \quad \times G_{\sigma}^{-+}(\epsilon + \epsilon' - \varepsilon_1) G_{\sigma'}^{+-}(\varepsilon_1) + \dots \\ &= - \left| \Gamma_{\sigma\sigma';\sigma'\sigma}^{-+;-+}(0, 0; 0, 0) \right|^2 Y_{\sigma\sigma'}^{-+}(\epsilon + \epsilon') + \dots. \quad (\text{C31b}) \end{aligned}$$

The symmetrized and antisymmetrized functions of these two components can be expressed in the following form,

$$\begin{aligned} & \rho_{d\sigma} \rho_{d\sigma'} \left[\Gamma_{\sigma\sigma';\sigma'\sigma}^{-+;-+}(\epsilon, \epsilon'; \epsilon', \epsilon) + \Gamma_{\sigma\sigma';\sigma'\sigma}^{-+;-+}(\epsilon, \epsilon'; \epsilon', \epsilon) \right] \\ &= i 2\pi \chi_{\sigma\sigma'}^2 \mathcal{W}_{\text{K}}^{\text{pp}}(\epsilon + \epsilon') + \dots, \quad (\text{C32}) \end{aligned}$$

$$\begin{aligned} & \rho_{d\sigma} \rho_{d\sigma'} \left[\Gamma_{\sigma\sigma';\sigma'\sigma}^{-+;-+}(\epsilon, \epsilon'; \epsilon', \epsilon) - \Gamma_{\sigma\sigma';\sigma'\sigma}^{-+;-+}(\epsilon, \epsilon'; \epsilon', \epsilon) \right] \\ &= i 2\pi \chi_{\sigma\sigma'}^2 \mathcal{W}_{\text{diff}}^{\text{pp}}(\epsilon + \epsilon') + \dots. \quad (\text{C33}) \end{aligned}$$

Note that the bosonic particle-particle collision integral $\mathcal{W}_{\text{diff}}^{\text{pp}}(\omega) \equiv \mathcal{W}^{\text{pp}}(\omega) - \mathcal{W}^{\text{hh}}(\omega)$ is defined in Eq. (7.24), and the explicit expression of $\mathcal{W}_{\text{K}}^{\text{pp}}(\omega)$ is given in TABLE VI.

d. Low-energy expansion of $\Gamma_{\sigma\sigma';\sigma'\sigma}^{-+;-+}$ & $\Gamma_{\sigma\sigma';\sigma'\sigma}^{++;-+}$

For multilevel Anderson impurity with $N > 2$, vertex corrections for $\sigma' \neq \sigma$ also arise from the diagram (d) of Fig. 10. In this case, the intermediate particle-hole pair can be excited in $N - 2$ different configurations of internal degrees of freedom σ'' as it is required that $\sigma'' \neq \sigma$ and $\sigma'' \neq \sigma'$. Thus, the contributions of the order U^2 process are given, taking $F'' = 2$, by

$$\begin{aligned} & \Gamma_{\sigma\sigma';\sigma'\sigma}^{(2)-+;-+}(\epsilon, \epsilon'; \epsilon', \epsilon) \\ &= (-1)^1 i^{2+1} (-1)^{F''} U^2 \int \frac{d\varepsilon_1}{2\pi} \sum_{\sigma'' (\neq \sigma, \sigma')} G_{\sigma''}^{+-}(\varepsilon_1) G_{\sigma''}^{-+}(\varepsilon_1) \\ &= \sum_{\sigma'' (\neq \sigma, \sigma')} U^2 X_{\sigma''\sigma''}^{+-}(0), \quad (\text{C34a}) \end{aligned}$$

$$\begin{aligned} & \Gamma_{\sigma\sigma';\sigma'\sigma}^{(2)++;-+}(\epsilon, \epsilon'; \epsilon', \epsilon) \\ &= (-1)^1 i^{2+1} (-1)^{F''} U^2 \int \frac{d\varepsilon_1}{2\pi} \sum_{\sigma'' (\neq \sigma, \sigma')} G_{\sigma''}^{-+}(\varepsilon_1) G_{\sigma''}^{+-}(\varepsilon_1) \\ &= \sum_{\sigma'' (\neq \sigma, \sigma')} U^2 X_{\sigma''\sigma''}^{-+}(0). \quad (\text{C34b}) \end{aligned}$$

These contributions are pure imaginary. Thus, similarly to the cases of the other components, contributions of the multiple scatterings of all orders in U can be deduced from the diagram Fig. 8 (d), up to linear order terms with respect to eV , T , and frequencies ϵ and ϵ' ,

$$\begin{aligned}
& \Gamma_{\sigma\sigma';\sigma'\sigma}^{-+;+-}(\epsilon, \epsilon'; \epsilon', \epsilon) \\
&= \int \frac{d\varepsilon_1}{2\pi i} \sum_{\sigma''(\neq\sigma, \sigma')} \Gamma_{\sigma\sigma'';\sigma''\sigma}^{-;-;--}(0, 0; 0, 0) \Gamma_{\sigma''\sigma';\sigma'\sigma''}^{++;++}(0, 0; 0, 0) \\
&\quad \times G_{\sigma''}^{+-}(\varepsilon_1) G_{\sigma''}^{-+}(\varepsilon_1) + \dots \\
&= \sum_{\sigma''(\neq\sigma, \sigma')} \Gamma_{\sigma\sigma'';\sigma''\sigma}^{-;-;--}(0, 0; 0, 0) \Gamma_{\sigma''\sigma';\sigma'\sigma''}^{-;-;--}(0, 0; 0, 0) \\
&\quad \times X_{\sigma''\sigma''}^{+-}(0) + \dots, \tag{C35a}
\end{aligned}$$

$$\begin{aligned}
& \Gamma_{\sigma\sigma';\sigma'\sigma}^{+-;-+}(\epsilon, \epsilon'; \epsilon', \epsilon) \\
&= \int \frac{d\varepsilon_1}{2\pi i} \sum_{\sigma''(\neq\sigma, \sigma')} \Gamma_{\sigma\sigma'';\sigma''\sigma}^{++;++}(0, 0; 0, 0) \Gamma_{\sigma''\sigma';\sigma'\sigma''}^{-;-;--}(0, 0; 0, 0) \\
&\quad \times G_{\sigma''}^{+-}(\varepsilon_1) G_{\sigma''}^{+-}(\varepsilon_1) + \dots \\
&= \sum_{\sigma''(\neq\sigma, \sigma')} \Gamma_{\sigma\sigma'';\sigma''\sigma}^{-;-;--}(0, 0; 0, 0) \Gamma_{\sigma''\sigma';\sigma'\sigma''}^{-;-;--}(0, 0; 0, 0) \\
&\quad \times X_{\sigma''\sigma''}^{-+}(0) + \dots. \tag{C35b}
\end{aligned}$$

Furthermore, the symmetrized and antisymmetrized functions of these two vertex components can also be written in the form,

$$\begin{aligned}
& \rho_{d\sigma} \rho_{d\sigma'} \left[\Gamma_{\sigma\sigma';\sigma'\sigma}^{-+;+-}(\epsilon, \epsilon'; \epsilon', \epsilon) + \Gamma_{\sigma\sigma';\sigma'\sigma}^{+-;-+}(\epsilon, \epsilon'; \epsilon', \epsilon) \right] \\
&= i 2\pi \sum_{\sigma''(\neq\sigma, \sigma')} \chi_{\sigma\sigma''} \chi_{\sigma''\sigma'} \mathcal{W}_K^{\text{ph}}(0) + \dots, \tag{C36}
\end{aligned}$$

$$\begin{aligned}
& \rho_{d\sigma} \rho_{d\sigma'} \left[\Gamma_{\sigma\sigma';\sigma'\sigma}^{-+;+-}(\epsilon, \epsilon'; \epsilon', \epsilon) - \Gamma_{\sigma\sigma';\sigma'\sigma}^{+-;-+}(\epsilon, \epsilon'; \epsilon', \epsilon) \right] \\
&= 0 + O((eV)^2, T^2). \tag{C37}
\end{aligned}$$

¹ A. C. Hewson, *The Kondo Problem to Heavy Fermions* (Cambridge University Press, 1993).
² M. Grobis, I. G. Rau, R. M. Potok, H. Shtrikman, and D. Goldhaber-Gordon, *Phys. Rev. Lett.* **100**, 246601 (2008).
³ G. D. Scott, Z. K. Keane, J. W. Ciszek, J. M. Tour, and D. Natelson, *Phys. Rev. B* **79**, 165413 (2009).
⁴ O. Zarchin, M. Zaffalon, M. Heiblum, D. Mahalu, and V. Umansky, *Phys. Rev. B* **77**, 241303(R) (2008).
⁵ T. Delattre, C. Feuillet-Palma, L. G. Herrmann, P. Morfin, J.-M. Berroir, G. FShu ve, B. PlaXun ais, D. C. Glatthli, M.-S. Choi, C. Mora, and T. Kontos, *Nature Physics* **5**, 208 (2009).
⁶ Y. Yamauchi, K. Sekiguchi, K. Chida, T. Arakawa, S. Nakamura, K. Kobayashi, T. Ono, T. Fujii, and R. Sakano, *Phys. Rev. Lett.* **106**, 176601 (2011).
⁷ M. Ferrier, T. Arakawa, T. Hata, R. Fujiwara, R. Delagrangé, R. Weil, R. Deblock, R. Sakano, A. Oguri, and K. Kobayashi, *Nat. Phys.* **12**, 230 (2016).
⁸ E. A. Laird, F. Kuemmeth, G. A. Steele, K. Grove-Rasmussen, J. Nygård, K. Flensberg, and L. P. Kouwenhoven, *Rev. Mod. Phys.* **87**, 703 (2015).
⁹ K. Ono, J. Kobayashi, Y. Amano, K. Sato, and Y. Takahashi, *Phys. Rev. A* **99**, 032707 (2019).
¹⁰ S. Yasui and S. Ozaki, *Phys. Rev. D* **96**, 114027 (2017).
¹¹ P. Nozières, *J. Low Temp. Phys.* **17**, 31 (1974).
¹² K. Yamada, *Prog. Theor. Phys.* **53**, 970 (1975).
¹³ K. Yosida and K. Yamada, *Prog. Theor. Phys.* **53**, 1286 (1975).
¹⁴ K. Yamada, *Prog. Theor. Phys.* **54**, 316 (1975).
¹⁵ H. Shiba, *Prog. Theor. Phys.* **54**, 967 (1975).
¹⁶ A. Yoshimori, *Prog. Theor. Phys.* **55**, 67 (1976).

¹⁷ S. Hershfield, J. H. Davies, and J. W. Wilkins, *Phys. Rev. B* **46**, 7046 (1992).
¹⁸ A. Oguri, *Phys. Rev. B* **64**, 153305 (2001).
¹⁹ A. A. Aligia, *J. Phys.: Condens. Matter* **24**, 015306 (2012).
²⁰ E. Muñoz, C. J. Bolech, and S. Kirchner, *Phys. Rev. Lett.* **110**, 016601 (2013).
²¹ B. Horvatić and V. Zlatić, *Phys. Status Solidi B* **111**, 65 (1982).
²² C. Mora, P. Vitushinsky, X. Leyronas, A. A. Clerk, and K. Le Hur, *Phys. Rev. B* **80**, 155322 (2009).
²³ P. Vitushinsky, A. A. Clerk, and K. Le Hur, *Phys. Rev. Lett.* **100**, 036603 (2008).
²⁴ C. Mora, X. Leyronas, and N. Regnault, *Phys. Rev. Lett.* **100**, 036604 (2008).
²⁵ C. Mora, *Phys. Rev. B* **80**, 125304 (2009).
²⁶ M. Filippone, C. P. Moca, A. Weichselbaum, J. von Delft, and C. Mora, *Phys. Rev. B* **98**, 075404 (2018).
²⁷ C. Mora, C. P. Moca, J. von Delft, and G. Zaránd, *Phys. Rev. B* **92**, 075120 (2015).
²⁸ A. Oguri and A. C. Hewson, *Phys. Rev. Lett.* **120**, 126802 (2018).
²⁹ A. Oguri and A. C. Hewson, *Phys. Rev. B* **97**, 045406 (2018).
³⁰ A. Oguri and A. C. Hewson, *Phys. Rev. B* **97**, 035435 (2018).
³¹ Y. Teratani, R. Sakano, T. Hata, T. Arakawa, M. Ferrier, K. Kobayashi, and A. Oguri, *Phys. Rev. B* **102**, 165106 (2020).
³² Y. Teratani, R. Sakano, and A. Oguri, *Phys. Rev. Lett.* **125**, 216801 (2020).
³³ Y. Teratani, R. Sakano, and A. Oguri, unpublished.
³⁴ H. R. Krishna-murthy, J. W. Wilkins, and K. G. Wilson, *Phys. Rev. B* **21**, 1003 (1980).

- ³⁵ H. R. Krishna-murthy, J. W. Wilkins, and K. G. Wilson, Phys. Rev. B **21**, 1044 (1980).
- ³⁶ T. Hata, Y. Teratani, T. Arakawa, S. Lee, M. Ferrier, R. Deblock, R. Sakano, A. Oguri, and K. Kobayashi, Nature Communications **12**, 3233 (2021).
- ³⁷ A. O. Gogolin and A. Komnik, Phys. Rev. Lett. **97**, 016602 (2006).
- ³⁸ E. Sela, Y. Oreg, F. von Oppen, and J. Koch, Phys. Rev. Lett. **97**, 086601 (2006).
- ³⁹ E. Sela and J. Malecki, Phys. Rev. B **80**, 233103 (2009).
- ⁴⁰ R. Sakano, T. Fujii, and A. Oguri, Phys. Rev. B **83**, 075440 (2011).
- ⁴¹ D. B. Karki, C. Mora, J. von Delft, and M. N. Kiselev, Phys. Rev. B **97**, 195403 (2018).
- ⁴² S. Hershfield, Phys. Rev. B **46**, 7061 (1992).
- ⁴³ L. P. Pitaevskii and E. M. Lifshitz, *Physical Kinetics* (Butterworth-Heinemann, 1981).
- ⁴⁴ H. Haug and A.-P. Jauho, *Quantum Kinetics in Transport and Optics of Semiconductors* (Springer, 2008).
- ⁴⁵ C. Caroli, R. Combescot, and P. Nozières, Phys. C: Solid State Phys **4**, 916 (1971).
- ⁴⁶ Y. Meir and N. S. Wingreen, Phys. Rev. Lett. **68**, 2512 (1992).
- ⁴⁷ A. C. Hewson, J. Phys.: Condens. Matter **13**, 10011 (2001).
- ⁴⁸ G. M. Eliashberg, Sov. Phys. JETP **14**, 886 (1962).
- ⁴⁹ G. M. Eliashberg, Sov. Phys. JETP **15**, 1151 (1962).
- ⁵⁰ Eq. (11) of Ref. 27. Their notation and our one correspond to each other such that $\alpha_{\sigma}^{(1)}/\pi = \chi_{\sigma\sigma}$, $\phi_{\sigma\sigma'}^{(1)}/\pi = -\chi_{\sigma\sigma'}$, $\alpha_{\sigma}^{(2)}/\pi = -\frac{1}{2}\chi_{\sigma\sigma\sigma}^{[3]}$, and $\phi_{\sigma\sigma'}^{(2)}/\pi = 2\chi_{\sigma\sigma'\sigma'}^{[3]}$ for $\sigma' \neq \sigma$.
- ⁵¹ Eq. (51) of Ref. 22, after inserting some parenthesis for correcting minor typos.
- ⁵² T. A. Costi and V. Zlatić, Phys. Rev. B **81**, 235127 (2010).
- ⁵³ NRG calculations for this case have been carried out, choosing the discretization parameter to be $\Lambda = 2.0$ and retaining typically 4000 low-lying excited states.
- ⁵⁴ A. Oguri and A. C. Hewson, Phys. Rev. B **98**, 079905(E) (2018).
- ⁵⁵ L. V. Keldysh, Sov. Phys. JETP **20**, 1018 (1965).
- ⁵⁶ A. A. Abrikosov, I. Dzyaloshinskii, and L. P. Gorkov, *Methods of Quantum Field Theory in Statistical Physics* (Pergamon, London, 1965).
- ⁵⁷ A. Oguri, J. Phys. Soc. Jpn. **70**, 2666 (2001).
- ⁵⁸ A. Oguri, J. Phys. Soc. Jpn. **72**, 3301 (2003).
- ⁵⁹ P. Morel and P. Nozières, Phys. Rev. **126**, 1909 (1962).
- ⁶⁰ K. Tsutsumi, Y. Teratani, R. Sakano, and A. Oguri, arXiv:2110.03226.
- ⁶¹ J. Schrieffer, *Theory of Superconductivity*, Advanced Book Program Series (Advanced Book Program, Perseus Books, 1983).
- ⁶² See also the very recent formulation of the spectral function for multipoint correlation functions by Kugler, Lee, and von Delft in Ref. 63.
- ⁶³ F. B. Kugler, Seung-Sup B. Lee, and J. von Delft, Phys. Rev. X **11**, 041006 (2021).